Topological Properties of Interacting Fermionic Systems

Dissertation advisor | Author

Professor Bertrand I. Halperin | **Luiz Henrique Bravo Dos Santos**

Topological Properties of Interacting Fermionic Systems

Abstract

This thesis is a study of three categories of problems in fermionic systems for which topology plays an important role: (i) The properties of zero modes arising in systems of fermions interacting with a bosonic background, with a special focus on Majorana modes arising in the superconductor state. We propose a method for counting Majorana modes and we study a mechanism for controlling their number parity in lattice systems, two questions that are of relevance to the protection of quantum bits. (ii) The study of dispersionless bands in two dimensions as a platform for correlated physics, where it is shown the possibility of stabilizing the fractional quantum Hall effect in a flat band with Chern number. (iii) The extension of the hierarchy of quantum Hall fluids to the case of time-reversal symmetric incompressible ground states describing a phase of strongly interacting topological insulators in two dimensions.

Contents

Citations to Previously Published Work

The content of Chapter 2 (except Sec. 2.4), apart from minor modifications, appeared in:

> "Topological qubits in graphenelike systems," Luiz Santos, Shinsei Ryu, Claudio Chamon, Christopher Mudry, *Phys. Rev. B* **82**, 165101 (2010).

The content of Chapter 3, apart from minor modifications, appeared in:

> "Counting Majorana zero modes in superconductors," Luiz Santos, Yusuke Nishida, Claudio Chamon, Christopher Mudry, *Phys. Rev. B* **83**, 104522 (2011).

The content of Chapter 4, apart from minor modifications, appeared in:

> "Isolated Flat Bands and Spin-1 Conical Bands in Two-Dimensional Lattices," Dmitry Green, Luiz Santos, Claudio Chamon, *Phys. Rev. B* **82**, 075104 (2010).

The content of Chapter 5 appeared in:

> "Fractional quantum Hall states at zero magnetic field," Titus Neupert, Luiz Santos, Claudio Chamon, Christopher Mudry, *Phys. Rev. Lett.* **106**, 236804 (2011).
>
> "Topological Hubbard model and its high-temperature quantum Hall effect," Titus Neupert, Luiz Santos, Shinsei Ryu, Claudio Chamon, Christopher Mudry, *Phys. Rev. Lett.* **108**, 046806 (2012).
>
> "Density algebra for three-dimensional topological insulators," Titus Neupert, Luiz Santos, Shinsei Ryu, Claudio Chamon, Christopher Mudry, `arXiv:1202.5188.`

The content of Chapter 6, apart from minor modifications, appeared in:

> "Time-reversal symmetric hierarchy of fractional incompressible liquids," Luiz Santos, Titus Neupert, Shinsei Ryu, Claudio Chamon, Christopher Mudry, *Phys. Rev. B* **84**, 165138 (2011).

Electronic preprints (shown in `typewriter font`) are available on the Internet at the following URL:

> `http://arXiv.org`

Acknowledgments

I have been very fortunate to have Claudio Chamon as my advisor *de facto*. Being his student for these past few years has taught me to develop an appreciation, on one hand, for elegantly formulated problems and, on the other hand, for the practical implications of scientific ideas. His intuitive approach to and his range of interests in physical problems will always be a source of inspiration for me. I am certain that crossing to the other side of the Charles River was the best decision I have taken as a graduate student. I am also deeply grateful to him and his family for having treated me as a friend and I hope that we will be able to nurture this friendship for the years ahead.

I immensely thank my Harvard advisor, Bert Halperin, and Amir Yacoby for being part of both my Qualifying Oral Exam Committee and Thesis Defense Committee, as well as for their valuable comments on my work. I had a great experience working as a Teaching Fellow in a statistical mechanics course taught by Bert. Through the discussions in our condensed matter seminars, I have been always amazed to by his deep knowledge of physics and his constant effort to reach to the core of ideas. I have also had the privilege to work as a Teaching Fellow in excellent courses taught by John Doyle, Arthur Jaffe and Bob Westervelt. I thank Melissa Franklin for demonstrating concern about my academic progress, for her support as Director of Graduate Studies, as well as for being part of my Thesis Defense Committee.

It was a great scientific experience to be able to interact with various people in different projects. I begin by acknowledging Dmitry Green for a collaboration in my first project on flat bands, a topic that has kept my attention since then. My colleagues Christopher Mudry, Titus Neupert and Shinsei Ryu had a great influence over my

views of physics and I wish to immensely thank them for our fruitful collaborations in various projects. I thank Yusuke Nishida for various collaborations and for enjoyable and informative physics discussions. From Roman Jackiw and So-Young Pi I had the privilege to learn about topics in quantum field theory and gravity and I will miss our weekly discussionss as well as our camaraderie. I would like to acknowledge Michael El-Batanouny and his laboratory members for given me the valuable opportunity to work closely with experimental data. I am also indebted to Denise Freed for the opportunity she gave me to join a year-long research project at Schlumberger-Doll Research.

I would like to take the moment to acknowledge many colleagues and friends at the Harvard Physics Department for their companionship: Ben Feldman, Clay Cordova, Chin Lin Wong, David Tempel, Eddie Schlafly, Eleanor Millman, Eli Visbal, Eun Gook Moon, Jack DiSciacca, Jayson Palouse, Laura Jeanty, Mark Morales, Peter Blair, Renee Meng-Ju Sher, Sofia Magkiriadou, Susanne Pielawa, Takuya Kitagawa, Tongyan Lin, Yang-Ting Chien and many others. I would also like express my deep appreciation to our former Graduate Student Program Coordinator Sheila Ferguson for being so attentive to the needs of the students.

I am highly thankful to Sumit Das, Ganpathy Murthy and Al Shapere for the positive scientific influence they had on me while I was at University of Kentucky. At that time, when I was trying to figure out in what area of physics I wanted to work on, they gave me precious advices, which I will never forget. I am also enormously grateful to my undergraduate advisor in Brazil, Carlos Pinheiro, for having instilled in me the desire to pursue my graduate studies in the United States and for his

relentless effort to help me achieve this goal.

I am indebted to my parents, Luiz Renato and Margarete, who have, through the years, faced tremendous hardships so that I could have good educational opportunities. I have always been inspired by their determination and I lack words to describe how important they are to me.

And finally I wholeheartedly thank my wife Sabrine for the unconditional love and support she has shown even in my worst moments of frustration towards physics or myself. On the difficult moments we went through, she has, despite her quiet personality, always demonstrated the courage to fight the good fight. She has kept me grounded through these years and to her and to our family, which will get a little bigger soon, I dedicate this thesis.

To my family and my lovely wife Sabrine.

Chapter 1

Introduction

1.1 Overview

Over the past 30 years, one of the central themes of condensed matter physics has been the description of physical properties of systems based on the notion of topology. In this context, a "topological property" refers to a property of the ground state, which remains invariant with respect to local perturbations applied on the system.

The best known example of such topological manifestation is given by the Quantum Hal Effect (QHE), whereby upon subjecting a two dimensional electron gas with high mobility to a strong uniform magnetic field at low temperatures, a series of plateaus for the Hall conductance are observed at values $\sigma_{xy} = \frac{p}{q}\frac{e^2}{h}$, where p and q are integer numbers. The quantization of σ_{xy} is robust so long as perturbations are unable to close the many-body gap.

A uniform magnetic field B in two dimensions organizes the single-particle spectrum into degenerate bands - Landau levels (LL) - equally separated from each other

by the cyclotron energy $\hbar\omega_c$, where $\omega_c \equiv eB/m_e c$ denotes the cyclotron frequency, e is the electron's charge, m_e is the electron's mass, c is the speed of light and $\hbar$ is the Planck's constant divided by 2π. The degeneracy of each LL is determined by the ratio Φ/ϕ_0 of the total magnetic flux $\Phi = BA$ (A is the total area of the system) threading the system divided by the fundamental magnetic flux quantum $\phi_0 \equiv hc/e$.

In the integer QHE (IQHE) [122], one deals with a scenario where the Fermi level $E_{\rm F}$ lies between, say, the p-th and the $(p+1)$-th LL's, i.e., $(p+1/2)\hbar\omega_{\rm c} < E_{\rm F} < (p+3/2)\hbar\omega_{\rm c}$. In such case, if one considers a cylinder geometry [69] or a ring geometry [45], the highest energy states far from the edges far are at energies $(p+1/2)\hbar\omega_{\rm c}$ in the limit of a clean sample and hence there is an excitation energy gap associated to these bulk states. Near the edges of sample, on the other hand, the confining potential pushes the single-particle energy levels up, which eventually end up crossing the Fermi level and give rise to gapless edge states. At equilibrium, the states localized near the two edges carry opposite currents and thus the net current in the whole sample is zero. On the other hand, if there is a difference $\Delta E_{\rm F} \equiv e\,\Delta\mu$ on the Fermi level at the edges, with $\Delta E_{\rm F}$ assumed to be small enough so that the bulk states do not cross the Fermi level, then near the edge where the Fermi level has been increased extra states will be populated, while near the edge where the Fermi level has been lowered states will be depopulated. This imbalance results in a net current $I = p\frac{e^2}{h}\,\Delta\mu$, which then implies a Hall conductance $\sigma = pe^2/h$. The effects of the Coulomb interaction and disorder do not change the quantized transport properties of the IQHE as long as their respective energy scales are much smaller than the cyclotron energy $\hbar\omega_c$ [69, 45].

Thouless, Kohmoto, Nightingale and den Nijs [120] have shown that, when applied to a non-interacting periodic band insulator subject to an external magnetic field in two dimensions, the Kubo formula for the Hall conductance σ_{xy} delivers an expression which, in units of e^2/h, equals the first Chern number computed over all the occupied bands. The first Chern number is an integer valued topological invariant that characterizes the mapping between the space of points $\boldsymbol{k}$ in the 2D Brillouin zone to the space of Bloch states $|\psi_{\boldsymbol{k}}\rangle$ (defined under the condition that $|\psi_{\boldsymbol{k}+\boldsymbol{G}}\rangle = |\psi_{\boldsymbol{k}}\rangle$, where $\boldsymbol{G}$ is a reciprocal lattice vector) forming an isolated band. A non-zero Chern number captures the inability to uniquely assign the phase of the Bloch states in the entire Brillouin zone [77] and exemplifies the concept of Berry phase [8, 109].

Differently from the above scenario, if a LL is partially filled and the effect of interactions is not taken into account, then a large number of many-body states become mutually degenerate, where such degeneracy cannot be lifted perturbatively by the effect of Coulomb interactions. The problem of a partially filled LL thus makes for a strongly correlated electronic states par excellence and, for some special values of the filling fraction (the ratio between the number of particles and the number of single-particle degenerate states which make up the LL's), the effects of the electronic correlations lift the large degeneracy by selecting an incompressible state with, σ_{xy} which is a fraction of e^2/h [121, 110]. The observation of the FQHE requires larger magnetic fields, cleaner samples and low temperatures as compared to the IQHE; while the latter can be formulated as a single-particle problem, the former is a quintessential strongly correlated state. Ref. [87] has extended the notion of a Chern number to an interacting many-body ground state by demonstrating that the Hall

conductance is related to the response of the ground state wave function to "twisted" boundary conditions.

The Hamiltonian of a free charged particle in a magnetic field has some special properties. The first aforementioned one is that adjacent LL's are separated by a constant energy gap $\hbar\omega_c$. Besides that, the lowest LL (LLL) plays a special role in that, modulo sign conventions, the single-particle wave functions (in so called symmetric gauge) pertaining to the LLL can be factorized into a Gaussian part (whose decay is controlled by the magnetic length $\ell_B = \sqrt{\hbar c/eB}$) and an analytic function of $z = x + \mathrm{i}\, y$, where x and y are the coordinates of the two dimensional plane. Laughlin has explored this analyticity property of the LLL, together with other general physical requirements, to propose wave functions for the ground state of the FQHE at filling fractions $1/(2m+1)$, $m \in \mathbb{Z}$ [70]. By applying gauge arguments to such family of wave functions, Laughlin was able to demonstrate that the elementary excitations of this compressible state are quasi-particles and quasi-holes with fractional charge $\pm e/m$, which were then shown in Refs. [47, 2] to have fractional statistics.

The experimental observation of a plethora of fractional Hall plateaus at a variety of filling fractions lead to the construction of a hierarchy of wave functions out of Laughlin's wave function, [46, 42, 47, 71, 36, 74, 73] and the development of the composite fermion picture. [59, 60] These approaches were later reconciled, and unified by the effective description of the FQHE in terms of multi-component Chern-Simons gauge field theories in $(2+1)$-dimensional space and time. [92, 136, 11, 12, 29, 137, 138, 28] These topological effective theories for the hierarchy of the FQHE deliver a correspondence between the physics in the two-dimensional bulk and the physics

along the edges of the sample. [69, 45, 129, 132, 131, 27]. The way in which the gauge fields of the Chern-Simons theory couple to one another is encoded in the so called K matrix. Despite the fact that these topological field theories do not depend on any energy scale of the physical system, i.e., the bulk Hamiltonian of such theories is exactly zero, still they provide a natural framework to study universal properties such as quasi-particle's mutual statistics. In addition, by studying these topological field theories in some 'non-trivial" geometry, one can determine the topological degeneracy of the ground state, which is encoded by the K matrix. The topological degeneracy of the ground state predicted by the Chern-Simons theory is of special relevance, for instance, in confronting the predictions of topological theories exact diagonalization studies performed, for example, on a toroidal geometry.

Building on the early connections of the characterization of the quantum Hall effect in terms of topological invariants [120, 87], Haldane [43] has pointed out the possibility of realizing the IQHE in a two dimensional lattice system with a *zero* magnetic flux per unit cell, in contrast to the Hofstadter model [51] . His model consists of spinless fermions hopping on a honeycomb lattice, where a complex valued second-nearest neighbor hopping parameter opens a gap in the single particle spectrum and gives rise to 2 topological bands with Chern numbers ± 1. At one electron per unit cell (half-filling) the system in a cylinder geometry is a bulk insulator with one unidirectional (chiral) current carrying mode at each edge (with opposite directions for opposite edges), i.e., the same properties fulfilled by a filled Landau level.

The parallelism between the Haldane model and a filled LL poses a question before us: Given that interactions can stabilize an incompressible many-body correlated

state at special filling fractions, what is the fate of interactions in a partially filled band with non-zero Chern number (hereafter referred to as a "Chern band")? Although similar at first sight, the two problems do not immediately map into one another. For example, the analytic properties shared by single particle wave functions in the LLL are absent in a Chern band. Moreover, while in the FQHE observed in semiconductors at uniform magnetic field the magnetic length ℓ_B is typically much larger than the underlying lattice spacing, thus justifying one to neglect the lattice effects to a very good approximation, in the case of a Chern band, the role of the magnetic length is played by the lattice spacing itself, such that the lattice effects are to be taken into account. If one partially fills a dispersionless Chern band, a natural candidate ground state is a charge density wave. Could it be, however, that for certain filling fractions a FQH state is energetically favored? Some of these issues pertaining to the properties of a Chern band and the effect of interactions will be addressed in this thesis.

Despite the fact that the model of Ref. [43] has not yet been realized experimentally to this date, the construction of Haldane is a breakthrough for the possibility that it opens to generalizations in lattice systems with time-reversal symmetry and spin degrees of freedom. For instance, if a two dimensional lattice model can be described as two spin-polarized and independent copies of the Haldane model with the opposite signs of the Hall conductance, then though the net charge transported by the two decoupled systems is zero, the spin transport is non-zero and quantized. In this scenario, the system would realize an integer spin quantum Hall effect (ISQHE).

The developments in the explorations of topological signatures in band theory have led to the recent prediction and experimental discovery of topological insulators

in two [62, 63, 7, 6, 68] and three [30, 32, 80, 90, 96, 53, 17, 143] dimensions, which are time-reversal symmetric band insulators whose band structure can be characterized by a $\mathbb{Z}_2$ topological invariant. This invariant measures the *parity* of the number of Krammer's pairs of boundary states and distinguishes whether or not the boundary states are immune to localization due to time-reversal invariant disorder.

All the recently discovered topological insulators are in a regime where the effect of interactions is negligible and thus much of their physical properties derive from the free particle picture. It is however possible to conceive the situation whereby the strength of interactions is adiabatically increased in a topological band insulator. What would then be the competing correlated ground states? Could any of these phases be an incompressible liquid-like ground state à la the FQHE, albeit with time reversal symmetry? In this thesis, we shall address this question, namely, the description of strongly correlated phases with time-reversal symmetry from the point of view of topological field theories in $(2+1)$ dimensions. In analogy with the FQHE, we shall provide a hierarchical construction of Chern-Simons topological field theories with fractionalized excitations and use it to derive the structure of the edge theory.

Another topic that has been receiving much attention recently and that has been influenced by ideas originated from topological properties of physical systems is quantum computation. The basic ingredient in quantum computation is the qubit, which is a two-level system on which information is stored. One of the major challenges in implementing realistic protocols of quantum computation is decoherence, i.e., the fact that the intrinsic coupling between the qubits with the environment generally leads to dephasing and subsequent loss of the coherence of the quantum state of in-

terest. It has been claimed to be possible to circumvent the problem of decoherence if the qubit is constructed non-locally by using spatially separated excitations of a many-body ground state. [66]

A possible way of implementing these non-local qubits is via systems whose excitations obey non-Abelian statistics. Two candidate systems to host these excitations, both in two spatial dimensions, are the $\nu = 5/2$ fractional quantum Hall state [79] and superconductors in which the presence of vortex order parameter binds a "zero mode", i.e., a fermionic excitation with zero energy localized at the core of the vortex. [94, 93, 54]

What makes zero modes so special in superconductors? To address this question we recall that because superconductance mixes particles and holes, the second quantized Bogoliubov quasi-particle operator γ_E at some energy E satisfies the particle-hole symmetric relation $\gamma_E = \gamma^\dagger_{-E}$. As such, the quantized operator γ_0 associated with the zero energy mode turns out to be self-adjoint, that is to say, $\gamma_0 = \gamma_0^\dagger$. It is in the sense of being a "real" fermion that a zero mode represents a condensed matter realization of Majorana fermions [75, 140]. With a pair of Majorana fermions $\gamma_{0,a}$ and $\gamma_{0,b}$ it is possible to assemble "complex" fermion operators $\psi = \frac{1}{\sqrt{2}}(\gamma_{0,a} + \mathrm{i}\,\gamma_{0,b})$ and $\psi^\dagger = \frac{1}{\sqrt{2}}(\gamma_{0,a} - \mathrm{i}\,\gamma_{0,b})$ acting on a two dimensional Hilbert space comprising the states $|0\rangle$ ("empty" fermion state) and $|1\rangle$ ("filled" fermion state), which constitute the qubit. The parity of the number of zero modes per vortex core turns out to be fundamental in determining the stability of the qubit. If, for example, two zero modes exist at each vortex, generic perturbations can split those modes apart causing the breaking down of the stability. The general statement is then that an odd (even)

number of zero modes per vortex implies that one can form, in principle, qubits that are stable (unstable) against decoherence.

Of particular importance is the question of the stability of Majorana qubits in realistic condensed matter systems where there is a natural tendency for a "doubling" of the degrees of freedom, either due to spin degeneracy or due the existence of an underlying lattice. To give a concrete example of this "doubling" phenomenon, we recall that in graphene, electrons hop on a two dimensional honeycomb lattice, where the band structure contains (per spin species) a pair of "Dirac points" in two momenta $\boldsymbol{K}_{\pm}$ at the Brillouin zone (see Ref. [82] for a review). If one induces superconductivity in graphene by the proximity effect with an s-wave superconductor, then a superconducting gap opens on the Dirac points. A superconductor vortex would give rise to one Majorana mode on the vortex core per spin species (2) and per Dirac points (2), resulting in a total of $2 \times 2 = 4$ Majorana modes per vortex, which turns out to be undesirable for stable qubits. In this thesis we shall provide a mechanism for obtaining an odd number of zero modes in graphene despite the even number of low energy degrees of freedom.

Aside from their interpretation as Majorana modes in superconductors, fermionic zero modes have a long and interesting history. It was first realized by Jackiw and Rebbi [56] and by Su, Schrieffer and Heeger [113, 114] that in one spatial dimension, fermions can interact with a scalar order parameter (which, in Refs. [113, 114], represents a bond dimerization on the polyacetylene chain) with a real space configuration forming a domain-wall. The non-zero order parameter being responsible for a mass gap in the fermionic spectrum, a domain wall configuration represents a region in

space where the sign of the fermion mass changes (π phase shift). The remarkable physical property shown in Refs. [56, 113, 114] is that the domain wall traps one zero energy mode per spin species with fermionic charge $\pm e/2$, where the signs ambiguity reflects whether the zero energy state is filled or empty. Therefore in the case of *spinless* fermions, this one dimensional example realizes, in the simplest form, the phenomenon of charge fractionalization. The account of the electron spin in a realistic system causes the charge of the domain-wall to reacquire integer values, however it still leaves room for a interesting possibility: (i) If both zero modes per spin species are either occupied or empty, the total charge $Q = \pm e/2 \pm e/2 = \pm e$ and the total spin $S = 0$ (single) or $S = 1$(triplet). (ii) If one of the spin states is occupied, the total charge $Q = \pm e/2 \mp e/2 = 0$ and the total spin $S = \pm 1/2$. We are then led conclude that the domain-wall produces the phenomenon of *spin-charge separation*.

The same phenomenon of charge fractionalization and spin-charge separation can also occur in higher dimensions. In graphene (see Ref. [82] for a review), for instance, the Kelulé bond order parameter, which opens a mass gap on the two inequivalent Dirac points in reciprocal space, also leads to fractional charge. [52] Being a complex $U(1)$ order parameter, the Kekulé allows for the possibility of a vortex configuration. It was shown in Ref. [52] that if the phase of the order parameter winds by 2π as it encircles the center of the vortex, a fermionic zero mode with charge $\pm e/2$ is exponentially localized at the core of the vortex. Mathematically, a common feature shared by these examples of charge fractionalization in one and two spatial dimensions is the existence of a sub-lattice symmetry represented by a unitary transformation S that anti-commutes with the Hamiltonian and guarantees a one to one relation

between positive and negative energy states. An isolated zero mode is thus protected by perturbations so long as they do not break the sub-lattice symmetry.

In the various examples cited above where point defects (domain-wall, vortex) in the fermion mass parameter give rise to zero modes, the search for zero modes relies on directly (either analytically or numerically) finding normalizable solutions to the zero eigenvalue equation and requires knowledge of microscopic information, such as, the boundary conditions obeyed by the wave function. It is known, on the other hand, that the existence of such interesting fermionic modes actually depends on "global" information of the Hamiltonian (for instance, the vorticity of the order parameter). Given the importance of zero modes associated to a variety of physical phenomena, it is natural to ask is one can predict the existence, as well as the multiplicity, of zero mode solutions in point defects by knowledge of the "global" properties of the Hamiltonian as opposed to directly relying on the solution of the zero energy eigenvalue problem. Such question shall be addressed in this thesis.

1.2 Organization of the thesis

Part I: Zero Modes and Majorana Fermions

Chapter 2

Chapter 2 studies the stability of Majorana qubits in the proximity-induced superconductor phase of graphene. If the Fermi energy lies close to the Dirac points, the number of low energy degrees of freedom that participate in the superconductor state is $4 = 2 \times 2$ (2 Dirac points and 2 spins), resulting in 4 zero modes per vortex, which

then imposes a serious barrier for the construction of Majorana qubits immune to the effects of decoherence. We shall address and answer the question: How to obtain an *odd* number of zero modes per vortex despite the fact that the system contains an *even* number of low-energy fermionic degrees of freedom? As we shall demonstrate, the answer to this question lies at the competition between the superconductor order parameter and fermionic bilinear terms (masses) which break time-reversal symmetry. In addition we shall also discuss the similarities and distinctions between the non-Abelian statistics of Majorana fermions and Dirac fermions.

Chapter 3

Zero modes are related to interesting physical effects such as charge fractionalization and Majorana fermions and appear in a variety of fermionic systems. In the special case of superconductors, the parity of the number of zero mode solutions per vortex is a measure of the ability to construct decoherence free qubits. Usually one relies on the solution of a differential equation in order to determine the number of zero mode solutions bound in a given point defect. We develop a method for counting the number of zero modes, which does not rely on solving a differential equation, rather it relies on computing the fermionic charge induced by the point defect in particle-hole symmetric Hamiltonians.

Part II: Flatbands and the Fractional Quantum Hall Effect

Chapter 4

Flatbands constitute a natural playground for studying strongly correlated physics. A remarkable example that illustrates this point is provided by the FQHE, in which the role of the flatbands is played by the Landau levels created by the external uniform magnetic field.

Lattice models offer another possibility of encountering dispersionless electronic bands. As it turns out in many instances such flatbands do not occur isolated from the other bands. Given the aforementioned importance of flatbands for understanding strongly correlated electronic phases, we study in a specific model, the conditions necessary for obtaining isolated flatbands. Similar to the Landau levels, the the breaking of time reversal symmetry is key to obtaining isolated flatbands. We shall also discuss how flatbands can be viewed as a critical point separating phases with opposite signs of the quantum Hall effect.

Chapter 5

We consider an example of electrons hopping on a two dimensional lattice for which the spectrum contains an isolated flat band with Chern number $C = 1$. A filled flatband with $C = 1$ is analogous to a filled Landau level in that both support a single chiral edge mode and a quantized Hall conductance $\sigma_{xy} = e^2/h$. Motivated by the onset of a fractional quantum Hall state at partial filling of a Landau level, we ask: What happens if one partially fills a flat band with $C = 1$? We present numerical

results which support the FQHE on a flatband at filling fraction $\nu = 1/3$. In addition to that we present a discussion of the relation between the spread of the Wannier functions and the Chern number of the band. Finally we discuss the effect of the non-uniformity of the Berry field in momentum space for the variational calculation of the spectrum of neutral excitations above the many-body ground state.

Part III: Topological Field Theories of 2D Fractional Topological Insulators

Chapter 6

Chapter 6 discusses strongly interacting electronic phases with time-reversal symmetry in two dimensions. These phases can be built, in some given limit, from pairs of fractional quantum Hall states related to each other by time-reversal. We construct a hierarchy of time-reversal symmetric topological field theories and describe the properties obeyed by the K matrix. By studying this field theory in a finite geometry, we are then able to construct the edge theory describing counter-propagating edge channels.

Part I

Zero Modes and Majorana Fermions

Chapter 2

Topological qubits in graphenelike systems

Abstract

The fermion-doubling problem can be an obstacle to getting half a qubit in two-dimensional fermionic tight-binding models in the form of Majorana zero modes bound to the core of superconducting vortices. We argue that the number of such Majorana zero modes is determined by a $\mathbb{Z}_2 \times \mathbb{Z}_2$ topological charge for a family of two-dimensional fermionic tight-binding models ranging from noncentrosymmetric materials to graphene. This charge depends on the dimension of the representation (i.e., the number of species of Dirac fermions – where the doubling problem enters) and the parity of the Chern number induced by breaking time-reversal symmetry. We show that in graphene there are as many as ten order parameters that can be used in groups of four to change the topological number from even to odd.

2.1 Introduction

A major hurdle in the realization of quantum computers is the problem of decoherence. Qubits generically do not last long in the presence of the environment. Overcoming decoherence is possible if the qubit is stored nonlocally using a many-body state, in such a way that the reservoir, which only couples locally to the system, is unable to damage the quantum information. [66] An implementation of this scheme can be achieved if the many-body ground state supports excitations obeying non-Abelian braiding statistics. Non-Abelian braiding statistics that departs from the Bose-Einstein or Fermi-Dirac statistics can only be realized in effectively two-dimensional (2D) systems, such as the $\nu = 5/2$ fractional quantum Hall state on the one hand, [79] or in chiral $p_x \pm ip_y$ 2D superconductors where a half vortex binds a zero-energy midgap state on the other hand. [94, 93, 54] In the latter example, due to particle-hole symmetry (PHS), this zero mode is a Majorana fermion. A two-state system – a qubit – can be assembled from one complex fermion made up of a pair of such Majorana fermions sitting at far away vortices. The splitting of the energies from exactly zero is exponentially small in the separation between the vortices and thus the time to degrade a quantum superposition is exponentially large in the distance between the vortices.

Majorana fermions bound to the core of vortices in a superconductor were discovered by Jackiw and Rossi. [57] There is a single zero-energy midgap state when the vorticity is $n = \pm 1$ (there are generically $|n|$ zero modes). However, these results are obtained for the case of the minimal representation of Dirac fermions whose support in space is the 2D continuum. The fermion-doubling problem, discovered in the con-

text of lattice-gauge theory, [84] prevents importing these results of Jackiw and Rossi to condensed-matter systems, which are models defined on lattices. In graphene, for instance, one does have the Majorana fermions from which it is possible to assemble the qubits, as shown by Ghaemi and Wilczek. [34] However, there are four of them in each vortex because there are two Dirac cones for each spin polarization in graphene. Even numbers of Majorana fermions are not stable, as local perturbations can move them away from zero energy.

One can get much insight into the problem of how many Majorana fermions can be realized in effectively 2D tight-binding models if one looks into ideas for addressing the fermion-doubling problem in lattice-gauge theories. There is the original proposal due to Wilson, which is achieved by adding perturbations (Wilson masses) to a lattice Hamiltonian that opens gaps at undesirable duplicate Dirac points. [141] However, from the point of view of a lattice-gauge regularization of quantum chromodynamics, this option has the undesirable property of breaking the chiral symmetry. Alternatively, the idea that the fermion doubling can be overcome by considering an n-dimensional system as a boundary of a $(n+1)$-dimensional one was put forth by Callan and Harvey in Ref. [13] (see also Refs. [24] and [64]). In fact, it is the Callan-Harvey effect that is at work in the remarkable results obtained by Fu and Kane: [31] (i) surface states in 3D topological insulators with time-reversal symmetry (TRS) realize an odd number of Dirac fermions in the minimal representation of the Clifford algebra. (ii) They can be used to achieve an odd number of Majorana fermions bound to vortex cores induced by the proximity to a type-II superconductor.

We argue in this paper that the Wilson prescription is a route to attain an odd

number of Majorana fermions in effectively 2D condensed-matter systems. The chief reason is that one is not constrained to impose chiral symmetry as in lattice-gauge theory. However, not any Wilson mass can be used for this purpose, only those that break TRS. This approach naturally leads to a $\mathbb{Z}_2 \times \mathbb{Z}_2$ topological charge that discerns whether the system has an even or odd number of Majorana fermions attached to a superconducting (SC) vortex. In essence, the parity of the number of zero modes is determined by the number of Dirac points which have not been knocked out by changing the Chern number via the TRS-breaking Wilson mass. For systems where the number of species is odd, like in the case of surface states of TRS topological insulators, odd numbers of zero modes occur without breaking TRS (odd×even case). In the case of graphene, which is one focus of this paper and where there is an even number of Dirac cones, TRS must be broken so as to obtain an odd Chern number and, in turn, an odd number of Majorana fermions (even×odd case). In all other cases, including graphene when TRS is unbroken (even×even case) and surface states of topological insulators with large enough magnetic field (odd×odd case), there are even numbers of Majorana fermions. Notice that, according to this $\mathbb{Z}_2 \times \mathbb{Z}_2$ classification, systems defined on 2D lattices must have both SC pairing correlations and a nonzero Chern number that accounts for a *thermal* Hall effect in order to have non-Abelian quasiparticles. This is "the poor cousin," i.e., the mean-field version, of the $\nu = 5/2$ quantum Hall state.

2.2 Tuning the number of Majorana fermions

To illustrate how it is possible to use a Wilson mass prescription to change at will the number of Majorana fermions in a 2D tight-binding model, we begin with the pure Rashba kinetic energy

$$H_\alpha := \sum_{\boldsymbol{r}} \sum_{\hat{\boldsymbol{n}}=\hat{\boldsymbol{x}},\hat{\boldsymbol{y}}} \left(i\alpha\, c^\dagger_{\boldsymbol{r}+\hat{\boldsymbol{n}}}\, \sigma_{\hat{\boldsymbol{n}}}\, c_{\boldsymbol{r}} + \text{H.c.} \right) \tag{2.1}$$

that we define on a square lattice with sites denoted by $\boldsymbol{r} = m\hat{\boldsymbol{x}} + n\hat{\boldsymbol{y}}$, where m and n are integers. Here, $c^\dagger_{\boldsymbol{r}} = (c^\dagger_{\boldsymbol{r},\mathrm{s}})$ is a doublet that creates on site $\boldsymbol{r}$ an electron with the spin projection s $=\uparrow,\downarrow$ along the quantization axis, $\sigma_{\hat{\boldsymbol{x}}} \equiv \sigma_x \equiv \sigma_1$ and $\sigma_{\hat{\boldsymbol{y}}} \equiv \sigma_y \equiv \sigma_2$ are the first two Pauli matrices while the third Pauli matrix σ_3 defines the quantization axis in spin space, and the real-valued number α sets the energy scale for the Rashba hopping. At half filling, i.e., at vanishing chemical potential, the Fermi surface collapses to the four nonequivalent Fermi points

$$\boldsymbol{p}_\mathrm{F} = (0,0), (0,\pi), (\pi,0), (\pi,\pi). \tag{2.2}$$

These Fermi points are TRS in that they change by a reciprocal wave vector under the inversion $\boldsymbol{p} \to -\boldsymbol{p}$. Linearization of the energy spectrum of H_α in the vicinity of these four Fermi points yields an 8×8 massless Dirac Hamiltonian, i.e., a reducible representation of the Clifford algebra four times larger than the minimal one in 2D continuum space. This is a manifestation of the fermion doubling. Hamiltonian (2.1) preserves TRS but breaks completely SU(2) spin-rotation symmetry (SRS).

We now introduce the same spectral gap at all the Fermi points, Eq. (2.2). We achieve this with the help of a singlet SC order parameter parametrized by a complex-

valued Δ,

$$H_\Delta := \sum_{\boldsymbol{r}} \left[\Delta \, c^\dagger_{\boldsymbol{r}} \, \left(i\sigma_{\hat{\boldsymbol{y}}} \right) \, c^\dagger_{\boldsymbol{r}} + \text{H.c.} \right], \tag{2.3}$$

that we add to Hamiltonian (2.1),

$$H_\alpha \to H_\alpha + H_\Delta. \tag{2.4}$$

This 2D tight-binding Hamiltonian is the relative to a noncentrosymmetric superconductor in the Rashba-Dirac limit and with singlet SC pairing studied in Ref. [102]. A TRS-breaking vortex

$$\Delta \to \Delta(r) \exp(i\theta) \tag{2.5}$$

with the profile $\Delta(r)$, where r and θ are polar coordinates, binds four Majorana fermions at the Fermi energy via the Jackiw-Rossi solutions. [102]

Finally, we define the three independent TRS-breaking Wilson masses

$$H_{\boldsymbol{h}} := \sum_{\boldsymbol{r}} \left(\sum_{\hat{\boldsymbol{n}}=\hat{\boldsymbol{x}},\hat{\boldsymbol{y}}} h_{\hat{\boldsymbol{n}}} \, c^\dagger_{\boldsymbol{r}+\hat{\boldsymbol{n}}} \, \sigma_3 c_{\boldsymbol{r}} + \text{H.c.} + 2h_3 \, c^\dagger_{\boldsymbol{r}} \, \sigma_3 c_{\boldsymbol{r}} \right) \tag{2.6}$$

parametrized by the triplet of energy scales,

$$\boldsymbol{h} = (h_1, h_2, h_3) \equiv (h_{\hat{\boldsymbol{x}}}, h_{\hat{\boldsymbol{y}}}, h_z) \equiv (h_x, h_y, h_z). \tag{2.7}$$

Each Wilson mass breaks TRS and breaks SU(2) SRS down to U(1).

We are going to show numerically on the lattice and analytically in the continuum limit that the Wilson masses $\boldsymbol{h}$ can be used to change the number of Majorana fermions bound to the core of the vortex, Eq. (2.5), in

$$H := H_\alpha + H_\Delta + H_{\boldsymbol{h}} \tag{2.8}$$

one by one from four to zero.

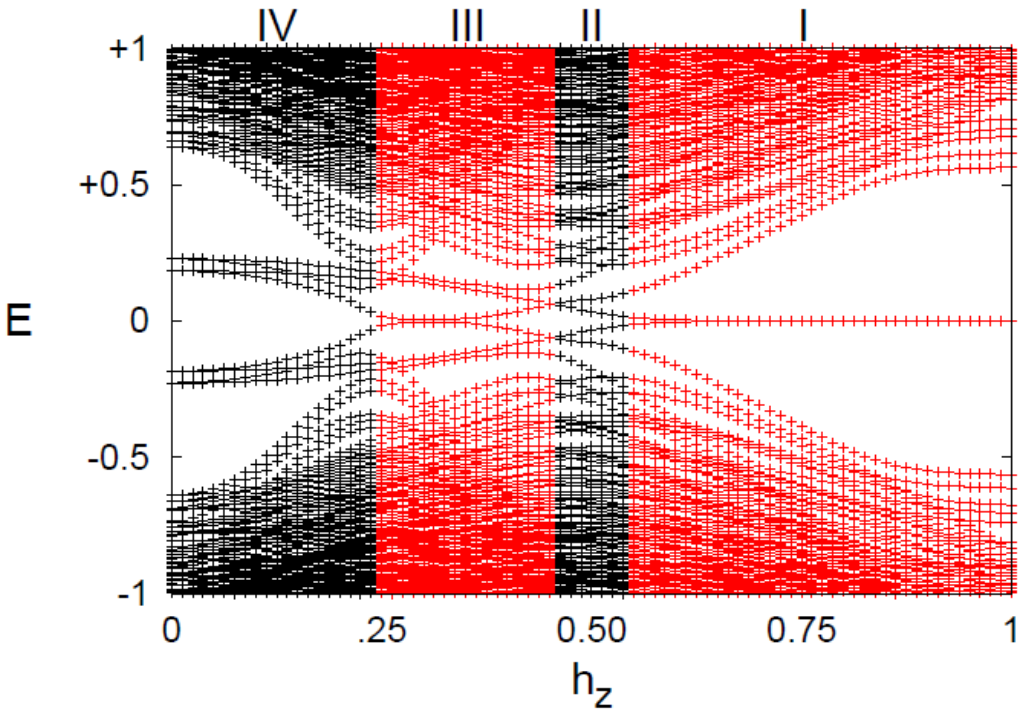

Figure 2.1: Energy levels for the lattice Hamiltonian (2.8) as a function of $h_3 \equiv h_z$ for $h_1 \equiv h_{\hat{\boldsymbol{x}}} = 0.55h_3$, $h_2 \equiv h_{\hat{\boldsymbol{y}}} = 0.45h_3$, and $\alpha = \Delta(r = \infty) = 1$. Although finite-size effects prevent the closing of the bulk gap, the vanishing curvature of the gap in the bulk is a footprint of each thermodynamic transition as a function of h_z. In region IV, there are 8 (=4×2) midgap states, four bound to the vortex and four bound to the antivortex. Their degeneracy is lifted by the combined effects of intravortex-level or intervortex-level repulsion. There are 6 (=3×2), 4 (=2×2), and 2 (=1×2) midgap states in regions III, II, and I, respectively. In the limit in which the vortex and antivortex separation goes to infinity, the intervortex-level repulsion is exponentially suppressed and midgap states can be converted to Majorana fermions. Thus, an odd number of Majorana fermions attached to an isolated vortex are found in regions III and I.

Figure 2.1 displays the energy spectrum of Hamiltonian (2.8) obtained from numerical diagonalization on a square lattice made of 39×39 sites. Periodic boundary conditions are imposed in the presence of a vortex and an anti-vortex with winding numbers ±1, respectively, that are as far apart as possible. A continuum of energy eigenstates is visible as are bulk-gap-closing transitions as a function of $h_3 \equiv h_z$. Midgap states are also visible although they are not located at the Fermi energy because of level repulsion for states attached to the same defect and because of the finite separation between the two defects. Starting from four midgap states per isolated vortex in the thermodynamic limit, increasing h_3 decreases their number by one after each bulk-gap-closing transition.

The same results follow analytically after linearization of the spectrum around the Fermi points, Eq. (2.2). Indeed, linearization of Hamiltonian (2.8) yields, in the Bogoliubov-de-Gennes single-particle representation, the 16×16-dimensional block-diagonal Hermitian matrix,

$$\mathcal{H} := \mathrm{diag}\left(\mathcal{H}_1, \mathcal{H}_2, \mathcal{H}_3, \mathcal{H}_4\right) \tag{2.9a}$$

with the 4×4 Hermitian blocks

$$\mathcal{H}_j = \begin{pmatrix} -\eta_j & p & \delta_j & 0 \\ \overline{p} & \eta_j & 0 & \delta_j \\ \overline{\delta_j} & 0 & -\eta_j & -p \\ 0 & \overline{\delta_j} & -\overline{p} & \eta_j \end{pmatrix} \tag{2.9b}$$

whereby the units $\hbar = v_{\mathrm{F}} = 1$ have been chosen, the complex notation $p \equiv p_1 + ip_2$ is

used for the momenta whereby $\overline{x}$ denotes the complex conjugate of x, and

$$\delta_1 = \delta_2 \equiv \Delta, \qquad \delta_3 = \delta_4 \equiv \overline{\Delta}, \tag{2.9c}$$

$$\eta_1 \equiv \eta_{(0,0)} = 2\left(h_3 + h_1 + h_2\right), \tag{2.9d}$$

$$\eta_2 \equiv \eta_{(0,\pi)} = -2\left(h_3 + h_1 - h_2\right), \tag{2.9e}$$

$$\eta_3 \equiv \eta_{(\pi,\pi)} = 2\left(h_3 - h_1 - h_2\right), \tag{2.9f}$$

$$\eta_4 \equiv \eta_{(\pi,0)} = -2\left(h_3 - h_1 + h_2\right). \tag{2.9g}$$

For the case where δ_j and η_j are spatially uniform, the spectrum of the Hamiltonian (2.9b) reads

$$E_j = \pm\sqrt{\boldsymbol{p}^2 + \left(\mid \delta_j \mid \pm \mid \eta_j \mid\right)^2}, \tag{2.10}$$

where the signs inside and outside the square root are not correlated. The mathematical form of any of the four matrices $\mathcal{H}_j$ is the same as that studied in Ref. [98], provided the SC order parameter Δ and each η_j are identified, respectively, with the Kekulé and Haldane masses in Ref. [98]. Thus, we can immediately borrow and tailor some of the results from Ref. [98] to the present case.

If all the η_j's are zero and the SC order parameter has a single vortex with unit winding number, there are four Majorana fermions bound to it. As the magnitudes of the $|\eta_j|$'s increase, there will be a phase transition every time that $|\eta_j| = |\Delta(r = \infty)|$. Any such transition is characterized by a decrease in the number of Majorana fermions by one unit and a corresponding change in the value of the Chern number by ± 1, depending on the sign of η_j. Therefore, by changing the Chern number of the system by ± 1 each time, one can knock out the Majorana fermions one by one.

Alternatively, one could start from the dominant Haldane masses limit defined by

$|\eta_j| > |\Delta(r=\infty)|$ with $j = 1, 2, 3, 4$. In this limit, the system sustains the *thermal* integer quantum Hall effect (IQHE) and supports four chiral Majorana fermions. [43]

One can then change $\boldsymbol{h}$ so as to cross successive quantum phase transitions at which any one of the $\eta_1, \ldots, \eta_4$ equals in magnitude the spectral gap controlled by $|\Delta(r=\infty)|$. As before, each time we cross a phase transition, the Chern number and hence the number of Majorana fermions at a SC vortex core changes.

We note that the presence of a nearest-neighbor-hopping dispersion

$$\epsilon(\boldsymbol{p}) = -2t(\cos p_x + \cos p_y) \tag{2.11}$$

with $t \ll \alpha$ is equivalent to adding a constant chemical potential

$$\mu_j \equiv \epsilon(\boldsymbol{p}_j) \tag{2.12}$$

for each one of the four Fermi momenta, Eq. (2.2). The effect of this term is to shift the gap closing condition to

$$|\eta_j| = \sqrt{|\Delta|^2 + \mu_j^2}, \tag{2.13}$$

i.e., our results can be generalized to systems with quadratic dispersions and naturally explain the results found in Ref. [105].

2.3 Tuning the number of Majorana fermions in graphene

We are now going to demonstrate that the very same control on the number of Majorana fermions achieved with Hamiltonian (2.9) is also possible in graphene. We recall that in graphene, electrons with spin s $=\uparrow, \downarrow$ hop on a honeycomb lattice that

is made of two triangular sublattices A and B. The conduction and valence bands touch at the two non-equivalent points $\boldsymbol{K}_{\pm}$ located at the opposite corners in the hexagonal first Brillouin zone (see Ref. [82] for a review). Finally, to account for the possibility of a SC instability, Nambu doublets are introduced with the index p and h to distinguish particles from their charge conjugate (holes). Hence, after linearization of the spectrum about the Fermi points $\boldsymbol{K}_{\pm}$, this leads to a single-particle kinetic energy represented by a 16×16-dimensional matrix

$$\mathcal{H}_{\mathrm{D}} := \alpha_1 p_1 + \alpha_2 p_2. \tag{2.14}$$

Here, α_1 and α_2 are two 16×16-dimensional Dirac matrices.

It was shown in Ref. [98] that there exists 36 distinct order parameters such that any one, when added to $\mathcal{H}_{\mathrm{D}}$, opens a spectral gap. These order parameters are identified by seeking all 16×16 matrices from the Clifford algebra that anticommute with $\mathcal{H}_{\mathrm{D}}$. One complex valued order parameter is that for singlet superconductivity. We shall denote the two corresponding 16×16 matrices from the Clifford algebra by M_{ReSSC} and M_{ImSSC} and define the perturbation

$$\mathcal{H}_{\Delta} := \Delta_1 M_{\mathrm{ReSSC}} + \Delta_2 M_{\mathrm{ImSSC}} \tag{2.15}$$

that opens the spectral gap $2|\Delta|$ with the complex-valued

$$\Delta \equiv \Delta_1 + i\Delta_2 \tag{2.16}$$

parametrized by the real-valued Δ_1 and Δ_2 when added to $\mathcal{H}_{\mathrm{D}}$. Next, we seek all 16×16 matrices from the Clifford algebra that (i) anticommute with $\mathcal{H}_{\mathrm{D}}$ and (ii) commute with $\mathcal{H}_{\Delta}$. In this way, we find all ten TRS-breaking order parameters

Table 2.1: The ten mass matrices with PHS that anticommute with α_1 and α_2 and commute with the singlet SC masses M_{ReSSC} and M_{ImSSC}. Each mass matrix can be assigned an order parameter for the underlying microscopic model. The latin subindex of the order parameter's name corresponds to the preferred quantization axis in SU(2) spin space. Each mass matrix either preserves or breaks TRS, SRS, and sublattice symmetry (SLS). Each mass matrix can be written as a tensor product $X_{\mu_1\mu_2\mu_3\mu_4} \equiv \rho_{\mu_1} \otimes s_{\mu_2} \otimes \sigma_{\mu_3} \otimes \tau_{\mu_4}$, where ρ_{μ_1}, s_{μ_2}, σ_{μ_3}, and τ_{μ_4} correspond to unit 2×2 and Pauli matrices that act on particle-hole, spin-1/2, valley, and sublattice indices, respectively.

Order parameter	TRS	SRS	SLS	Here	$X_{\mu_1\mu_2\mu_3\mu_4}$
IQHE	False	True	False	M_{IQHE}	X_{3003}
ReVBS_x	False	False	True	M_{ReVBS_x}	X_{3110}
ReVBS_y	False	False	True	M_{ReVBS_y}	X_{0210}
ReVBS_z	False	False	True	M_{ReVBS_z}	X_{3310}
ImVBS_x	False	False	True	M_{ImVBS_x}	X_{0120}
ImVBS_y	False	False	True	M_{ImVBS_y}	X_{3220}
ImVBS_z	False	False	True	M_{ImVBS_z}	X_{0320}
$\mathrm{Néel}_x$	False	False	False	$M_{\mathrm{Néel}_x}$	X_{3133}
$\mathrm{Néel}_y$	False	False	False	$M_{\mathrm{Néel}_y}$	X_{0233}
$\mathrm{Néel}_z$	False	False	False	$M_{\mathrm{Néel}_z}$	X_{3333}

listed in Table 2.1 that alone would open a gap in the Dirac spectrum if not for their competition with the gap induced by singlet superconductivity. Within this set of ten matrices one can form groups of at most four matrices that are mutually commuting and therefore can be simultaneously diagonalized. Here, we choose the four-tuplet $\{\mathrm{ReVBS}_x, \mathrm{ImVBS}_y, \mathrm{Néel}_z, \mathrm{IQHE}\}$ for concreteness but the results hereafter apply to any other such four-tuplet of commuting mass matrices among the set of ten. Our main result regarding graphene is the fact that

$$\begin{aligned}\mathcal{H} &= \boldsymbol{p}\cdot\boldsymbol{\alpha} + \Delta_1 M_{\mathrm{ReSSC}} + \Delta_2 M_{\mathrm{ImSSC}} \\ &\quad + m_1 M_{\mathrm{ReVBS}_x} + m_2 M_{\mathrm{ImVBS}_y} \\ &\quad + m_3 M_{\mathrm{Néel}_z} + \eta M_{\mathrm{IQHE}} \end{aligned} \tag{2.17a}$$

is unitarily similar to Eqs. (2.9a) and (2.9b) with

$$\delta_{1,2,3,4} \equiv \Delta, \tag{2.17b}$$

$$\eta_1 \equiv -m_1 + m_2 + m_3 + \eta, \tag{2.17c}$$

$$\eta_2 \equiv \ m_1 - m_2 + m_3 + \eta, \tag{2.17d}$$

$$\eta_3 \equiv \ m_1 + m_2 - m_3 + \eta, \tag{2.17e}$$

$$\eta_4 \equiv -m_1 - m_2 - m_3 + \eta. \tag{2.17f}$$

The phase diagram in Figure 2.2 follows.

There is a total of four SC pair potentials that open a uniform gap at $\boldsymbol{K}_\pm$ in graphene. [98] One is the singlet SC pair potential, which we have discussed so far and the remaining three are all triplet SC pair potentials. For each such triplet SC mass, as in the singlet SC, there are four competing orders that commute pairwise

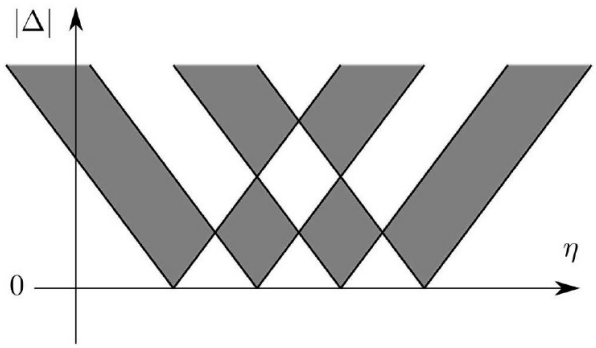

Figure 2.2: Schematic phase diagram of the competition between the singlet SC (Δ), thermal IQH (η), magnetic bond ($m_{1,2}$), and Néel (m_3) orders near the Dirac point in graphene. Here, $m_{1,2,3}$ are fixed while $|\eta|$ and $|\Delta|$ vary. When $m_{1,2,3} = 0$, there are three phases (two large $|\eta|$ phases with $\eta > 0$ and $\eta < 0$ and one large $|\Delta|$ phase, according to Ref. [98]). If we choose $m_{1,2,3}$ in such a way that $m_1 + m_2 + m_3$, $m_1 + m_2 - m_3$, $-m_1 + m_2 - m_3$, and $-m_1 - m_2 + m_3$ are all different, there are 15 phases as we change η and Δ. Shaded (nonshaded) regions represent a phase with the odd (even) Chern number. In phases that are adiabatically connected to a nonsuperconducting state (the horizontal axis $|\Delta| = 0$), one can switch off the pairing without closing the gap. In these phases, the number of Majorana fermions is thus even.

and can be used, in principle, to knock out one by one Majorana fermions bound to the cores of isolated vortices.

2.4 Zero modes and non-Abelian statistics

Consider the 4×4 Hamiltonian (2.9b) in the limit $\eta_j = 0$.

$$\mathcal{H} = \begin{pmatrix} 0 & \partial_+ & \Delta(\boldsymbol{r}) & 0 \\ \partial_- & 0 & 0 & \Delta(\boldsymbol{r}) \\ \overline{\Delta}(\boldsymbol{r}) & 0 & 0 & -\partial_+ \\ 0 & \overline{\Delta}(\boldsymbol{r}) & -\partial_- & 0 \end{pmatrix} \tag{2.18}$$

where $\partial_\pm \equiv -\mathrm{i}(\partial_x \pm \partial_y)$. Let

$$\mathcal{H}\,\Phi(\boldsymbol{r}) = 0, \tag{2.19}$$

be the zero mode equation with $\Phi(\boldsymbol{r}) = (\,\tilde{u}(\boldsymbol{r}), u(\boldsymbol{r}), v(\boldsymbol{r}), \tilde{v}(\boldsymbol{r})\,)$. Eq. (2.19) reduces to the pair of equations for (u, v)

$$\partial_+ u(\boldsymbol{r}) + \Delta(\boldsymbol{r}) v(\boldsymbol{r}) = 0 \tag{2.20a}$$

$$\overline{\Delta}(\boldsymbol{r}) u(\boldsymbol{r}) - \partial_- v(\boldsymbol{r}) = 0, \tag{2.20b}$$

and another equivalent pair of equations for $(\tilde{u}, \tilde{v})$. Eqs. (2.20) have the property that a change of the phase of the order parameter by $\Delta \to e^{\,\mathrm{i}\phi}\Delta$ transforms the eigenmodes by

$$u \to e^{\,\mathrm{i}\phi/2} u, \quad v \to e^{\,-\mathrm{i}\phi/2} v, \tag{2.21}$$

implying that for a change of phase $\phi = 2\pi$, the eigenmodes transform as $(u, v) \to (-u, -v)$. For a vortex at the origin $r = 0$, i.e., $\Delta(\boldsymbol{r}) = \Delta_0(r)\, e^{\,-\mathrm{i}\theta}$, there is a single normalizable solution of Eqs. (2.20) which is exponentially localized at the vortex core, satisfying $v = \overline{u}$, while no normalizable solution exists for the pair of equations satisfied by $(\tilde{u}, \tilde{v})$. [57] The fermionic operator representing this zero mode is expressed as

$$\gamma = \int \mathrm{d}^2\boldsymbol{r}\, \left(u(\boldsymbol{r}) c + \overline{u}(\boldsymbol{r}) c^\dagger\right) \tag{2.22}$$

and, thus, is a Majorana fermion, since $\gamma = \gamma^\dagger$. As shown by Ivanov [54], as a consequence of the transformations (2.21), the braiding of two vortices, each supporting Majorana fermions γ_1 and γ_2 satisfying the anti-commutation relation $\{\,\gamma_i, \gamma_j\,\} = 2\delta_{ij}$, induces the transformation

$$\gamma_1 \to \gamma_2, \quad \gamma_2 \to -\gamma_1. \tag{2.23}$$

As shown in Ref. [54] the unitary transformation

$$\mathcal{U}_{12} \equiv e^{\frac{\pi}{4}\gamma_1\gamma_2} \tag{2.24}$$

implements (2.23). Braiding operations in a degenerate system with N Majorana fermions sufficiently far from each other are represented by successive unitary transformations of the form $\mathcal{U}_{ij}$, for $i, j = 1, ..., N$ acting on the degenerate subspace of the zero modes. Since these unitary transformation do not commute, the order in which these braiding transformations are performed matters and this realizes an example of non-Abelian statistics.

Hamiltonian (2.18) also applies to spinless electrons graphene, where Δ has the interpretation of the Kekulé order parameter [52]. As shown in Ref. [52], the zero mode is a complex fermionic mode with fractional charge $e/2$ and is represented by the operator

$$\psi = \int \mathrm{d}^2\boldsymbol{r}\ \left(u(\boldsymbol{r})c_+ + \overline{u}(\boldsymbol{r})c_-\right), \tag{2.25}$$

where $c_\pm$ are annihilation operators of the of the two Dirac cones of graphene's band structure. [82] By virtue of the transformation (2.21) satisfied by the mode functions, the analysis of Ref. [54] still applies leading to the transformation rule

$$\psi_i \to \psi_j, \quad \psi_j \to -\psi_i, \tag{2.26}$$

when two complex fermions ψ_i and ψ_j are braided.

A complex fermion can always be represented by a pair of Majorana operators. For the case of 2 vortices hosting complex fermions ψ_1 and ψ_2, we have

$$\psi_1 = \frac{1}{2}\left(\alpha_1 + \mathrm{i}\,\alpha_2\right) \tag{2.27}$$

$$\psi_2 = \frac{1}{2}\left(\beta_1 + \mathrm{i}\,\beta_2\right) \tag{2.28}$$

where $\{\alpha_i, \alpha_j\} = \{\beta_i, \beta_j\} = 2\delta_{ij}$, $\{\alpha_i, \beta_j\} = 0$, $\alpha_i^\dagger = \alpha_i$ and $\beta_i^\dagger = \beta_i$. It follows then that the unitary transformation

$$\mathbb{U}_{12} \equiv e^{\frac{\pi}{4}\alpha_2\beta_2}\, e^{\frac{\pi}{4}\alpha_1\beta_1} = e^{\frac{\pi}{4}\left(\psi_1^\dagger - \psi_1\right)\left(\psi_2^\dagger - \psi_2\right)}\, e^{\frac{\pi}{4}\left(\psi_1^\dagger + \psi_1\right)\left(\psi_2^\dagger + \psi_2\right)} \tag{2.29}$$

implements the transformation (2.26). Similar to the case of superconductors, the brading operations in a set of N complex zero modes would be realized by the unitary transformations $\mathbb{U}_{ij}$ of the form (2.29), for $i, j = 1, ..., N$, and would provide a realization of non-Abelian statistics. There is, however, an important physical distinction between these two cases, for, in a superconductor the Majorana modes are protected by particle-hole symmetry of the mean-field superconductor state, while in the charge conserving case considered in Ref. [52], perturbations which break the symmetry between positive and negative energy states are able to lift the energy of the zero mode and thus cause the degeneracy of the zero mode subspace to be less robust than in a superconductor.

2.5 Conclusions

In summary, we have identified a mechanism to overcome the fermion-doubling barrier that can prevent the attachment of an odd number of Majorana fermions to the core of SC vortices in graphenelike tight-binding models. This mechanism relies on a $\mathbb{Z}_2 \times \mathbb{Z}_2$ topological charge that measures the parity in the number of Majorana fermions attached to an isolated vortex and the use of TRS-breaking order parameters that compete with each other and with the SC order parameter to knock out one by one the Majorana fermions. In this surgical way, an odd number of Majorana fermions

can be made to bind the vortices in a singlet SC order parameter, whereas this could only be achieved for the more elusive triplet SC order parameter in Refs. [94, 93], [54], and [104]. This mechanism applies to graphene with superconductivity induced by the proximity effect, provided a way can be found to also induce and select from the remarkably large variety of coexisting and competing order parameters that graphene supports those with odd $\mathbb{Z}_2 \times \mathbb{Z}_2$ topological charge and thus odd number of Majorana fermions attached to isolated vortices.

Chapter 3

Counting Majorana zero modes in superconductors

Abstract

A counting formula for computing the number of (Majorana) zero modes bound to topological point defects is evaluated in a gradient expansion for systems with charge-conjugation symmetry. This semi-classical counting of zero modes is applied to some examples that include graphene and a chiral p-wave superconductor in two-dimensional space. In all cases, we explicitly relate the counting of zero modes to Chern numbers.

3.1 Introduction

The counting of zero modes, eigenstates annihilated by a single-particle Hamiltonian $\mathcal{H}$, has a long history in physics. Charge-conjugation symmetry, the existence of a norm-preserving linear or anti-linear transformation $\mathcal{C}$ that anticommutes with $\mathcal{H}$,

protects the parity of the number of zero modes. When the parity is odd, at least one zero mode must be robust to any perturbation that preserves the charge-conjugation symmetry. This chapter aims at calculating the parity of zero modes of a single-particle Hamiltonian $\mathcal{H}\big(\hat{\boldsymbol{p}}, \boldsymbol{\varphi}(\boldsymbol{x})\big)$ when (1) it obeys charge-conjugation symmetry, (2) it describes fermionic quasiparticles, and (3) it depends on a position dependent order parameter $\boldsymbol{\varphi}(\boldsymbol{x})$. These three assumptions are often met in mean-field treatments of electrons interacting with each other or with collective excitations such as phonons or magnons in condensed matter physics.

Zero mode solutions can be found by direct means, in practice solving a differential equation. This requires a non-universal definition of the model since both microscopic and macroscopic data must be supplied, say the boundary conditions to be obeyed at the origin and at infinity in space.

Is there an alternative approach to calculating the parity in the number of zero modes that is more universal? The celebrated index theorem for elliptic differential operators gives a positive answer to this question for those problems in physics for which this theorem applies (Dirac Hamiltonians for example). [5, 76, 35] The index theorem achieves this by relating some (not all!) zero modes to a topological number (a global property of the Hamiltonian that can only take integer values). However, the index theorem cannot be applied to most Hamiltonians of relevance to condensed matter physics.

In this chapter, we start from an exact integral representation of the total number of *unoccupied* [1] zero modes (up to exponential accuracy) N for fermionic single-

[1]The assumption underlying this statement, here and throughout this chapter, is that the chemical potential is chosen to be arbitrarily small and negative ($\mu = 0^-$) so that all the zero mode states

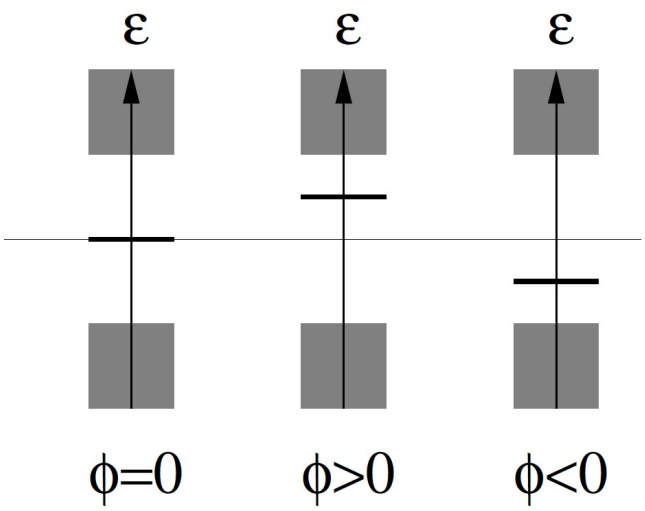

Figure 3.1: The charge-conjugation-symmetry-breaking parameter ϕ moves in energy a mid-gap state upward or downward depending on its sign. The continuum parts of the energy-eigenvalue spectrum are denoted by the shaded boxes. The thin horizontal line denotes the band center about which the spectrum is symmetric when $\phi = 0$.

particle Hamiltonians with charge-conjugation symmetry in terms of a charge Q,

$$N = -2Q. \tag{3.1}$$

This counting formula appears implicitly in Ref. [112] and explicitly in Ref. [58], both in the context of polyacetylene. [139] For polyacetylene, it relates the number of unoccupied zero modes to the *conserved electric charge* Q_{dw} induced by domain walls in the spontaneous bond ordering triggered by the coupling of electrons to phonons. Remarkably, the electric charge $Q_{\mathrm{dw}} = \pm 1/2$ induced by a single domain wall is fractional and counts a single zero mode, with the sign ambiguity resolved by whether the midgap state is filled or empty. [56, 113, 114] Alternatively, this sign ambiguity

are above the chemical potential. In this situation, the charge induced by each of these unoccupied states is $Q = -1/2$.

can be removed by the application of a small charge-conjugation-symmetry-breaking perturbation that shifts the energy of the zero mode up or down (see Figure 3.1). Hence, the counting formula (3.1) becomes

$$N = 2Q \bmod 2 \tag{3.2}$$

if no prescription is given as to whether the filled Fermi sea includes or not a zero mode. The same assignment of quantum numbers also relates a single zero mode and the conserved electric charge Q_{Kekule} induced by a vortex with unit vorticity in the Kekulé dimerization pattern of graphene. [52, 55, 14, 15, 98]

For polyacetylene and graphene, the charge-conjugation symmetry is approximate, for it originates from a sublattice symmetry that is broken as soon as next-nearest-neighbor hopping is included in the tight-binding model. To the extend that the Bardeen-Cooper-Schrieffer (BCS) mean-field approximation to superconductivity is empirically observed to be excellent, single-particle Bogoliubov-de-Gennes (BdG) Hamiltonians realize a much more robust charge-conjugation symmetry. For BdG Hamiltonians, zero modes are associated to Majorana fermions. Majorana fermions do not carry a well-defined electric charge since global electro-magnetic gauge invariance is broken in any mean-field treatment of superconductivity. The counting formula (3.1) nevertheless applies to any BdG Hamiltonian $\mathcal{H}_{\text{BdG}}$ with the important caveat that the conserved quasiparticle charge Q_{BdG} is unrelated to the electric charge. Rather, the conservation of Q_{BdG} encodes, for any local BdG Hamiltonian, a local continuity equation obeyed by the Bogoliubov quasiparticles that is responsible for the conservation of the thermal flow in the mean-field treatment of superconductivity. [1, 108, 107]

In this chaper, we represent the counting formula (3.1) in terms of single-particle Green functions. The advantage of this choice is that it easily lends itself to a perturbative (gradient) expansion of the conserved quasiparticle charge Q that forgoes the non-universal short-distance data. [85, 124, 125] To leading order, this expansion is akin to an adiabatic approximation. We thus propose the adiabatic approximation to the conserved quasiparticle charge Q as an efficient mean to compute the parity in the number N of unoccupied zero modes of charge-conjugation-symmetric single-particle Hamiltonians.

We then apply this formula to charge-conjugation-symmetric Dirac insulators with time-reversal symmetry in arbitrary dimensions and chiral p-wave BdG superconductor in two-dimensional space that all support a point defect. One of the main results of this chapter is an integral representation for the number (zero or one) of unoccupied zero mode induced by a unit vortex in a two-dimensional chiral p-wave BdG superconductor. A by-product of this integral representation is that it is closely related to *the second Chern number*. We also relate *the d-th Chern number* to the number of unoccupied zero modes for Dirac fermions in d-dimensional space that interact with a d-tuplet of Higgs field supporting point defects.

The gradient expansion is presented in Sec. 3.2 and applied to point defects in Sec. 3.3. We conclude in Sec. 3.4.

3.2 Gradient expansion of the counting formula

Let the charge-conjugation-symmetric single-particle Hamiltonian $\mathcal{H}\big(\hat{\boldsymbol{p}}, \boldsymbol{\varphi}(\boldsymbol{x})\big)$ be such that its dependence on the space coordinate

$$\boldsymbol{x} \in \mathbb{R}^d \tag{3.3}$$

is implicit through that of a static vector-valued order parameter

$$\boldsymbol{\varphi}(\boldsymbol{x}) \in \mathbb{R}^D, \tag{3.4}$$

while its dependence on the canonical momentum

$$\hat{\boldsymbol{p}} \equiv -\mathrm{i}\boldsymbol{\partial} \equiv -\mathrm{i}\frac{\partial}{\partial \boldsymbol{x}} \tag{3.5}$$

is explicit. (We have chosen natural units, i.e., $\hbar = 1$.)

The single-particle Hamiltonian in second quantization reads

$$\widehat{H} = \int\limits_{\boldsymbol{x}} \widehat{\Psi}^\dagger(\boldsymbol{x})\, \mathcal{H}\big(\hat{\boldsymbol{p}}, \boldsymbol{\varphi}(\boldsymbol{x})\big)\, \widehat{\Psi}(\boldsymbol{x}). \tag{3.6a}$$

The creation operators $\widehat{\Psi}^\dagger(\boldsymbol{x})$ and the annihilation operators $\widehat{\Psi}(\boldsymbol{x})$ obey here the fermion algebra

$$\begin{aligned} \Big\{ \widehat{\Psi}_r(\boldsymbol{x}), \widehat{\Psi}^\dagger_{r'}(\boldsymbol{x}') \Big\} &= \delta_{r,r'} \delta(\boldsymbol{x} - \boldsymbol{x}'), \\ \Big\{ \widehat{\Psi}_r(\boldsymbol{x}), \widehat{\Psi}_{r'}(\boldsymbol{x}') \Big\} &= 0, \qquad r, r' = 1, \cdots, R, \end{aligned} \tag{3.6b}$$

in some R-dimensional representation of the charge-conjugation-symmetric single-particle Hamiltonian

$$\mathcal{H}\big(\hat{\boldsymbol{p}}, \boldsymbol{\varphi}(\boldsymbol{x})\big) = -\, \mathcal{C}^{-1}\, \mathcal{H}\big(\hat{\boldsymbol{p}}, \boldsymbol{\varphi}(\boldsymbol{x})\big)\, \mathcal{C}. \tag{3.6c}$$

The norm-preserving operation for charge conjugation in the R-dimensional single-particle representation is denoted by $\mathcal{C}$. The short-hand notation $\int\limits_{\boldsymbol{x}}$ stands for the space integration $\int \mathrm{d}^d\boldsymbol{x}$. The quasi-particle charge is measured with respect to a fixed background state.

We begin with an expression for a quasiparticle charge density in the vicinity of a point $\boldsymbol{x}$. To do so, we shall assume that the static vector-valued order parameter can be decomposed additively, i.e.,[2]

$$\boldsymbol{\varphi}(\boldsymbol{x}) = \boldsymbol{\varphi}_0 + \delta\boldsymbol{\varphi}(\boldsymbol{x}), \tag{3.7}$$

in such a way that:

- (i) the single-particle Hamiltonian

$$\mathcal{H}_0(\hat{\boldsymbol{p}}) \equiv \mathcal{H}\big(\hat{\boldsymbol{p}}, \boldsymbol{\varphi}_0\big) \tag{3.8}$$

  is translation invariant,

- (ii) the single-particle eigenvalue spectrum of $\mathcal{H}_0(\hat{\boldsymbol{p}})$ is fully gaped with the gap $2\Delta_0 > 0$,

- (iii) the changes between $\delta\boldsymbol{\varphi}(\boldsymbol{x})$ and $\delta\boldsymbol{\varphi}(\boldsymbol{y})$ when $\boldsymbol{x}$ and $\boldsymbol{y}$ are a distance of order $1/\Delta_0$ apart are small.

Condition (iii) implies that the gradient of $\delta\boldsymbol{\varphi}(\boldsymbol{x})$ can be viewed as a smooth and small perturbation that can be treated perturbatively in the gradient expansion that will follow shortly.

[2]This additive decomposition is very similar to the spin-wave approximation. It is only valid locally and fails to capture the non-trivial topology of a defect such as a vortex. However, we will remedy this difficulty by the introduction of an additional charge-symmetry-breaking component to the Higgs multiplet for which this additive decomposition becomes meaningful globally.

Condition (i) implies that

$$\widehat{H}_0 \equiv \int\limits_{\boldsymbol{x}} \widehat{\Psi}^\dagger(\boldsymbol{x})\, \mathcal{H}_0(\hat{\boldsymbol{p}})\, \widehat{\Psi}(\boldsymbol{x}) = \int\limits_{\boldsymbol{p}} \widehat{\Psi}^\dagger(\boldsymbol{p})\, \mathcal{H}_0(\boldsymbol{p})\, \widehat{\Psi}(\boldsymbol{p}) \tag{3.9a}$$

with the symmetric Fourier conventions

$$\begin{aligned} \widehat{\Psi}^\dagger(\boldsymbol{x}) &= (2\pi)^{+d/2} \int\limits_{\boldsymbol{p}} e^{-\mathrm{i}\boldsymbol{p}\cdot\boldsymbol{x}}\, \widehat{\Psi}^\dagger(\boldsymbol{p}), \\ \widehat{\Psi}^\dagger(\boldsymbol{p}) &= (2\pi)^{-d/2} \int\limits_{\boldsymbol{x}} e^{+\mathrm{i}\boldsymbol{p}\cdot\boldsymbol{x}}\, \widehat{\Psi}^\dagger(\boldsymbol{x}), \end{aligned} \tag{3.9b}$$

for the annihilation (creation) operators and the asymmetric convention

$$\begin{aligned} \mathcal{K}(\boldsymbol{x}) &= \int\limits_{\boldsymbol{p}} e^{+\mathrm{i}\boldsymbol{p}\cdot\boldsymbol{x}} \mathcal{K}(\boldsymbol{p}), \\ \mathcal{K}(\boldsymbol{p}) &= \int\limits_{\boldsymbol{x}} e^{-\mathrm{i}\boldsymbol{p}\cdot\boldsymbol{x}} \mathcal{K}(\boldsymbol{x}), \end{aligned} \tag{3.9c}$$

for any kernel $\mathcal{K}$ (such as the Hamiltonian $\mathcal{H}$). Here, $\int\limits_{\boldsymbol{p}}$ is a short-hand notation for the momentum-space integration $\int \mathrm{d}^d\boldsymbol{p}/(2\pi)^d$.

Condition (ii) implies the existence of the characteristic length scale $1/\Delta_0$.

Define the quasiparticle charge density

$$\rho_\gamma(\boldsymbol{x}) \equiv \int\limits_\gamma \frac{\mathrm{d}\omega}{2\pi} \left\langle \boldsymbol{x} \left| \mathrm{tr}_R \left[\mathcal{G}(\omega) - \mathcal{G}_0(\omega) \right] \right| \boldsymbol{x} \right\rangle . \tag{3.10a}$$

Here, tr_R denotes the trace over the R-dimensional degrees of freedom and we have introduced the Euclidean single-particle Green functions

$$\mathcal{G}(\omega) = \frac{1}{\mathrm{i}\omega - \mathcal{H}}, \qquad \mathcal{G}_0(\omega) = \frac{1}{\mathrm{i}\omega - \mathcal{H}_0}. \tag{3.10b}$$

The quasiparticle charge density $\rho_\gamma(\boldsymbol{x})$ depends on the contour of integration γ. The latter is chosen as in Appendix A.1 so that the integration over the ω-complex plane

picks up *only the first-order poles from the non-vanishing and negative energy eigenvalues* of $\mathcal{H}$ and of $\mathcal{H}_0$ [see Eq. (A.15)].

It is shown in Appendix A.1 [see Eq. (A.16c)] that Eq. (3.6c) and condition (ii) imply that the *total number N of unoccupied zero modes* of $\mathcal{H}$ is related to the charge Q_γ by

$$\frac{N}{2} = -\int \mathrm{d}^d\boldsymbol{x}\, \rho_\gamma(\boldsymbol{x}) \equiv -Q_\gamma. \tag{3.11}$$

According to the counting formula (3.11), computing N reduces to computing the conserved quasiparticle charge Q_γ induced by the smooth variation of $\delta\boldsymbol{\varphi}(\boldsymbol{x})$ through space defined in Eq. (3.3). The counting formula (3.11) appears implicitly in Ref. [112] and explicitly in Ref. [58].

There is an alternative to specifying γ in the counting formula (3.11). We can regulate the first-order pole of the Green function $\mathcal{G}(\omega)$ at $\omega = 0$ by adding a perturbation that moves all zero modes to strictly positive energies. This perturbation must be small if all these positive energy increments are to remain much smaller than the threshold Δ_0 to the continuum. We can then safely replace the contour of integration γ in the counting formula (3.11) by $\mathbb{R}$ since the subtraction of $\mathcal{G}_0$ from $\mathcal{G}$ insures the convergence of the ω integration for large ω.

For example, we imagine that it is possible to augment the vector-valued order parameter (3.7) by the conjugation-symmetry-breaking real-valued field ϕ without

loosing conditions (i)-(iii). More precisely, we define the $(D+1)$-tuplet

$$\boldsymbol{\phi}(\boldsymbol{x}) \equiv \begin{pmatrix} \phi_1(\boldsymbol{x}) \\ \vdots \\ \phi_D(\boldsymbol{x}) \\ \phi_{D+1} \end{pmatrix} \equiv \begin{pmatrix} \varphi_1(\boldsymbol{x}) \\ \vdots \\ \varphi_D(\boldsymbol{x}) \\ \phi \end{pmatrix} \tag{3.12a}$$

and we assume that Eq. (3.6c) becomes

$$\mathcal{H}\big(\hat{\boldsymbol{p}}, \boldsymbol{\varphi}(\boldsymbol{x}), \phi\big) = -\,\mathcal{C}^{-1}\,\mathcal{H}\big(\hat{\boldsymbol{p}}, \boldsymbol{\varphi}(\boldsymbol{x}), -\phi\big)\,\mathcal{C}. \tag{3.12b}$$

It then follows that

$$Q(\phi) = \int \mathrm{d}^d\boldsymbol{x}\,\rho(\boldsymbol{x}, \phi) = -Q(-\phi) \tag{3.13}$$

where the quasiparticle charge density $\rho(\boldsymbol{x}, \phi)$ is obtained from Eq. (3.10) with $\mathbb{R}$ substituting for γ, Hamiltonian (3.12b) substituting for $\mathcal{H}\big(\hat{\boldsymbol{p}}, \boldsymbol{\varphi}(\boldsymbol{x})\big)$, and $\mathcal{H}_0 \equiv \mathcal{H}\big(\hat{\boldsymbol{p}}, \boldsymbol{\varphi}_0, \phi\big)$ substituting for $\mathcal{H}_0 \equiv \mathcal{H}\big(\hat{\boldsymbol{p}}, \boldsymbol{\varphi}_0\big)$. The smoking gun for the *unoccupied zero modes* is now a discontinuity at the conjugation-symmetric point $\phi = 0$ of the odd function $Q(\phi)$ of ϕ, i.e., the counting formula (3.11) has become

$$\frac{N}{2} = -\lim_{\phi\to 0}\int \mathrm{d}^d\boldsymbol{x}\,\rho(\boldsymbol{x}, \phi) \equiv -\lim_{\phi\to 0} Q(\phi) \tag{3.14}$$

where the sign of ϕ is to be chosen so as to move the N zero modes along the energy axis to positive energies. Furthermore, we can relax the condition that the symmetry breaking ϕ is constant everywhere in space $(\boldsymbol{x})$ provided that the condition

$$\boldsymbol{\phi}^2(\boldsymbol{x}) \approx \boldsymbol{\varphi}_0^2 \equiv \Delta_0^2 \tag{3.15}$$

holds everywhere in $\mathbb{R}^d$. Condition (iii) then means that $\delta\boldsymbol{\phi}(\boldsymbol{x})$ varies slowly on the characteristic length scale $1/\Delta_0$.

Rather than computing $\rho(\boldsymbol{x})$ exactly, say with the help of numerical tools, we are after the leading contribution to the gradient expansion of the quasiparticle charge density $\rho(\boldsymbol{x})$, which we shall denote as $\rho_{\text{adia}}(\boldsymbol{x})$ where the subscript "adia" refers to the adiabatic approximation contained in condition (iii).

The order parameter (3.12a) enters linearly in all the single-particle Hamiltonians that we shall consider explicitly in this chapter. Hence, there follows the additive law

$$\begin{aligned}\mathcal{H}\big(\hat{\boldsymbol{p}}, \boldsymbol{\phi}(\boldsymbol{x})\big) &= \mathcal{H}\big(\hat{\boldsymbol{p}}, \boldsymbol{\phi}_0\big) + \mathcal{V}\big(\hat{\boldsymbol{p}}, \delta\boldsymbol{\phi}(\boldsymbol{x})\big) \\ &\equiv \mathcal{H}_0 + \mathcal{V}\big(\hat{\boldsymbol{p}}, \delta\boldsymbol{\phi}(\boldsymbol{x})\big)\end{aligned} \tag{3.16}$$

upon insertion of

$$\boldsymbol{\phi}(\boldsymbol{x}) = \boldsymbol{\phi}_0 + \delta\boldsymbol{\phi}(\boldsymbol{x}). \tag{3.17}$$

Upon second-quantization, this implies that

$$\widehat{H} = \int_{\boldsymbol{p}} \int_{\boldsymbol{q}} \widehat{\Psi}^\dagger(\boldsymbol{p}) \left[\mathcal{H}_0(\boldsymbol{p})\, \delta(\boldsymbol{p}-\boldsymbol{q}) + \mathcal{V}(\boldsymbol{p};\boldsymbol{q})\right] \widehat{\Psi}(\boldsymbol{q}) \tag{3.18a}$$

holds with

$$\mathcal{V}(\boldsymbol{p};\boldsymbol{q}) = \left(\frac{\partial \mathcal{H}}{\partial \boldsymbol{\phi}}\right)_0 \left(\frac{\boldsymbol{p}+\boldsymbol{q}}{2}\right) \cdot \delta\boldsymbol{\phi}(\boldsymbol{p}-\boldsymbol{q}). \tag{3.18b}$$

The subscript 0 means setting $\delta\boldsymbol{\phi}$ to zero so that the gradient

$$\left(\frac{\partial \mathcal{H}}{\partial \boldsymbol{\phi}}\right)_0 = -\left(\frac{\partial \mathcal{G}^{-1}}{\partial \boldsymbol{\phi}}\right)_0 \tag{3.18c}$$

depends only on the single-particle canonical momentum operator $\hat{\boldsymbol{p}} \equiv -\mathrm{i}\boldsymbol{\partial}$. We have also adopted the convention that matrix elements of $\hat{\boldsymbol{p}}$ are to be symmetrized, i.e.,

$$\left(f^* \hat{\boldsymbol{p}} g\right)(\boldsymbol{x}) \equiv -\frac{\mathrm{i}}{2}\left(f^* \left(\frac{\partial g}{\partial \boldsymbol{x}}\right) - \left(\frac{\partial f^*}{\partial \boldsymbol{x}}\right) g\right)(\boldsymbol{x}) \tag{3.18d}$$

for any differentiable functions f and g.

We now expand the quasiparticle charge density up to the first non-trivial order in an expansion in powers of $\mathcal{V}$ with the help of the geometrical series

$$\mathcal{G}(\omega) - \mathcal{G}_0(\omega) = \sum_{n=1}^{\infty} \left(\mathcal{G}_0(\omega)\mathcal{V}\right)^n \mathcal{G}_0(\omega). \tag{3.19}$$

This gives the expansion

$$\rho(\boldsymbol{x}) = \sum_{n=1}^{\infty} \rho_n(\boldsymbol{x}) \tag{3.20a}$$

with

$$\rho_n(\boldsymbol{x}) = \int\limits_{\omega} \int\limits_{\boldsymbol{p}} \int\limits_{\boldsymbol{q}_1} \cdots \int\limits_{\boldsymbol{q}_n} e^{\mathrm{i}(\boldsymbol{q}_1+\cdots+\boldsymbol{q}_n)\cdot\boldsymbol{x}} \sum_{\mathsf{a}_1,\cdots,\mathsf{a}_n=1}^{D+1} I_{\mathsf{a}_n,\cdots,\mathsf{a}_1}(\omega, \boldsymbol{p}, \boldsymbol{q}_1, \cdots, \boldsymbol{q}_n) \times \delta\phi_{\mathsf{a}_n}(\boldsymbol{q}_n) \cdots \delta\phi_{\mathsf{a}_1}(\boldsymbol{q}_1) \tag{3.20b}$$

where $\int\limits_{\omega} \equiv \int \frac{\mathrm{d}\omega}{2\pi}$ and the integrand

$$\begin{aligned}
&I_{\mathsf{a}_n,\cdots,\mathsf{a}_1}(\omega, \boldsymbol{p}, \boldsymbol{q}_1, \cdots, \boldsymbol{q}_n) \\
&\quad = \mathrm{tr}_R \Bigg[\mathcal{G}_0\left(\omega, \boldsymbol{p} + \boldsymbol{q}_1 + \boldsymbol{q}_2 + \cdots + \boldsymbol{q}_n\right) \\
&\qquad \times \left(\frac{\partial \mathcal{H}}{\partial \phi_{\mathsf{a}_n}}\right)_0 \left(\omega, \boldsymbol{p} + \boldsymbol{q}_1 + \boldsymbol{q}_2 + \cdots + \boldsymbol{q}_{n-1} + \frac{\boldsymbol{q}_n}{2}\right) \\
&\qquad \times \mathcal{G}_0\left(\omega, \boldsymbol{p} + \boldsymbol{q}_1 + \boldsymbol{q}_2 + \cdots + \boldsymbol{q}_{n-1}\right) \\
&\qquad \times \left(\frac{\partial \mathcal{H}}{\partial \phi_{\mathsf{a}_{n-1}}}\right)_0 \left(\omega, \boldsymbol{p} + \boldsymbol{q}_1 + \boldsymbol{q}_2 + \cdots + \boldsymbol{q}_{n-2} + \frac{\boldsymbol{q}_{n-1}}{2}\right) \\
&\qquad \vdots \\
&\qquad \times \mathcal{G}_0\left(\omega, \boldsymbol{p} + \boldsymbol{q}_1\right) \left(\frac{\partial \mathcal{H}}{\partial \phi_{\mathsf{a}_1}}\right)_0 \left(\omega, \boldsymbol{p} + \frac{\boldsymbol{q}_1}{2}\right) \mathcal{G}_0\left(\omega, \boldsymbol{p}\right) \Bigg].
\end{aligned} \tag{3.20c}$$

Finally, we expand the integrand (3.20c) in powers of the coordinates q_{1i_1}, $\cdots$, q_{ni_n} of the momenta $\boldsymbol{q}_1$, $\cdots$, $\boldsymbol{q}_n$, which are then to be integrated over. Condition (iii)

suggests that we keep only first-order derivatives in the slowly varying fluctuations $\delta\boldsymbol{\phi}(\boldsymbol{x})$ of the order parameter (3.7). This approximation yields the leading contribution $\rho_{\text{adia}}(\boldsymbol{x})$ in the gradient expansion of the quasiparticle charge density (3.20a) and becomes exact in the limit when the ratio between the characteristic length scale $1/\Delta_0$ and the characteristic length scale over which the change in $\delta\boldsymbol{\phi}(\boldsymbol{x})$ becomes significant vanishes.

However, to each order n in this expansion there are terms for which not all $\delta\boldsymbol{\phi}(\boldsymbol{x})$ are differentiated. These terms do not have to be small. Hence, they should be treated non-perturbatively. This is achieved by replacing the Euclidean single-particle Green function

$$\mathcal{G}_0(\omega, \boldsymbol{p}) = \frac{1}{\mathrm{i}\omega - \mathcal{H}\big(\boldsymbol{p}, \boldsymbol{\phi}_0\big)} \tag{3.21}$$

with the Euclidean semi-classical Green function

$$\mathcal{G}_{\text{s-c}}(\omega, \boldsymbol{p}, \boldsymbol{x}) = \frac{1}{\mathrm{i}\omega - \mathcal{H}\big(\boldsymbol{p}, \boldsymbol{\phi}(\boldsymbol{x})\big)} \tag{3.22}$$

to any given order n in the expansion (3.20). This result is rooted in the fact that the choice of $\boldsymbol{\phi}_0$ in the additive decomposition (3.17) is arbitrary from the point of view of the expansion (3.20). Such arbitrariness should not appear in the final result, i.e., the final result should only depend on $\boldsymbol{\phi}(\boldsymbol{x})$ or $\partial_i \phi_{\mathsf{a}}(\boldsymbol{x}) \equiv \frac{\partial \phi_{\mathsf{a}}}{\partial x^i}(\boldsymbol{x})$ with $\mathsf{a} = 1, \cdots, d+1$ and $i = 1, \cdots, d$.

Thus, by collecting the appropriate derivatives of the spatially varying order parameter $\delta\boldsymbol{\phi}(\boldsymbol{x})$, we arrive at expressions for the induced quasiparticle charge density. We now analyze this expression according to which term is the first non-vanishing contribution to the expansion.

When the adiabatic approximation for the quasiparticle charge density is the non-vanishing $n = 1$ term in the gradient expansion, it is given by

$$\rho_{\text{adia}}(\boldsymbol{x}) = \mathcal{I}_{i_1\mathsf{a}_1}(-\mathrm{i})\left(\partial_{i_1}\phi_{\mathsf{a}_1}\right)(\boldsymbol{x}). \tag{3.23a}$$

Here, the summation convention is assumed over repeated indices and the coefficients are given by

$$\mathcal{I}_{i_1\mathsf{a}_1} = \int_\omega \int_{\boldsymbol{p}} \frac{1}{2}\mathrm{tr}_R\left(\left[\frac{\partial\mathcal{G}^{-1}}{\partial\phi_{\mathsf{a}_1}}, \frac{\partial\mathcal{G}}{\partial p_{i_1}}\right]\mathcal{G}\right)_0(\omega, \boldsymbol{p}). \tag{3.23b}$$

The subscript 0 refers to the semi-classical Green function (3.22). This case is the relevant one for the study of point defects in one-dimensional space.

When the first non-vanishing contribution to the adiabatic expansion occurs at $n = 2$, then the quasiparticle charge density contains two gradients and is given by

$$\rho_{\text{adia}}(\boldsymbol{x}) = \mathcal{I}_{i_2\mathsf{a}_2 i_1\mathsf{a}_1}(-\mathrm{i})^2\left(\partial_{i_2}\phi_{\mathsf{a}_2}\right)\left(\partial_{i_1}\phi_{\mathsf{a}_1}\right)(\boldsymbol{x}). \tag{3.24a}$$

By assumption, $\mathcal{I}_{i_1\mathsf{a}_1}$ defined by Eq. (3.23b) vanishes, but

$$\begin{aligned}\mathcal{I}_{i_2\mathsf{a}_2 i_1\mathsf{a}_1} = -\int_\omega \int_{\boldsymbol{p}} \frac{1}{2}\mathrm{tr}_R\Bigg(& 2\frac{\partial\mathcal{G}}{\partial p_{i_2}}\frac{\partial\mathcal{G}^{-1}}{\partial\phi_{\mathsf{a}_2}}\mathcal{G}\frac{\partial\mathcal{G}^{-1}}{\partial\phi_{\mathsf{a}_1}}\frac{\partial\mathcal{G}}{\partial p_{i_1}} + \mathcal{G}\frac{\partial^2\mathcal{G}^{-1}}{\partial p_{i_2}\partial\phi_{\mathsf{a}_2}}\mathcal{G}\frac{\partial\mathcal{G}^{-1}}{\partial\phi_{\mathsf{a}_1}}\frac{\partial\mathcal{G}}{\partial p_{i_1}} \\ &+ \frac{\partial\mathcal{G}}{\partial p_{i_2}}\frac{\partial\mathcal{G}^{-1}}{\partial\phi_{\mathsf{a}_2}}\mathcal{G}\frac{\partial^2\mathcal{G}^{-1}}{\partial p_{i_1}\partial\phi_{\mathsf{a}_1}}\mathcal{G}\Bigg)_0(\omega, \boldsymbol{p})\end{aligned} \tag{3.24b}$$

does not. Again, the summation convention is assumed over repeated indices and the subscript 0 refers to the semi-classical Green function (3.22). We have chosen to represent Eq. (3.24) so as to make the reality of $\rho_{\text{adia}}(\boldsymbol{x})$ manifest. This case is the relevant one for the study of point defects in two-dimensional space.

Observe that, whenever $n > 1$, we must allow for the possibility that

$$\frac{\partial^2\mathcal{H}}{\partial p_i\partial\phi_{\mathsf{a}}} \equiv -\frac{\partial^2\mathcal{G}^{-1}}{\partial p_i\partial\phi_{\mathsf{a}}} \tag{3.25}$$

is non-vanishing for some $i = 1, \cdots, d$ and some $\mathsf{a} = 1, \cdots, D+1$. These terms occur when dealing with a p-wave superconductor in $d = 2$ dimensions as we do in Sec. 3.3.2; however, we find by explicit calculation that these terms vanish upon integration over ω and $\boldsymbol{p}$.

When the order parameter is independent of momentum,

$$\frac{\partial^2 \mathcal{H}}{\partial p_i \partial \phi_{\mathsf{a}}} \equiv -\frac{\partial^2 \mathcal{G}^{-1}}{\partial p_i \partial \phi_{\mathsf{a}}} = 0 \tag{3.26a}$$

for any $i = 1, \cdots, d$ and any $\mathsf{a} = 1, \cdots, D+1$. For example this is the case with $D = d$ for Dirac fermions in d-dimensional space interacting with $(d+1)$ real-valued Higgs fields, in which case it is the coefficient

$$\mathcal{I}_{i_n \mathsf{a}_n \cdots i_1 \mathsf{a}_1} = -\,\mathrm{i} \int\limits_{\omega} \int\limits_{\boldsymbol{p}} \mathrm{tr}_R \left[\left(\mathcal{G} \frac{\partial \mathcal{G}^{-1}}{\partial p_{i_n}} \mathcal{G} \frac{\partial \mathcal{G}^{-1}}{\partial \phi_{\mathsf{a}_n}} \right) \cdots \left(\mathcal{G} \frac{\partial \mathcal{G}^{-1}}{\partial p_{i_1}} \mathcal{G} \frac{\partial \mathcal{G}^{-1}}{\partial \phi_{\mathsf{a}_1}} \right) \left(\mathcal{G} \frac{\partial \mathcal{G}^{-1}}{\partial \omega} \right) \right]_0 (\omega, \boldsymbol{p}) \tag{3.26b}$$

that controls the adiabatic approximation to n-th order through

$$\rho_{\mathrm{adia}}(\boldsymbol{x}) = (-\mathrm{i})^d \mathcal{I}_{i_n \mathsf{a}_n \cdots i_1 \mathsf{a}_1} \left(\partial_{i_n} \phi_{\mathsf{a}_n} \right) \cdots \left(\partial_{i_1} \phi_{\mathsf{a}_1} \right) (\boldsymbol{x}) \tag{3.26c}$$

as we shall show in Sec. 3.3.3. The subscript 0 refers to the semi-classical Green function (3.22).

Finally, with the expression for the *local* quasiparticle charge density $\rho_{\mathrm{adia}}(\boldsymbol{x})$ within the adiabatic approximation in hand, we can compute the *total* quasiparticle charge Q_{adia}. Naturally, one goes from the local density to the total charge by integrating the former over all space. We conclude that

$$\begin{aligned} Q_{\mathrm{adia}} &= \int \mathrm{d}^d x \, \rho_{\mathrm{adia}}(\boldsymbol{x}) \\ &= \int \mathrm{d}^d x \, (-\mathrm{i})^d \, \mathcal{I}_{i_n \mathsf{a}_n \cdots i_1 \mathsf{a}_1}(\boldsymbol{x}) \times \left(\partial_{i_n} \phi_{\mathsf{a}_n} \right) \cdots \left(\partial_{i_1} \phi_{\mathsf{a}_1} \right) (\boldsymbol{x}), \end{aligned} \tag{3.27a}$$

where it is the Euclidean semi-classical Green function

$$\mathcal{G}_{\text{s-c}}(\omega, \boldsymbol{p}, \boldsymbol{x}) := \frac{1}{\mathrm{i}\omega - \mathcal{H}\big(\boldsymbol{p}, \boldsymbol{\phi}(\boldsymbol{x})\big)} \tag{3.27b}$$

that enters the kernel $\mathcal{I}$.

3.3 Zero modes induced by point defects

We are going to apply the adiabatic expansion from Sec. 3.2 to the case of point defects supported by the static order parameter

$$\boldsymbol{\phi}(\boldsymbol{x}) \equiv \begin{pmatrix} \phi_1(\boldsymbol{x}) \\ \vdots \\ \phi_D(\boldsymbol{x}) \\ \phi_{D+1}(\boldsymbol{x}) \end{pmatrix} \equiv \begin{pmatrix} \varphi_1(\boldsymbol{x}) \\ \vdots \\ \varphi_D(\boldsymbol{x}) \\ \phi(\boldsymbol{x}) \end{pmatrix} \in \mathbb{R}^{d+1} \tag{3.28a}$$

and

$$\boldsymbol{\phi}^2(\boldsymbol{x}) \approx \boldsymbol{\varphi}_0^2 \equiv \Delta_0^2 \tag{3.28b}$$

when space is d-dimensional, i.e., when

$$\boldsymbol{x} \in \mathbb{R}^d. \tag{3.28c}$$

The component $\phi_{D+1}(\boldsymbol{x}) \equiv \phi(\boldsymbol{x})$ breaks locally the charge conjugation symmetry. This component determines if a zero mode bound to a defect at $\boldsymbol{x}$ is occupied or unoccupied. All remaining components of the order parameter (3.28a) are compatible with the charge-conjugation symmetry of the single-particle Hamiltonian. The condition (3.28b) suggests that the homotopy group

$$\Pi_d(S^d) = \mathbb{Z} \tag{3.29}$$

of smooth maps from the compactification of $\mathbb{R}^d$ into the d-sphere S^d to the d-sphere S^d in order-parameter space $\mathbb{R}^{d+1}$ might play an important role.

We begin in one dimensional space (x) with a generic single-particle Hamiltonian. We show that the charge Q_{adia} that enters the counting formula (3.11) is *the first Chern number* if we relax the condition that the charge-symmetry-breaking component ϕ of the order parameter is infinitesimally small and if we compactify space (3.28c) and the order-parameter space (3.28a).

We continue with the chiral p-wave superconductor in two-dimensions when the superconducting order parameter supports a vortex. We show that the number of unoccupied zero modes bound to a vortex with unit vorticity computed from the adiabatic approximation agrees with the direct construction of zero modes once all microscopic data have been supplied. Moreover, we show that the charge Q_{adia} that enters the counting formula (3.11) is also related to *the second Chern number* after compactification of both space (3.28c) and order-parameter space (3.28a). This is apriori surprising since the superconducting order parameter couples to the momentum contrary to the simpler case of Dirac fermions.

We also study Dirac single-particle Hamiltonians in d-dimensional space (3.28c) that are represented by Dirac matrices of dimension $R = 2^d$. We show how the charge Q_{adia} that enters the counting formula (3.11) is related to *the d-th Chern number* when the Dirac spinor couples to a $(d+1)$-tuplet of Higgs field.

We close by discussing how to interpret the adiabatic approximation.

3.3.1 Generic single-particle $\mathcal{H}$ when $d = 1$

We compactify space and the order-parameter space,

$$x \in S^1, \qquad \boldsymbol{\phi}(\theta) \in S^1 \subset \mathbb{R}^2, \tag{3.30}$$

respectively, such that

$$\boldsymbol{\phi}(x) = \begin{pmatrix} \phi_1(x) \\ \\ \phi_2(x) \end{pmatrix} = m \begin{pmatrix} \sin\theta(x) \\ \\ \cos\theta(x) \end{pmatrix}, \tag{3.31}$$

and denote with $\mathcal{G} = (\mathrm{i}\omega - \mathcal{H})^{-1}$ the single-particle Green function in Euclidean space for any suitable $R \times R$ matrix-valued single-particle Hamiltonian $\mathcal{H}\big(\hat{p}, \boldsymbol{\phi}(x)\big)$. Suitability means that the dependence on the momentum operator $\hat{p} \equiv -\mathrm{i}\partial_x$ in $\mathcal{H}\big(\hat{p}, \boldsymbol{\phi}(x)\big)$ is only restricted by locality while that on the two-component order parameter $\boldsymbol{\phi}(x)$ is linear. Furthermore, $\mathcal{H}\big(\hat{p}, \boldsymbol{\phi}(x)\big)$ obeys Eq. (3.12) for $D = 1$ and supports the spectral gap $2m$ for a uniform $\boldsymbol{\phi}_0$. Under these conditions, for any p the semi-classical $R \times R$ matrix $\mathcal{H}\big(p, \boldsymbol{\phi}(x)\big)$ is traceless and its square is proportional to the unit matrix with the smallest nonvanishing eigenvalue no smaller than m^2. We have introduced the spherical coordinate θ of the one-sphere $S^1 \subset \mathbb{R}^2$ in order-parameter space.

According to Eq. (3.23), the conserved quasiparticle charge Q_{adia} becomes

$$Q_{\mathrm{adia}} = \int\limits_{\omega} \int\limits_{p \in S^1} \int\limits_{x \in S^1} \frac{1}{2} \mathrm{tr}_R \Big(\mathcal{G}\partial_p \mathcal{G}^{-1} \mathcal{G} \partial_\theta \mathcal{G}^{-1} \mathcal{G} - \mathcal{G}\partial_\theta \mathcal{G}^{-1} \mathcal{G} \partial_p \mathcal{G}^{-1} \mathcal{G} \Big)_0 (-\mathrm{i})\, \partial_x \theta. \tag{3.32}$$

The subscript 0 refers to the semi-classical Green function (3.22). We use the identity $\partial_\omega \mathcal{G}^{-1} = \mathrm{i}$, introduce the family of indices labeled by $\nu_1, \nu_2, \nu_3 = 0, 1, 2$, and the Euclidean 3-momentum $K_\nu := (\omega, p, \theta)$. With the help of the manipulations made

between Eqs. (A.50) and (A.61), it is possible to re-write Eq. (3.32) as

$$Q_{\text{adia}} = -\frac{1}{24\pi^2}\int \mathrm{d}\omega \int_0^{2\pi} \mathrm{d}p \int_0^{2\pi} \mathrm{d}\theta\, \epsilon_{\nu_1\nu_2\nu_3} \times \mathrm{tr}_R\Big(\mathcal{G}\partial_{\nu_1}\mathcal{G}^{-1}\mathcal{G}\partial_{\nu_2}\mathcal{G}^{-1}\mathcal{G}\partial_{\nu_3}\mathcal{G}^{-1}\Big)_0. \quad (3.33)$$

Equation (3.33) is *the first Chern number*. [123] Thus, the charge Q_{adia} obeying Eq. (3.33) takes integer values. We defer to Sec. 3.3.4 and Appendix A.2.1 for a more detailed discussion of the connection between *the first Chern number* and the number of unoccupied zero modes.

3.3.2 Chiral p-wave superconductor when $d = 2$

Definition

One of the main results of this chapter consists in applying the counting formula (3.14) to the two-dimensional chiral p-wave superconductor with the single-particle BdG Hamiltonian

$$\mathcal{H}^{\text{BdG}}_{p_x+\mathrm{i}p_y} = \begin{pmatrix} \varepsilon(\hat{\boldsymbol{p}}) & \frac{1}{2}\{\hat{p}_1 - \mathrm{i}\hat{p}_2, \Delta(\boldsymbol{x})\} \\ \frac{1}{2}\{\hat{p}_1 + \mathrm{i}\hat{p}_2, \Delta^*(\boldsymbol{x})\} & -\varepsilon(\hat{\boldsymbol{p}}) \end{pmatrix} \quad (3.34)$$
$$\varepsilon(\hat{\boldsymbol{p}}) = \frac{\hat{\boldsymbol{p}}^2}{2m} - \mu,$$

for the case when the superconducting order parameter supports the vorticity $n_{\text{v}} = \pm 1$ at the origin of two-dimensional Euclidean space, i.e., when

$$\Delta(\boldsymbol{x}) = \Delta_0(r)\, e^{\mathrm{i}\, n_{\text{v}}\, \theta} \quad (3.35)$$

where r and θ are the polar coordinates of $\boldsymbol{x} \in \mathbb{R}^2$.

The applicability of the counting formula (3.14) follows from the antiunitary conjugation symmetry

$$\mathcal{C}_{\text{ph}}^{-1}\, \mathcal{H}^{\text{BdG}}_{p_x+\mathrm{i}p_y}\, \mathcal{C}_{\text{ph}} = -\mathcal{H}_{p_x+\mathrm{i}p_y}, \quad (3.36a)$$

where

$$\mathcal{C}_{\rm ph} = \rho_1 \, \mathsf{K}. \tag{3.36b}$$

The Pauli matrices ρ_1, ρ_2, and ρ_3 encode the particle and hole block structure of the single-particle BdG Hamiltonian (3.34). Complex conjugation is denoted by K.

For a unit vorticity, Read and Green have shown in Ref. [94] the existence of a single zero mode bound to the vortex by solving the eigenvalue problem at zero energy. A zero mode in a single-particle BdG Hamiltonian realizes a Majorana fermion, for it cannot be distinguished from its particle-hole conjugate. For an arbitrary vorticity $n_{\rm v} \in \mathbb{Z}$, it is shown in Refs. [116] and [41] by solving the eigenvalue problem at zero energy that the number of Majorana fermions is one if $n_{\rm v}$ is odd and zero otherwise.

We do not expect the adiabatic approximation to the counting formula (3.14) to capture this subtle parity effect since it is only sensitive to the net vorticity $n_{\rm v}$ trapped in region of space much larger than the characteristic length scale $\ell \gg 1/\Delta_0$ over which $|\delta\boldsymbol{\varphi}|$ changes by the amount of order Δ_0. The adiabatic approximation fails to distinguish the case of a single vortex with vorticity $n_{\rm v}$ and $n_{\rm v}$ vortices with unit vorticity that are separated by a distance of order ℓ. This parity effect is a non-perturbative effect from the point of view of the gradient expansion that we now present.

Counting zero modes

To count the unoccupied zero modes induced by a vortex in the superconducting order parameter with the gradient expansion of Sec. 3.2, we need to simultaneously move in energy the zero mode and properly regulate the singularity at the core of the

vortex. Achieving both goals is impossible with the 2×2 BdG Hamiltonian for the chiral p-wave single-particle Hamiltonian. On the other hand, both conditions are met after doubling the BdG single-particle Hamiltonian so as to introduce an auxiliary chiral-symmetry-breaking perturbation in two ways (denoted by the subscripts $\mp$),

$$\mathcal{H}^{\text{aux}}_{\mp}\big(\hat{\boldsymbol{p}}, \boldsymbol{\phi}(\boldsymbol{x})\big) = \begin{pmatrix} \mathcal{H}^{\text{BdG}}_{p_x+\mathrm{i}p_y} & \frac{1}{2}\rho_0 \left\{\hat{p}_{\mp}, \phi_3(\boldsymbol{x})\right\} \\ \frac{1}{2}\rho_0 \left\{\hat{p}_{\pm}, \phi_3(\boldsymbol{x})\right\} & -\mathcal{H}^{\text{BdG}}_{p_x+\mathrm{i}p_y} \end{pmatrix}. \tag{3.37a}$$

The short-hand notations $\hat{p}_{\pm} \equiv \hat{p}_x \pm \mathrm{i}\hat{p}_y$ was introduced and ρ_0 is the 2×2 unit matrix. The triplet

$$\boldsymbol{\phi}(\boldsymbol{x}) \equiv \begin{pmatrix} \phi_1(\boldsymbol{x}) \\ \phi_2(\boldsymbol{x}) \\ \phi_3(\boldsymbol{x}) \end{pmatrix} = \begin{pmatrix} \Delta_1(\boldsymbol{x}) \\ \Delta_2(\boldsymbol{x}) \\ \phi_3(\boldsymbol{x}) \end{pmatrix} \tag{3.37b}$$

is real-valued and is made of the static superconducting order parameter $\Delta(\boldsymbol{x}) \equiv \Delta_1(\boldsymbol{x}) + \mathrm{i}\Delta_2(\boldsymbol{x})$ and of the static auxiliary charge-conjugation-symmetry-breaking field $\phi_3(\boldsymbol{x})$.

The spectrum of the pair of auxiliary single-particle Hamiltonians (3.37a) given a uniform order parameter $\boldsymbol{\phi}_0$ in Eq. (3.37b) is

$$\varepsilon_0^2(\boldsymbol{p}) = \left(\frac{\boldsymbol{p}^2}{2m} - \mu\right)^2 + \boldsymbol{p}^2\boldsymbol{\phi}_0^2. \tag{3.38}$$

Conditions (i) and (ii) from Sec. 3.2 are thus fulfilled since the Fermi surface $\boldsymbol{p}^2 = 2m\mu$ is fully gaped.

When $\phi_3 = 0$, the auxiliary single-particle Hamiltonian (3.37) represents two independent copies of the original chiral p-wave BdG Hamiltonian (3.34). When $\phi_3 = 0$, the spectrum of $\mathcal{H}^{\text{aux}}_{\mp}$ is identical to the spectrum of $\mathcal{H}^{\text{BdG}}_{p_x+\mathrm{i}p_y}$ up to a two-fold

degeneracy arising from the doubling. Furthermore, $\phi_3 = 0$ implies that, in addition to the antiunitary charge conjugation symmetry

$$\mathcal{C}_{\rm ph}^{-1}\,\mathcal{H}_{\mp}^{\rm aux}\big(\hat{\boldsymbol{p}},\boldsymbol{\phi}(\boldsymbol{x})\big)\,\mathcal{C}_{\rm ph} = -\mathcal{H}_{\mp}^{\rm aux}\big(\hat{\boldsymbol{p}},\boldsymbol{\phi}(\boldsymbol{x})\big) \tag{3.39a}$$

with

$$\mathcal{C}_{\rm ph} = \begin{pmatrix} \rho_1 & 0 \\ 0 & \rho_1 \end{pmatrix} \mathsf{K}, \tag{3.39b}$$

where K denotes as before the operation of complex conjugation, that originates from Eq. (3.36), there exists an auxiliary unitary charge-conjugation symmetry

$$\mathcal{C}_{\rm ch}^{-1}\mathcal{H}_{\mp}^{\rm aux}\big(\hat{\boldsymbol{p}},\boldsymbol{\phi}(\boldsymbol{x})\big)\,\mathcal{C}_{\rm ch} = -\mathcal{H}_{\mp}^{\rm aux}\big(\hat{\boldsymbol{p}},\boldsymbol{\phi}(\boldsymbol{x})\big) \tag{3.40a}$$

with the generator of the auxiliary chiral transformation

$$\mathcal{C}_{\rm ch} = \begin{pmatrix} 0 & \rho_0 \\ \rho_0 & 0 \end{pmatrix}. \tag{3.40b}$$

Although neither $\mathcal{C}_{\rm ph}$ nor $\mathcal{C}_{\rm ch}$ are symmetries as soon as $\phi_3 \neq 0$, their product $\mathcal{T}_{\rm aux} \equiv \mathcal{C}_{\rm ph}\mathcal{C}_{\rm ch}$ is a symmetry for any ϕ_3. The antiunitary operation $\mathcal{T}_{\rm aux}$ can be thought of as implementing an auxiliary time-reversal symmetry. As a result all eigenstates of $\mathcal{H}_{\mp}^{\rm aux}\big(\hat{\boldsymbol{p}},\boldsymbol{\phi}(\boldsymbol{x})\big)$, including zero modes, have a two-fold Kramers degeneracy.

As we shall see in Sec. 3.3.3, Dirac Hamiltonians can also share unitary and antiunitary charge-conjugation symmetries. There are differences with Sec. 3.3.3 however. A first difference with Sec. 3.3.3 is that

$$\mathcal{C}_{\rm ch}^{-1}\mathcal{H}_{\mp}^{\rm aux}\big(\hat{\boldsymbol{p}},\boldsymbol{\phi}(\boldsymbol{x})\big)\,\mathcal{C}_{\rm ch} = -\mathcal{H}_{\pm}^{\rm aux}\big(\hat{\boldsymbol{p}},C_{\rm ch}\boldsymbol{\phi}(\boldsymbol{x})\big) \tag{3.41a}$$

with

$$C_{\rm ch}\begin{pmatrix}\phi_1(\boldsymbol{x})\\ \phi_2(\boldsymbol{x})\\ \phi_3(\boldsymbol{x})\end{pmatrix}\equiv\begin{pmatrix}\phi_1(\boldsymbol{x})\\ \phi_2(\boldsymbol{x})\\ -\phi_3(\boldsymbol{x})\end{pmatrix}. \tag{3.41b}$$

A second difference with Sec. 3.3.3 is the absence of relativistic invariance. A third difference is that Eq. (3.25) is non-vanishing.

We start from the expansion (3.20) of the quasiparticle charge density induced by the order parameter, the static triplet $\boldsymbol{\phi}$. We compute first the contribution from $n = 1$ for the pair of auxiliary Hamiltonians. It vanishes. The adiabatic approximation to the quasiparticle charge density for any one of the pair of auxiliary Hamiltonians is given by Eq. (3.24), which delivers

$$\rho^{\rm aux}_{\mp{\rm adia}}(\boldsymbol{x}) = \pm\,\frac{1+{\rm sgn}(\mu)}{2\pi\,|\boldsymbol{\phi}(\boldsymbol{x})|^4}\epsilon_{\mathsf{abc}}\Big(\,(\partial_1\phi_{\mathsf{a}})\,(\partial_2\phi_{\mathsf{b}})\,\phi_{\mathsf{c}}\phi_3\Big)(\boldsymbol{x}). \tag{3.42}$$

When $\mu < 0$, Eq. (3.42) gives $\rho^{\rm aux}_{\mp}(\boldsymbol{x}) = 0$. This is consistent with the absence of a normalizable zero energy solution for negative values of the chemical potential.[94, 116, 41]

When $\mu > 0$ and ϕ_3 is independent of space ($\boldsymbol{x}$), the adiabatic approximation to the conserved quasiparticle charge of the auxiliary Hamiltonian is

$$Q^{\rm aux}_{\mp{\rm adia}}(\phi_3) = \pm\frac{1}{\pi}\int {\rm d}\Theta\int_0^{\Delta_0}{\rm d}\rho\,\rho\,\frac{\phi_3^2}{\left(\rho^2+\phi_3^2\right)^2}, \tag{3.43a}$$

where the parametrization

$$\begin{pmatrix}\phi_1\\ \phi_2\end{pmatrix} = \begin{pmatrix}\rho(r)\cos\Theta(\theta)\\ \rho(r)\sin\Theta(\theta)\end{pmatrix} \tag{3.43b}$$

is assumed for the superconducting order parameter with r and θ denoting the polar coordinates of $\boldsymbol{x} \in \mathbb{R}^2$. In the limit in which ϕ_3 tends to zero, we get for the induced charge of the auxiliary Hamiltonian

$$\begin{aligned} Q^{\text{aux}}_{\mp\text{adia}} &= \pm \frac{1}{2\pi} \int \mathrm{d}\Theta \\ &= \pm \text{ winding number in } (\phi_1, \phi_2). \end{aligned} \tag{3.44}$$

To compute the number N^{aux} of unoccupied zero modes with the counting formula (3.14) induced by a vortex with vorticity unity, we choose the charge-conjugation-symmetry-breaking perturbation such that it shifts the zero mode in energy above the chemical potential. In the limit $\phi_3 \to 0$, we find that

$$N^{\text{aux}} = 2. \tag{3.45}$$

Equation (3.45) implies that the adiabatic approximation for the number N of unoccupied zero modes of the original BdG Hamiltonian (3.34) induced by a vortex with unit vorticity is

$$N = 1. \tag{3.46}$$

Chern number

Next, we compactify space (3.28c) and the order-parameter space (3.28a),

$$\boldsymbol{x} \in S^2, \qquad \boldsymbol{\phi}(\boldsymbol{\theta}) \in S^2 \subset \mathbb{R}^3 \tag{3.47}$$

where we have introduced the spherical coordinates $\boldsymbol{\theta} = (\theta_1, \theta_2)$ of the two-sphere $S^2 \subset \mathbb{R}^3$. Motivated by Eq. (3.24), we separate the adiabatic approximation to the conserved quasiparticle charge of the auxiliary Hamiltonian into two contributions,

$$Q^{\text{aux}}_{\text{adia}} = Q^{\text{aux}\prime}_{\text{adia}} + Q^{\text{aux}\prime\prime}_{\text{adia}} \tag{3.48a}$$

where

$$Q^{\text{aux}\prime}_{\text{adia}} = -\int\limits_{\omega}\int\limits_{\boldsymbol{p}\in S^2}\int\limits_{\boldsymbol{x}\in S^2} \text{tr}_4\Big(\mathcal{G}\partial_{i_2}\mathcal{G}^{-1}\mathcal{G}\partial_{\mathsf{a}_2}\mathcal{G}^{-1}\times\mathcal{G}\partial_{\mathsf{a}_1}\mathcal{G}^{-1}\mathcal{G}\partial_{\mathsf{i}_1}\mathcal{G}^{-1}\mathcal{G}\Big)_0\partial_{i_1}\phi_{\mathsf{a}_1}\partial_{i_2}\phi_{\mathsf{a}_2} \tag{3.48b}$$

while

$$Q^{\text{aux}\prime\prime}_{\text{adia}} = \frac{1}{2}\int\limits_{\omega}\int\limits_{\boldsymbol{p}\in S^2}\int\limits_{\boldsymbol{x}\in S^2} \text{tr}_4\Big(\mathcal{G}\partial^2_{i_2\mathsf{a}_2}\mathcal{G}^{-1}\mathcal{G}\partial_{\mathsf{a}_1}\mathcal{G}^{-1}\partial_{i_1}\mathcal{G}+\partial_{i_2}\mathcal{G}\partial_{\mathsf{a}_2}\mathcal{G}^{-1}\mathcal{G}\partial^2_{i_1\mathsf{a}_1}\mathcal{G}^{-1}\mathcal{G}\Big)_0\partial_{i_1}\phi_{\mathsf{a}_1}\partial_{i_2}\phi_{\mathsf{a}_2} \tag{3.48c}$$

and $\mathcal{G} = (\mathrm{i}\omega - \mathcal{H}^{\text{aux}}_{\mp})^{-1}$. The subscript 0 refers to the semi-classical Green function (3.22). The first contribution comes about when the order parameter decouples from the momentum. The second contribution arises when the order parameter and the momentum couple.

By explicit computation of the trace in Eq. (3.48b), one verifies that this trace is fully antisymmetric in all the indices $i_2, \mathsf{a}_2, i_1, \mathsf{a}_1$ where the family i and the family a of indices are distinct with

$$i_1, i_2 = 1, 2, \qquad \mathsf{a}_1, \mathsf{a}_2 = 1, 2, 3. \tag{3.49}$$

Furthermore, the trace in Eq. (3.48b) gives an integrand with even contributions in ω so that it does not vanish upon integration over ω. By explicit computation of the trace in Eq. (3.48c), one verifies that this trace yields an integrand that is odd in ω and thus vanishes upon integration over ω,

$$Q^{\text{aux}\prime\prime}_{\text{adia}} = 0. \tag{3.50}$$

With the help of the manipulations made between Eqs. (A.50) and (A.61), it is

possible to write

$$Q^{\rm aux}_{\rm adia} = Q^{\rm aux\prime}_{\rm adia} = \frac{-{\rm i}(2\pi)^2}{60} \int\limits_K \epsilon_{\nu_1 \cdots \nu_5} {\rm tr}_4 \left(\mathcal{G} \partial_{\nu_1} \mathcal{G}^{-1} \cdots \mathcal{G} \partial_{\nu_5} \mathcal{G}^{-1} \right)_0 \tag{3.51a}$$

where we have introduced the family of indices labeled by $\nu_1, \cdots, \nu_5 = 1, \cdots, 5$, the five-momentum $K_\nu = (\omega, p_1, p_2, \theta_1, \theta_2)$, and the domain of integration

$$\int\limits_K \equiv \int \frac{{\rm d}\omega}{2\pi} \int\limits_{\boldsymbol{p} \in S^2} \frac{{\rm d}\Omega_2(\boldsymbol{p})}{(2\pi)^2} \int\limits_{\boldsymbol{\theta} \in S^2} \frac{{\rm d}\Omega_2(\boldsymbol{\theta})}{(2\pi)^2}. \tag{3.51b}$$

The "surface" element of the sphere S^2 is here denoted by ${\rm d}\Omega_2$. The subscript 0 refers to the semi-classical Green function (3.22). Equation (3.51) is *the second Chern number*. [90] It takes integer values only. It should be compared with Eq. (A.44). We defer to Secs. 3.3.3, 3.3.4, and A.2.2 for a more detailed discussion of the connection between *this second Chern number* and the number of unoccupied zero modes.

We have verified that the *second Chern number* (3.51) vanishes for a s-wave superconducting order parameter that supports an isolated vortex with unit vorticity.

3.3.3 Dirac single-particle $\mathcal{H}_d^{\rm Dirac}$ for any d

Our purpose here is to apply the counting formula (3.14) to a Dirac single-particle Hamiltonian defined in the d-dimensional Euclidean space with the coordinates (3.3). We choose the dimensionality of the Dirac matrices to be

$$R = 2^d. \tag{3.52a}$$

The integer R is the smallest dimensionality compatible with an irreducible representation of the Clifford algebra generated by the unit $R \times R$ matrix $\hat{1}$ and the traceless

and Hermitian matrices

$$\Gamma_{\mu} = \Gamma_{\mu}^{\dagger}, \quad \mathrm{tr}_R\, \Gamma_{\mu} = 0, \quad \big\{\Gamma_{\mu}, \Gamma_{\nu}\big\} = 2\delta_{\mu,\nu}\hat{1}, \tag{3.52b}$$

where $\mu, \nu = 1, \cdots, 2d+1$. [147] We choose the single-particle Dirac Hamiltonian such that a R-dimensional spinor is coupled to a $(d+1)$-tuplet of real-valued static Higgs fields

$$\boldsymbol{\phi}(\boldsymbol{x}) \in \mathbb{R}^{d+1}, \qquad \boldsymbol{x} \in \mathbb{R}^{d}. \tag{3.52c}$$

Accordingly,

$$\mathcal{H}_d^{\mathrm{Dirac}}\big(\hat{\boldsymbol{p}}, \boldsymbol{\phi}(\boldsymbol{x})\big) = \sum_{i=1}^{d} \Gamma_i \hat{p}_i + \sum_{\mathsf{a}=1}^{d+1} \Gamma_{d+\mathsf{a}} \phi_{\mathsf{a}}(\boldsymbol{x}). \tag{3.52d}$$

The decomposition (3.7) is generalized to

$$\boldsymbol{\phi}(\boldsymbol{x}) = \boldsymbol{\phi}_0 + \delta\boldsymbol{\phi}(\boldsymbol{x}) \tag{3.53}$$

and is assumed to hold together with conditions (iii) from Sec. 3.2, once we have established the existence of charge-conjugation symmetry. Conditions (i) and (ii) follow from the spectrum

$$\varepsilon_0^2(\boldsymbol{p}) = \boldsymbol{p}^2 + \boldsymbol{\phi}_0^2 \tag{3.54}$$

of $\mathcal{H}_d^{\mathrm{Dirac}}\big(\hat{\boldsymbol{p}}, \boldsymbol{\phi}_0\big)$.

The Dirac Hamiltonian (3.52d) has the charge-conjugation symmetry

$$\mathcal{H}_d^{\mathrm{Dirac}} = -\Gamma_{d+\mathsf{a}} \mathcal{H}_d^{\mathrm{Dirac}} \Gamma_{d+\mathsf{a}} \tag{3.55a}$$

for any $\mathsf{a} = 1, \cdots, d+1$ as soon as $\phi_{\mathsf{a}} = 0$ everywhere in space. Without loss of generality, we choose the generator of the so-called chiral symmetry (3.55a) to be Γ_{2d+1}, i.e., we identify the charge-conjugation symmetry (3.6c) with the unitary

operation represented by

$$\mathcal{C}_{\text{ch}} := \Gamma_{2d+1} = (-\mathrm{i})^d \, \Gamma_1 \cdots \Gamma_{2d}. \tag{3.55b}$$

Equation (3.55) follows from $2d+1$ being an odd integer. [147] With this choice, the vector-valued order parameter (3.4) is

$$\varphi_a := \phi_a, \qquad a = 1, \cdots, d, \tag{3.56}$$

i.e.,

$$D = d. \tag{3.57}$$

We present our main result for Dirac fermions in three steps. The reader is referred to Appendix A.2 for their detailed derivations when $d = 1$ and $d = 2$, and a sketch of the derivation when $d > 2$.

First, the adiabatic approximation to the counting formula (3.14) is determined by the adiabatic charge Q_{adia}. However, Q_{adia} can be computed without assuming charge-conjugation symmetry. It is only when using the counting formula (3.14) that Q_{adia} must be restricted to a charge-conjugation-symmetric configuration of the Higgs order parameter (3.28a). After relaxing the condition of charge-conjugation symmetry, we find

$$\begin{aligned} Q_{\text{adia}} &= \text{Chern}_d \\ &\equiv \frac{(-1)^{d(d-1)/2}(-\mathrm{i})^{d+1} d!}{(2d+1)!} (2\pi)^d \int_K \epsilon_{\nu_1 \cdots \nu_{2d+1}} \times \text{tr}_R \left(\mathcal{G} \partial_{\nu_1} \mathcal{G}^{-1} \cdots \mathcal{G} \partial_{\nu_{2d+1}} \mathcal{G}^{-1} \right)_0 \end{aligned} \tag{3.58a}$$

if we compactify momentum space and the target manifold, i.e., we have introduced the Euclidean momentum $K_\nu := (\omega, p_1, \cdots, p_d, \theta_1, \cdots, \theta_d)$ with $(p_1, \cdots, p_d) \in S^d$

and the spherical coordinates $\boldsymbol{\theta} \equiv (\theta_1, \cdots, \theta_d)$ with $\boldsymbol{\phi}(\boldsymbol{\theta}) \in S^d \subset \mathbb{R}^{d+1}$. The last inclusion serves to emphasize that the coordinates on the d-sphere in order-parameter space can involve a sizable breaking of the conjugation symmetry through $\phi_{d+1}(\boldsymbol{\theta}) \equiv \phi(\boldsymbol{\theta})$. The short-hand notation $\int\limits_K$ stands for the integral over $\mathbb{R} \times S^d \times S^d$ defined in Eq. (A.61a). The Euclidean single-particle Green function $\mathcal{G} = \left(\mathrm{i}\omega - \mathcal{H}_d^{\mathrm{Dirac}}\right)^{-1}$ is the one for the Dirac Hamiltonian. The subscript 0 refers to the semi-classical Green function (3.22). The second equality in Eq. (3.58a) *defines the d-th Chern number* in term of these Dirac Euclidean single-particle Green functions. It takes integer values and, conversely, to each integer N_{hedgehog} there corresponds a static $\boldsymbol{\phi}_{N_{\mathrm{hedgehog}}}(\boldsymbol{x}) \in S^d$ for which $Q_{\mathrm{adia}} = N_{\mathrm{hedgehog}}$. We call $\boldsymbol{\phi}_{N_{\mathrm{hedgehog}}}(\boldsymbol{x}) \in S^d$ a hedgehog with *the d-th Chern number* N_{hedgehog}.

Second, if we relax the condition that $\boldsymbol{\phi}(\boldsymbol{\theta}) \in S^d$ and replace it with Eq. (3.28b) instead, then the local quasiparticle current induced by the adiabatic variations of the Higgs fields in space ($\boldsymbol{x}$) and time (x_0) is

$$j^\nu = \frac{\Omega_d^{-1}}{|\boldsymbol{\phi}|^{d+1}} \frac{\epsilon^{\nu\nu_1\cdots\nu_d}}{d!} \epsilon_{\mathsf{a}\mathsf{a}_1\cdots\mathsf{a}_d} \phi_{\mathsf{a}} \partial_{\nu_1} \phi_{\mathsf{a}_1} \cdots \partial_{\nu_d} \phi_{\mathsf{a}_d}. \tag{3.59a}$$

It obeys the continuity equation

$$\partial_\nu j^\nu = 0. \tag{3.59b}$$

Here,

$$|\boldsymbol{\phi}| = \sqrt{\phi_1^2 + \cdots + \phi_{d+1}^2}, \tag{3.59c}$$

the $(d+1)$ indices $\nu, \nu_1, \cdots, \nu_d$ run over space ($\boldsymbol{x}$) and time (x_0), and the $(d+1)$ indices $\mathsf{a}_1, \cdots, \mathsf{a}_{d+1}$ run over the $(d+1)$ components of the vector-valued Higgs field (3.52c). The Minkowski metric is used in space ($\boldsymbol{x}$) and time (x_0). Finally, Ω_d denotes the

area of the d-sphere S^d. Equation (3.59a) was obtained by Goldstone an Wilczek in Ref. [39] when $d = 1$ and $d = 3$ and by Jaroszewicz in Ref. [61] when $d = 2$. The conserved quasiparticle charge induced by a hedgehog configuration is the integer

$$Q_{\text{adia}} = \int \mathrm{d}^d \boldsymbol{x}\, j^0_{\text{adia}}(\boldsymbol{x}) = \frac{1}{\Omega_d} \int_{S^d} \mathrm{d}\Omega_d = N_{\text{hedgehog}} \in \mathbb{Z}. \tag{3.60}$$

The "surface" element ("area") of the sphere S^d is here denoted by $\mathrm{d}\Omega_d$ (Ω_d).

Third, we need to define a point defect that is compatible with the charge-conjugation symmetry and consistent with the adiabatic approximation (see Sec. 3.3.4 for a discussion of the latter caveat). A charge-conjugation symmetric point defect is a half hedgehog, i.e., a static Higgs $(d + 1)$-tuplet (3.28a) that satisfies Eq. (3.28b) and wraps the d-sphere S^d the half integer $\pm 1/2$ number of times (a domain wall in $d = 1$, a vortex with unit vorticity in $d = 2$, etc). The counting formula (3.14) predicts that there is one unoccupied zero modes for a half-hedgehog provided we choose the sign of the infinitesimal conjugation-symmetry-breaking ϕ in Eq. (3.28a) to be opposite to the sign of $\pm 1/2$.

The *d-th Chern number* (3.58) is non-vanishing for any single-particle Hamiltonian topologically equivalent to the Dirac Hamiltonian (3.52).

3.3.4 Physical interpretation of the adiabatic approximation

The relevant length scales in d-dimensional space are: (1) the characteristic linear size $\mathfrak{a}$ of a point defect, (2) the characteristic linear size $\xi_0 = 1/\Delta_0$ of the support in space of the zero modes bound to the point defect, (3) the characteristic length ℓ over which the variation of the order parameter $\boldsymbol{\phi}$ is of order of the gap $2\Delta_0$,

$$|\boldsymbol{\nabla}\boldsymbol{\phi}|\, \ell = \Delta_0, \tag{3.61}$$

(4) and the linear size R of the region of space in which the conserved quasiparticle charge Q and the total number N of unoccupied zero modes is to be computed (measured). The gradient approximation relies on the hierarchy

$$\mathfrak{a} < \xi_0 \ll \ell \ll R. \tag{3.62}$$

In the gradient approximation, all microscopic data for length scales smaller than ℓ are dispensed with. This fact dictates how to properly interpret the results from the gradient approximation when point defects can be assigned an additive label q_{def}. Here, the subscript stands for point defect.

When $d = 1$, $q_{\text{def}} \equiv q_{\text{dw}}$, with $q_{\text{dw}} = +1$ representing a domain wall and $q_{\text{def}} = -1$ representing an antidomain wall. Observe that we can exchange the terminology domain and antidomain wall, for there is no absolute notion of a positive or negative q_{dw}. When $d = 2$, $q_{\text{def}} \equiv q_{\text{vor}} \in \mathbb{Z}$ encodes the vorticity of the vortex. In either case, these charges can be thought of as "classical Coulomb charges".

Any two point defects with the labels $q_{\text{def}}^{(1)}$ and $q_{\text{def}}^{(2)}$ within a distance of order $\mathfrak{a}$ of each other fuse into a point defect with the label

$$q_{\text{def}}^{(1+2)} = q_{\text{def}}^{(1)} + q_{\text{def}}^{(2)}. \tag{3.63}$$

When $d = 1$, domain walls are necessarily ordered. Consecutive domain walls necessarily carry the opposite label. Fusion of two domain walls in $d = 1$ necessarily results in their annihilation. When $d = 2$, vortices can fuse to yield larger vorticities.

When $d = 1$, we have shown in Sec. A.2.1 that the number of unoccupied zero modes N bound to a single domain wall in a large region of size R is $N = 1$ in the adiabatic approximation. This result agrees with solving the differential equation for

the zero mode once all microscopic data have been supplied. [56] However, we have also shown in Sec. 3.3.1 and Sec. A.2.1 that the number of unoccupied zero modes N in a large region of size R can be made to be an arbitrary integer number in the adiabatic approximation, in apparent contradiction with the fact that the net number of domain walls is either 0 or 1 along any finite segment of the line. This is explained with the help of Figure 3.2 as follows.

Occupying or leaving empty any single-particle level is a physical operation forcing a fermionic quasiparticle in or out of this single-particle level. This physical process is, for zero modes, achieved by the local sign of the charge-conjugation-symmetry-breaking ϕ_2. In Figure 3.2 (a), we plot as a function of position x along the line the dependence of the order parameter ϕ_1 and of the charge-conjugation-symmetry-breaking ϕ_2. Given the shape of the domain wall and its asymptotic value φ_0, we choose the sign $\phi_2(x) = +\phi$ so that the zero mode bound to the domain wall is shifted to a positive energy. If the chemical potential is chosen to be at 0, then the zero mode is unoccupied. The zero mode bound to an antidomain wall remains unoccupied if we choose the sign $\phi_2(x) = -\phi$ as depicted in Figure 3.2 (b). In Figure 3.2 (c) a domain wall is followed by an antidomain wall a distance ℓ apart. The closing of the gap $|\boldsymbol{\phi}|$ at the center of each domain walls when $\phi_1 = 0$ is avoided by the charge-conjugation-symmetry-breaking field saturating to its asymptotic magnitude ϕ. A phase twist in ϕ by π half way between the two consecutive domain walls insures that the zero-modes are shifted to positive energies and thus remain unoccupied. Gap closing at this phase twist is again avoided because ϕ_1 has healed to its asymptotic value. Everywhere along the line, $|\boldsymbol{\nabla\phi}|$ can thus be made as small as needed. The

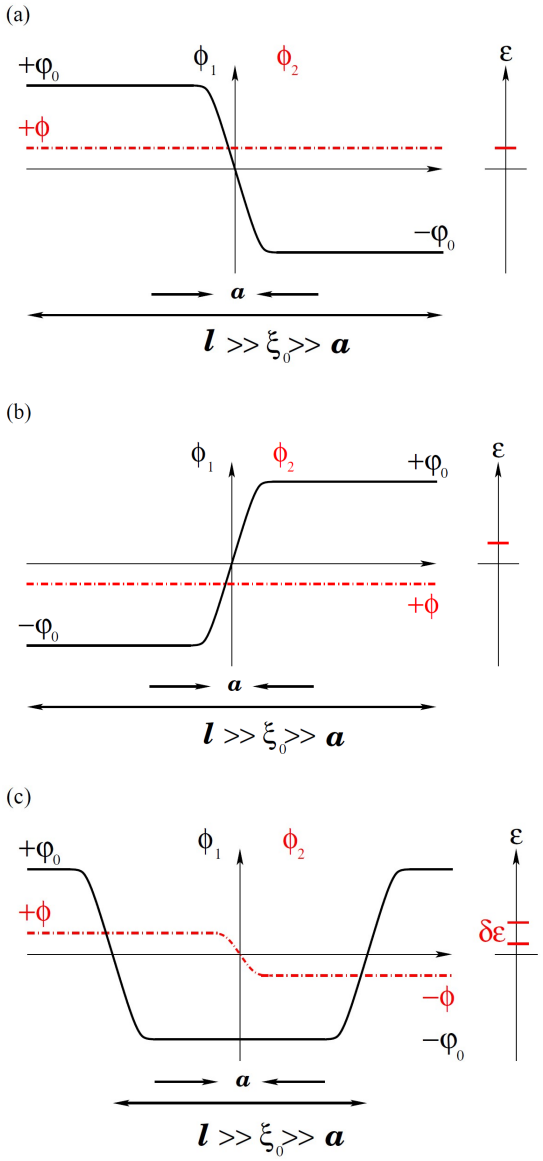

Figure 3.2: The dependence on space (x) of the Higgs doublet in Eq. (A.17) is depicted in panels (a), (b), and (c) together with the number and position of the zero modes along the single-particle energy eigenvalue axis ε. The magnitude of the asymptotic value of the order parameter ϕ_1 is $\varphi_0 > 0$. The magnitude of the asymptotic value of the charge-conjugation symmetry ϕ_2 is $\phi > 0$. The size of the point defect, a domain wall, is $\mathfrak{a}$. The exponential decay of the envelope of the bound state is controlled by the length scale $\xi_0 = 1/|\boldsymbol{\phi}_0|$. The characteristic length ℓ is defined in Eq. (3.61).

energy splitting $\delta\varepsilon$, which is of order $\Delta_0 \exp(-2\ell/\xi_0)$, is exponentially small in ℓ/ξ_0. In the gradient approximation, the order of limit is $\ell/\xi_0 \to \infty$ first followed by $\phi \to 0$. Evidently, this order of limit does not commute with $\phi \to 0$ first followed by $\ell/\xi_0 \to \infty$. In the latter order of limits, the unoccupied number of zero modes always vanishes.

We close the discussion of the results in one-dimensional space from Sec. 3.3.1 by observing that since the number of unoccupied zero mode is an integer, all higher contributions to the gradient expansion beyond the adiabatic (leading) order must vanish identically. We have verified this expectation explicitly for the first sub-leading order.

When $d = 2$, the adiabatic approximation of Sec. 3.3.2 applied to a chiral p-superconductor predicts that the total number of unoccupied zero modes in a large region of size R equals in magnitude the net vorticity in this region. On the other hand, it is known from solving the differential equation for a single vortex of vorticity q_{vort} in a p-wave superconductor that the number of zero modes is one if q_{vort} is odd or zero otherwise. [94, 116, 41] This is not a paradox if the adiabatic approximation in this chapter is limited to point defects each of which bind at most a single zero mode. We now argue that this interpretation of the adiabatic approximation is a necessary one.

The adiabatic approximation is not sensitive to the microscopic data on length scales smaller than ℓ. However, it is precisely those microscopic data that determines if more than one zero modes can be bound to a point defect. Consider the case of the relativistic Dirac Hamiltonian in two-dimensional space from Sec. A.2.2. It

respects two charge-conjugation symmetries, the chiral symmetry and the particle-hole symmetry. Correspondingly, the order parameter $\boldsymbol{\varphi}$ can either be interpreted as a bond-order (Kekulé order), [52] in which case the electron charge is a good quantum number, or as an s-wave superconductor, [57] in which case the electron charge is not anymore a good quantum number (the thermal quasiparticle charge is). In either interpretations, an index theorem guarantees that the number of zero modes equals in magnitude the vorticity of the order parameter. [128] For example, a vorticity of two implies that there are two zero modes. Of course, they must be orthogonal. Perturb now the Dirac Hamiltonian with a perturbation, whose characteristic energy scale is η, that breaks the chiral symmetry but preserves the particle-hole symmetry. [98] We assume that η is not sufficiently large to close the gap. The delicate balance that allowed the two zero modes to be orthogonal is destroyed by the perturbation η. The two zero modes split pairwise, one migrating to positive energy, the other migrating to negative energy. This level repulsion is encoded by the microscopic data in a region centered about the point defect of linear size ξ_0, a window of length scales inaccessible to the adiabatic approximation. If we split the single vortex with vorticity two into two vortices with vorticity one separated by a distance ℓ, we can use the adiabatic approximation. The energy shift induced by the chiral-symmetry-breaking ϕ is of order $\phi \exp(-2\ell/\xi_0)$. The level splitting induced by the particle-hole-symmetric η is of order $\eta \exp(-2\ell/\xi_0)$. They vanish in the adiabatic limit $\ell/\xi_0 \to \infty$ first, $\phi \to 0$ second.

The adiabatic approximation saturates the number of unoccupied zero modes N. Consistency demands that higher-order corrections vanish identically. This suggests

that the adiabatic approximation cannot capture the parity effect by which a charge-conjugation-symmetric perturbation splits pairwise the degeneracy of zero modes. Such a parity effect is an essential singularity for the adiabatic expansion presented in this chapter.

3.4 Conclusion

In chapter, we have derived a procedure to count the zero-energy eigenvalues of a single-particle Hamiltonian $\mathcal{H}\big(\hat{\boldsymbol{p}}, \boldsymbol{\varphi}(\boldsymbol{x})\big)$ that possesses a charge-conjugation symmetry, when the order parameter $\boldsymbol{\varphi}(\boldsymbol{x})$ supports point defects. This procedure is based on counting the charge Q induced by a point defect of $\boldsymbol{\varphi}(\boldsymbol{x})$.

We showed that one can use counting arguments similar to those appearing implicitly in Ref. [112] and explicitly in Ref. [58] to compute the fractional charge Q induced by a point defect. Once one observes that the number of unoccupied zero modes N can be related to Q through $N = -2Q$, one can concentrate the efforts into computing Q near a point defect of the position-dependent order parameter $\boldsymbol{\varphi}(\boldsymbol{x})$. We carry out this procedure within a gradient expansion for smoothly spatially varying fluctuations of the charge-conjugation-symmetric order parameter $\boldsymbol{\varphi}(\boldsymbol{x})$.

The resulting expression is then applied to generic systems in one-dimensional space, the chiral p-wave superconductor in two-dimensional space, and to Dirac fermions in d-dimensional space. In one-dimensional space, we find that the number of unoccupied zero modes is related to the first Chern number. For the p-wave superconductor in two-dimensional space, it is related to the second Chern number. For the Dirac Hamiltonians in d-dimensional space, the number of zero modes is de-

termined by the d-th Chern number. Therefore, we can establish in a logical and constructive way the relation between the number of zero modes induced by a point defect and topological invariants (the Chern numbers) in a number of cases.

There has been a resurgence of efforts dedicated to counting zero modes induced by defective order parameters in the condensed matter community. [103, 97] Fukui and Fujiwara in Ref. [33] have revisited Dirac fermions in up to three spatial dimensions. They use the chiral anomaly to carry the counting. Our general counting formula reproduces their and previous results, and extends them to arbitrary d dimensions of space. An elegant formulation of the Dirac problem in d dimensions in the presence of an isotropic hedgehog has been carried out by Herbut. [49] (See also Freedman *et al.* in Ref. [25].) The number of zero modes should not depend on deformations away from the isotropic case, and this result is captured by our counting formula, which we can express as the d-th Chern number. Finally, Teo and Kane in Ref. [115] have studied defects of arbitrary dimensions r coupled to noninteracting fermionic quasiparticles with the help of the classification scheme of Schnyder *et al* for topological band insulators and superconductors. [106, 67, 99] They conjecture that the topological invariant for a given symmetry class is related to the number of zero modes attached to r-dimensional defects, but cannot make any direct connection between these two integer numbers. Our explicit construction provides this relation, although, only for specific examples and for point defects. We do not have yet a proof for generic Hamiltonians that have a momentum-dependent coupling to the order parameter.

In summary, we showed that one can count zero modes using the charge induced by point defects for any mean-field Hamiltonian with charge-conjugation symmetry. This

counting supports a direct relation between topological invariants and the number of zero modes bound to defective order parameters.

Part II

Flatbands and the Fractional Quantum Hall Effect

Chapter 4

Isolated flat band and spin-1 conical bands in two-dimensional lattices

Abstract

Dispersionless bands, such as Landau levels, serve as a good starting point for obtaining interesting correlated states when interactions are added. With this motivation in mind, we study dispersionless ("flat") band structures that arise in tight-binding Hamiltonians defined on a kagome lattice with staggered fluxes. The flat bands and their neighboring dispersing bands have several notable features: (a) Flat bands can be isolated from other bands by breaking time reversal symmetry, allowing for an extensive degeneracy when these bands are partially filled; (b) An isolated flat band corresponds to a critical point between regimes where the band is electron-like or hole-like, with an anomalous Hall conductance that changes sign across the transition; (c) When the gap between a flat band and two neighboring bands closes, the system is described by a single spin-1 conical-like spectrum, extending to higher angu-

lar momentum the spin-1/2 Dirac-like spectra in topological insulators and graphene; and (d) We find that the Chern number of the isolated flat band is zero.

4.1 Introduction

One of the reasons why dispersionless (or "flat") bands are interesting is that they accommodate, when partially filled, an exponentially large number of states. This macroscopic degeneracy can be lifted when interactions are added, often leading to rich strongly correlated phenomena. The best known example is the fractional quantum Hall effect, which arises from the degeneracy within flat Landau bands for particles in a magnetic field.

In addition to the Landau problem, other models with flat bands have been studied at least since the 1970's, such as amorphous semiconductors [126, 127, 118]. This system is idealized by a lattice made up of clusters of sites. Both inter- and intra-cluster hopping are allowed. From a mathematical point of view, it turns out that the intra-cluster hopping term in the Hamiltonian is a projection operator, leading to the existence of flat bands [111]. [1] In the 1980's, flat bands were studied in relation to the Nielson-Ninomiya theorem [84] by Dagotto, Fradkin and Moreo [20]. They showed that it is possible to escape the fermion-doubling problem at the price of having an extra flat band in the spectrum. In this way, the low energy degrees of freedom of the theory can be described as a single Weyl species.

[1] In models for amorphous semiconductors, the Hamiltonian can be written as $H = \hat{A} + \hat{T}$ where $\hat{A}$ accounts for the intra-cluster hopping and satisfies $\hat{A}^2 = \hat{A}$, *i.e.* it is a projection operator, and $\hat{T}$ is the operator responsable for the hopping between nearest neighbor clusters and satisfies $\hat{T}^2 = I$. These properties of $\hat{A}$ and $\hat{T}$ endow the spectrum with dispersionless bands.

More recently, Ohgushi, Murakami, and Nagaosa [88] studied flux phases in the kagome lattice, which is the planar section of ferromagnetic textured pyrochlores. If the flux is staggered then electrons accumulate a spin Berry phase as they hop. This system contains *isolated* flat bands, *i.e.*, they are protected by a gap. On the other hand, Bergman, Wu and Balents have studied flat bands *without a gap* in similar lattices [4] not threaded by fluxes. In their models, a flat band is degenerate with one or more other bands at a single point, and the touching is topologically protected. Each of the works above has identified interesting, but seemingly disconnected, properties of flat bands.

The purpose of this chapter is to understand the different types of flat band spectra, the conditions to obtain them, and the properties that follow. This chapter is organized around five main findings. First, flat bands can be isolated by breaking time reversal symmetry (TRS). Second, isolated flat bands can be viewed as critical points. On either side of the phase boundary the flat band becomes positively or negatively curved, which corresponds to transitioning from a particle-like to a hole-like band. We also find an anomalous Hall effect on either side of the transition, whose sign depends on whether the band is electron- or particle-like. Third, when the gap between a flat band and its neighboring bands closes with the flat band in the middle, the system is described by a single spin-1 conical-like spectrum. This extends to higher angular momentum the spin-1/2 Dirac-like spectra in topological insulators and in graphene. Forth, we find that the Chern number of the isolated flat band is zero. So as opposed to Landau levels, we get no quantized Hall conductance for this particular flat band.

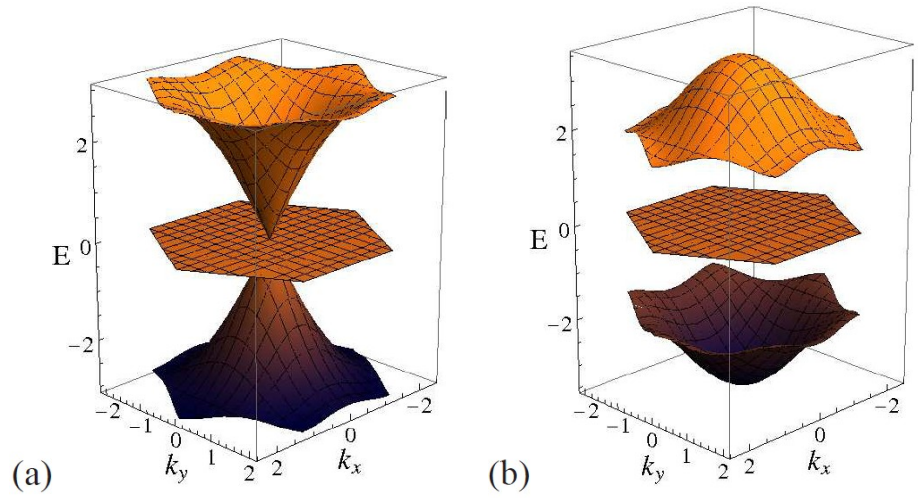

Figure 4.1: Energy dispersions with staggered flux phases ϕ_+ and ϕ_- on the up and down triangles of the kagome lattice . The dispersion on the left, Type I , corresponds to $\phi_+ = 2\pi$ and $\phi_- = -\pi$ while the dispersion on the right, Type II , corresponds to $\phi_+ = \phi_- = 3\pi/2$.

The model which we will analyze is a simple kagome lattice with a tight-binding interaction, and two staggered fluxes, ϕ_+ and ϕ_-, on alternating triangles. Depending on the values of $\phi_\pm$, dispersions can be classified into three Types:

- Type (I): a flat band touches two linearly dispersing bands at the same point, where the linear bands are reminiscent of a "Dirac-like" point, but with spin-1 behavior,
- Type (II): an isolated flat band that is separated from bands above and below by a gap, and
- Type (III): a gapless flat band that touches a single massive energy band either above or below. The energy dispersions corresponding to Types I and II are plotted in Figure 4.1.

Type III has been discussed recently [144, 142, 4] in hexagonal and kagome lattices without magnetic flux, and it was found that in this case the zero gap is protected by topological arguments [4]. Type III has been also shown to exhibit a topological insulator phase in the presence of spin-orbit interactions [40]. Type II appears when electrons accumulate a spin Berry phase as they hop from site to site, which is equivalent to both up and down triangles with the same magnetic flux [88]. Type I necessitates the staggered fluxes $\phi_+ \neq \phi_-$ that we analyze below.

We will show that the condition for a flat band to occur at $E = 0$ is $\phi_+ + \phi_- \equiv \pi \,(\mathrm{mod}\, 2\pi)$. By changing the value of the fluxes in such a way that their sum differs slightly from π, the flat band acquires a small curvature, which can be positive or negative depending on the values of $\phi_\pm$. Interestingly, the band curvature implies that if the Fermi energy is chosen to be zero, then by tuning the fluxes it is possible to change the center of the band from an electron-like pocket to a hole-like pocket. This leads to an inversion of the sign of the anomalous Hall response [44]. Therefore, the flat band condition $\phi_+ + \phi_- \equiv \pi \,(\mathrm{mod}\, 2\pi)$ represents a quantum critical point separating two regions with different anomalous Hall responses.

Type I is remarkable in that it displays linearly dispersing modes, akin to those of graphene, but differing in two important ways. First, the conical points do not appear in pairs as in graphene, but instead there is only one such point within the first Brillouin zone (see Figure 4.1). Second, these are not Dirac fermions (this is why it is possible to evade the doubling problem), but instead the effective Hamiltonian in momentum space is of the form $H = v_F\, \vec{k}\cdot\vec{L}$, where $\vec{L}$ is the spin-1 angular momentum operator (v_F is the Fermi velocity). The spin-1 type spectrum (like the spin-1/2 Dirac

type spectrum of graphene) can be viewed as a single quantum spin in a magnetic field, as in Berry's original work on quantum phases [8], but with the wavevector $\mathbf{k}$ playing the role of the magnetic field. Type I does not require the breaking of TRS. However, we show that a gap can be opened while leaving the flat band untouched by breaking TRS, and thus Type (I) is continuously connected to Type II . In Type II the degenerate states within the flat band are protected by the gap at finite temperature, and would provide a fertile base to construct correlated states.

4.2 Flat zero-mode band in the staggered-flux kagome lattice

Consider the tight-binding Hamiltonian defined on a kagome lattice, where staggered fluxes ϕ_+ and ϕ_- are applied within alternating triangles ("up" and "down" triangles, respectively), as shown in Figure 4.2.

For convenience define the phase factors $\alpha_\pm = e^{i\phi_\pm/3}$. Let $\mathbf{s}_1 = (0,-1)$, $\mathbf{s}_2 = (\sqrt{3}/2, 1/2)$ and $\mathbf{s}_3 = (-\sqrt{3}/2, 1/2)$ be the vectors pointing from the centers of an up triangle to its three down neighbors, and define $d_{\mathbf{k}}^{ij} = e^{-i\mathbf{k}\cdot(\mathbf{s}_i - \mathbf{s}_j)}$, $j = 1, 2, 3$. In momentum space, the Hamiltonian can be written as:

$$H_{\mathbf{k}} = g \begin{pmatrix} 0 & \alpha_+ + \alpha_- d_{\mathbf{k}}^{12} & \overline{\alpha}_+ + \overline{\alpha}_- d_{\mathbf{k}}^{13} \\ \overline{\alpha}_+ + \overline{\alpha}_- d_{\mathbf{k}}^{21} & 0 & \alpha_+ + \alpha_- d_{\mathbf{k}}^{23} \\ \alpha_+ + \alpha_- d_{\mathbf{k}}^{31} & \overline{\alpha}_+ + \overline{\alpha}_- d_{\mathbf{k}}^{32} & 0 \end{pmatrix} , \tag{4.1}$$

where g is the hopping strength. The characteristic polynomial for this matrix is

$$P(E) = -E^3 + g^2 a_1(\mathbf{k})\, E + g^3 a_0(\mathbf{k}) \, , \tag{4.2}$$

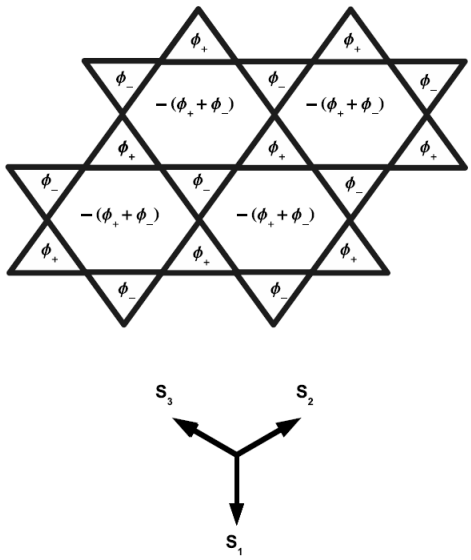

Figure 4.2: The kagome lattice with fluxes ϕ_+ and ϕ_- on alternating triangles, which correspond to a flux $-(\phi_+ + \phi_-)$ inside each hexagon. $\mathbf{s}_{1,2,3}$ are vectors pointing from the center of a down triangle to its three up neighbors.

where

$$\begin{aligned} a_1(\mathbf{k}) &= [3 + \overline{\alpha}_+\alpha_- \, q(\mathbf{k})] + c.c. \\ a_0(\mathbf{k}) &= [(\alpha_+^3 + \alpha_-^3) + (\alpha_+^2\alpha_- + \overline{\alpha}_+\overline{\alpha}_-{}^2)\, q(\mathbf{k})] + c.c. \, , \end{aligned}$$

and $q(\mathbf{k}) = d_{\mathbf{k}}^{12} + d_{\mathbf{k}}^{23} + d_{\mathbf{k}}^{31}$. The condition for a flat ($\mathbf{k}$-independent) band is obtained by setting the overall factor of $q(\mathbf{k})$ in $P(E)$ to zero,

$$g^2\overline{\alpha}_+\alpha_- E + g^3(\alpha_+^2\alpha_- + \overline{\alpha}_+\overline{\alpha}_-{}^2) = 0 \, , \tag{4.3}$$

which is equivalent to

$$E = -g(\alpha_+^3 + \overline{\alpha}_-{}^3) \, . \tag{4.4}$$

Combining Eqs.(4.2), (4.3) and (4.4) gives the following equation for the energy eigen-

values of the flat bands

$$E(E - 4g^2) = 0 \,, \tag{4.5}$$

which has 3 possible solutions:

(a) $E = 0$ flatband: this configuration is achieved for $\phi_+ + \phi_- = \pi \,(\mathrm{mod}\, 2\pi)$;

(b) $E = -2g$ flatband: this configurations is achieved for $\phi_\pm = 2\pi n_\pm$, with $n_\pm$ integer valued numbers;

(c) $E = 2g$ flatband: this configurations is achieved for $\phi_\pm = \pi(2n_\pm + 1)$, with $n_\pm$ integer valued numbers.

The cases $E = \pm 2g$ (Type III) are similar to those discussed in Refs. [144, 142, 4], where the flat band touches a parabolic electron-like band at its bottom (for $E = -2|g|$) or a hole-like band at its top (for $E = +2|g|$). Here we shall focus instead in the case where the flat band is at $E = 0$. In Figure 4.1 (I) and (II) we show two particular choices for $\phi_\pm$, which are representative of what we classify as Types I and II spectra. Type I contains a cone vertex touching at the point $\mathbf{k} = 0$, which we illustrate by setting $\phi_+ = 3\pi$ and $\phi_- = 0$ (this choice of phase can be interpreted as tight-binding hoppings $-g$ for up triangles and $+g$ for down triangles). Type II contains an isolated flat band, which we illustrate by setting $\phi_\pm = 3\pi/2$ (this choice can be interpreted as tight-binding matrix elements $\pm ig$ for hopping anti-clockwise or clock-wise around the triangles). Notice that because $\mathrm{tr}(\, H_{\mathbf{k}}\,) = 0$ and one of the

eigenvalues is $E = 0$, the other two eigenenergies must satisfy $E_+(\mathbf{k}) + E_-(\mathbf{k}) = 0$, so the spectrum is symmetric with respect to zero in both Types I and (II).

The general condition for nodal touching, Type I , can be obtained by requiring that there is another $E = 0$ eigenvalue, so that at least one other band touches the flat band. When such a solution exists, the derivative of the characteristic polynomial $P'(E)$ also has a zero at $E = 0$ for some value of $\mathbf{k}$. This condition translates to

$$a_1(\mathbf{k}) = 0 \Rightarrow \overline{\alpha}_+\alpha_- q(\mathbf{k}) = -3 \,, \tag{4.6}$$

which admits three different solutions:

(A) Nodal point at $\Gamma = (0, 0)$: this Type I configuration is obtained if the condition $\phi_+ - \phi_- = 3\pi + 6\pi n$ is satisfied, where n is an integer, and it is illustrated in Figure 4.1 (I);

(B) Nodal point at $\mathbf{k} = K_+ = (\frac{4\pi}{3\sqrt{3}}, 0)$: this Type I configuration is obtained if the condition $\phi_+ - \phi_- = 5\pi + 6\pi n$ is satisfied, where n is an integer;

(C) Nodal point at $\mathbf{k} = K_- = (-\frac{4\pi}{3\sqrt{3}}, 0)$: this Type I configuration is obtained if the condition $\phi_+ - \phi_- = \pi + 6\pi n$ is satisfied, where n is an integer;

Even though Types (I) and (II) are particle-hole symmetric with a flat band at $E = 0$ and have staggered fluxes obeying the constraint $\phi_+ + \phi_- = \pi \,(\text{mod } 2\pi)$, Type (II) lacks the nodal conditions **(A)**, **(B)** and **(C)** above mentioned.

4.2.1 Nodal touching and the spin-1 cone

Let us now expand the Hamiltonian, in Type I , near the vertex point for small $|\mathbf{k}| = \sqrt{k_x^2 + k_y^2}$. At the same time we move into Type II by applying a slight flux offset from the condition for the touching: $\phi_+ = 3(\pi + \delta)$ and $\phi_- = -3\delta$. We will interpret δ as a "mass" term. To first order in δ and $\mathbf{k}$ the Hamiltonian becomes:

$$\begin{aligned} H_{\mathbf{k}} &= g\,\frac{3}{\sqrt{2}}\,\left[k_x\,L'_x + k_y\,L'_y + 2\sqrt{\frac{2}{3}}\,\delta\,L'_z\right] \\ &= g\,\frac{3}{\sqrt{2}}\,(k_x, k_y, m)\cdot\vec{L}'\,, \end{aligned} \tag{4.7}$$

where $m = 2\sqrt{2/3}\,\delta$. It is straightforward to check that the matrices

$$L'_x = \frac{i}{\sqrt{6}}\begin{pmatrix} 0 & 1 & -1 \\ -1 & 0 & -2 \\ 1 & 2 & 0 \end{pmatrix} \tag{4.8a}$$

$$L'_y = \frac{i}{\sqrt{2}}\begin{pmatrix} 0 & 1 & 1 \\ -1 & 0 & 0 \\ -1 & 0 & 0 \end{pmatrix} \tag{4.8b}$$

$$L'_z = \frac{i}{\sqrt{3}}\begin{pmatrix} 0 & -1 & 1 \\ 1 & 0 & -1 \\ -1 & 1 & 0 \end{pmatrix} \tag{4.8c}$$

satisfy the angular momenta algebra $[L'_x, L'_y] = iL'_z$ (along with the cyclic permutations of x, y and z), and that they have eigenvalues $-1, 0, +1$, *i.e.*, they form a spin-1 representation of $SU(2)$.

The eigenvalues of the Hamiltonian Eq. (4.7) are $E_{\mathbf{k}} = g\,\frac{3}{\sqrt{2}}\,\sqrt{k_x^2+k_y^2+m^2}\;\;\ell_{\mathbf{k}}$, where $\ell_{\mathbf{k}} = -1, 0, +1$ is the eigenvalue of angular momentum along the direction (k_x, k_y, m). Therefore we obtain the three bands, with the flat band being the one with zero angular momentum. The other two bands describe the cone when $\delta = 0$, and two parabolic bands separated from the flat band by a gap $\Delta = g\,2\sqrt{3}\,\delta$ when δ is non-zero. (A particular instance of the $\delta = 0$ spectrum has recently also been predicted in $\mathcal{T}_3$ optical lattices by Bercioux et. al. [3]).

The spin-1 structure has interesting topological properties, namely it can be viewed as a generalization of the Berry phase for the spin-1/2 spectrum of graphene. One implication is that, when the gap is open by breaking TRS, the upper and lower bands have a quantized Hall conductance.

4.2.2 Time reversal and particle-hole symmetries

First, we discuss time reversal symmetry. Consider a tight-binding model of spinless fermions described by

$$\mathcal{H} = \sum_{\mathbf{k}} \psi_i^\dagger(\mathbf{k}) H_{ij}(\mathbf{k}) \psi_j(\mathbf{k}) \;, \tag{4.9}$$

where ψ is an anihilation fermionic operator and $\mathbf{k}$ takes values on the first Brillouin zone. Under time reversal transformation,

$$\mathcal{H} \;\;\rightarrow\;\; \sum_{\mathbf{k}} \psi_i^\dagger(-\mathbf{k}) H_{ij}^*(\mathbf{k}) \psi_j(-\mathbf{k}) = \sum_{\mathbf{k}} \psi_i^\dagger(\mathbf{k}) H_{ij}^*(-\mathbf{k}) \psi_j(\mathbf{k}) \;. \tag{4.10}$$

For $\mathcal{H}$ to be time reversal invariant, one way would be to have $H(\mathbf{k}) = H^*(-\mathbf{k})$. Looking at our Hamiltonian more carefully, though, we see that there is a freedom to

redefine the hopping matrix elements without changing the fluxes ϕ_+ and ϕ_-. This freedom can be mathematically described by the following gauge transformation

$$H(\mathbf{k}) \to \tilde{H}(\mathbf{k}) = \Lambda H(\mathbf{k}) \Lambda^\dagger \,, \tag{4.11}$$

where

$$\Lambda = \begin{pmatrix} e^{i\alpha_1} & 0 & 0 \\ 0 & e^{i\alpha_2} & 0 \\ 0 & 0 & e^{i\alpha_3} \end{pmatrix} . \tag{4.12}$$

Hamiltonians $H(\mathbf{k})$ and $\tilde{H}(\mathbf{k})$ related by the gauge transformation Eq. (4.11) represent physically equivalent descriptions of the system. The requirement of time reversal symmetry, taking into account the gauge invariance given by Eq. (4.11) becomes then

$$H(\mathbf{k}) = \Lambda H^*(-\mathbf{k}) \Lambda^\dagger \,, \tag{4.13}$$

from which we get the following conditions

$$e^{\frac{2i}{3}\phi_\pm} = e^{i(\alpha_1 - \alpha_2)} = e^{i(\alpha_2 - \alpha_3)} = e^{i(\alpha_3 - \alpha_1)} \,. \tag{4.14}$$

Eq. (4.14) immediately implies that symmetry under time reversal is satisfied if $\phi_+ = n_+\pi$ and $\phi_- = n_-\pi$, for integers n_+ and n_- such that $n_+ - n_- = 3l$ (l integer). This is exactly equivalent to the condition for $\phi_\pm$ such that the spectrum has a gapless flat band at $E = 0$, *i.e.*, Type I . Therefore, we conclude, for this given model, that in order to have an isolated flat band *time reversal symmetry must be broken.*

Now consider particle-hole symmetry. The key observation is the following: when the spectrum of $\mathcal{H}$ has three bands, as in the kagome lattice, particle-hole symmetry

only exists when there is a flat band at $E = 0$ and the two other bands have opposite energies. We have already worked out the conditions for the existence of a flat $E = 0$ band in the kagome lattice to be $\phi_+ + \phi_- = \pi$, which also dictates the conditions for particle-hole symmetry (if the Hamiltonian is a traceless matrix). Notice that $\mathcal{H}$ can be particle-hole symmetric without being time reversal invariant. (A spin-1 cone is a situation where both symmetries are present). We will use this important aspect when we calculate the Chern number of the bands in Sec. 4.2.3

4.2.3 Chern numbers for bands in the staggered flux system

Haldane [43] has shown that it is possible for a system to exhibit the quantum Hall effect without Landau levels provided the system breaks TRS. Here we compute explicitly the band Chern numbers in the Type II spectrum of our kagome model.

Recall that when $\phi_+ + \phi_- = \pi$ and $\phi_+ - \phi_- = 3\pi$ we have a flat band with a Dirac point as shown in Figure 4.1. For this choice of fluxes, as discussed previously, the Hamiltonian is time-reversal invariant and the system presents no Hall response (Type I). However, when the flat band is maintained but a gap is opened, time reversal invariance is lost and we have the possibility of bands with non-zero Chern numbers (Type II). We parameterize the gap by a mass term, δ, such that the fluxes $\phi_+ = 2\pi + \delta$ and $\phi_- = -\pi - \delta$. $\delta = 0$ corresponds to a Dirac cone at the center of the Brillouin zone (BZ). For reference we give the complete energy spectrum, although we will expand around small $\vec{k}$ below: $E_\pm = \pm\sqrt{f(\mathbf{k})}$ and $E_0 = 0$, where $f(\mathbf{k}) = 6 - 2\sum_{i,j} \cos\left[\mathbf{k} \cdot (\mathbf{s}_j - \mathbf{s}_i) - 2\delta/3\right]$, and the summation is over the cyclic permutations $(i, j) = (1, 2)$, $(2, 3)$, and $(3, 2)$.

The Chern number of the n-th band is defined as

$$\begin{aligned} C_n &= \frac{-i}{2\pi}\sum_{m\neq n}\sum_{\mathbf{k}\in BZ}\frac{\langle n\mathbf{k}|J_x|m\mathbf{k}\rangle\langle m\mathbf{k}|J_y|n\mathbf{k}\rangle - (J_x \leftrightarrow J_y)}{[\,E_n(\mathbf{k}) - E_m(\mathbf{k})\,]^2} \\ &= \frac{1}{2\pi}\sum_{\mathbf{k}\in BZ}\nabla_{\mathbf{k}}\times\vec{A}_n(\mathbf{k}) \\ &= \frac{1}{2\pi}\sum_{\mathbf{k}\in BZ}B_n(\mathbf{k}). \end{aligned} \tag{4.15}$$

$B_n(\mathbf{k})$ is the field strength associated with the Berry field $\vec{A}_n(\mathbf{k}) = -i\langle n\mathbf{k}|\nabla_{\mathbf{k}}|n\mathbf{k}\rangle$ and $\boldsymbol{J} = (J_x, J_y)$ is the current operator given by $\boldsymbol{J} = \nabla_{\mathbf{k}}H$. One can see that $\sum_n C_n = 0$ by the antisymmetry of C_n as x and y are interchanged. Because the Chern numbers of the bands are topological quantities [120, 87], their values can only change when a band touching occurs. Chosing δ to be very small, an arbitrarily small gap $m \sim \delta$ is opened (still maintaining the flat band) and a near degeneracy appears for $\mathbf{k} \approx 0$. Around this point, the Hamiltonian is that of a spin-1 system with $H_{\mathbf{k}} \approx k_x L_x + k_y L_y + mL_z$.

To perform the summation explicitly it is convenient to define the vector $\boldsymbol{f} \equiv (k_x, k_y, m) \equiv |\boldsymbol{f}|(\sin\theta\cos\phi, \sin\theta\sin\phi, \cos\theta)$, which can be viewed as a magnetic field in momentum space coupled to the spin operator (c.f., Berry [8]). First, we compute the eigenvectors of $H_{\mathbf{k}}$ with the respect to the $z-$axis and then we apply a rotation to bring the spin states to an arbitrary (θ, ϕ) direction. Let $\{|\chi_+\rangle, |\chi_0\rangle, |\chi_-\rangle\}$ be the eigenstates of L_z with eigenvalues $1, 0, -1$ respectively. The eigenvectors of $H_{\mathbf{k}}$ in a general direction (θ, ϕ) are given by

$$|\psi_n\rangle = e^{-i\phi L_z}e^{-i\theta L_y}|\chi_n\rangle\ , \tag{4.16}$$

with $n = +, -, 0$, which in explicit form reads

$$|\psi_+\rangle = |\ e^{-i\phi}\left(\tfrac{1+\cos\theta}{2}\right),\ \ \tfrac{\sin\theta}{\sqrt{2}},\ \ e^{i\phi}\left(\tfrac{1-\cos\theta}{2}\right)\ \rangle \tag{4.17a}$$

$$|\psi_0\rangle = |\ -e^{-i\phi}\tfrac{\sin\theta}{\sqrt{2}},\ \ \cos\theta,\ \ e^{i\phi}\tfrac{\sin\theta}{\sqrt{2}}\ \rangle \tag{4.17b}$$

$$|\psi_-\rangle = |\ e^{-i\phi}\left(\tfrac{1-\cos\theta}{2}\right),\ \ -\tfrac{\sin\theta}{\sqrt{2}},\ \ e^{i\phi}\left(\tfrac{1+\cos\theta}{2}\right)\ \rangle\ , \tag{4.17c}$$

and $H_{\mathbf{k}}|\psi_\pm\rangle = \pm\sqrt{|\mathbf{k}|^2 + m^2}|\psi_\pm\rangle$ and $H_{\mathbf{k}}|\psi_0\rangle = 0$. A straightforward calculation of the the field strengths gives us

$$B_\pm(\mathbf{k}) = \pm\frac{m}{(m^2 + |\mathbf{k}|^2)^{3/2}}\ \ ,\ \ B_0(\mathbf{k}) = 0\ . \tag{4.18}$$

The contribution of these fluxes to the Chern numbers are found to be $\pm\mathrm{sgn}(m)$ and 0. We have also confirmed this result numerically over the entire BZ without linearizing around the Γ point. As we cross the gap, δ (equivalently, m) changes sign and the Chern numbers of the upper and lower bands change sign as well, while the Chern number of the flat band remains zero. Because the topological nature of the Chern numbers, their values will remain unaltered until a new band touching occurs, which will happen for $\delta = \pm\pi$, when the Dirac point moves to one of the corners of the BZ.

4.2.4 Transitioning between electron and hole bands

We now consider deviations from the flat band condition for the case when the middle band is isolated, as in Type II . For concreteness, consider the case $\phi_+ = \phi_- = 3(\pi/2 - \epsilon)$. For small ϵ, the energy of the middle band will be close to $E = 0$, so we can obtain the dispersion for the middle band by dropping the cubic term in the

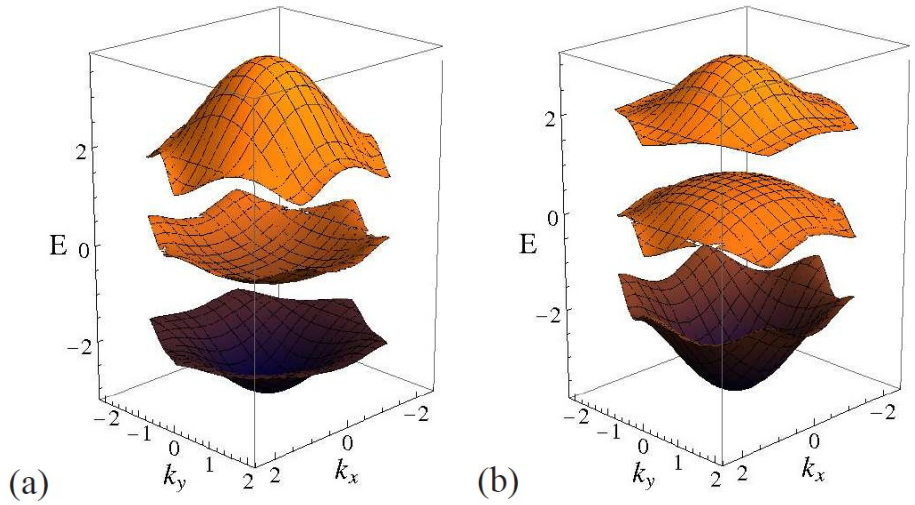

Figure 4.3: Left (right): middle band showing electron (hole)-like dispersion corresponding to $\epsilon < 0 (> 0)$ in Eq. (4.20).

characteristic polynomial $P(E)$:

$$E(\mathbf{k}) = -g\,\frac{a_0(\mathbf{k})}{a_1(\mathbf{k})} + \mathcal{O}(\epsilon^3)\ . \tag{4.19}$$

Expanding $a_0(\mathbf{k}), a_1(\mathbf{k})$ up to order $|\mathbf{k}|^2$ and ϵ, one obtains

$$E(\mathbf{k}) = g\left(4\epsilon - \frac{3\epsilon}{4}\,|\mathbf{k}|^2\right)\ , \tag{4.20}$$

corresponding to a band mass $m_\epsilon = -3\epsilon/2\,g$ for the middle band, so it has a hole-like dispersion for $\epsilon > 0$ and an electron-like dispersion for $\epsilon < 0$, as depicted in Figure 4.3. This trivial mathematical result is physically remarkable in that one can, in principle, change the character of a band from electron-like to hole-like by varying one parameter in the Hamiltonian.

Notice that there is also a band shift $4\epsilon g$, which adds to the chemical potential. There is an interesting result when the chemical potential is fixed to $\mu = 0$: the Fermi surface is pinned and independent of ϵ. It is best to see this effect prior to any

perturbation in ϵ or expansion in $|\mathbf{k}|$. The Fermi surface is in this case the locus of $\mathbf{k}$ points for which $P(E=0)=0$, those that satisfy $a_0(\mathbf{k})=0$. For the electron-like case, the Fermi sea is in the region bounded by the $a_0(\mathbf{k})=0$ surface that contains the Γ-point, whereas for the hole-like case the Fermi sea is the complementary region in the Brillouin zone. The anomalous Hall effect is given by the integral of the Berry curvature over the Fermi sea. As showed in sec. 4.2.3, the Chern number, the Berry curvature integrated over the complete Brillouin zone, for the middle flat band is zero. This means that the sum of the anomalous Hall effect for the electron- and hole-like Fermi seas is zero. Thus, as one tunes across holding $\mu=0$, the anomalous Hall effect will change sign. Of course, by tuning μ one can vary the anomalous Hall effect continuously.

4.3 Summary

Dispersionless bands can be the starting point for constructing strongly correlated electronic states. The lack of electron kinetic energy leads to a macroscopic degeneracy when dispersionless bands are partially filled, and interactions become responsible for lifting the degeneracy and selecting the many-body ground state. This situation is the case for Landau levels, which are flat bands created by an external magnetic field.

In this chapter, we have analyzed different types of spectra that contain flat bands in tight-binding systems in the presence of staggered fluxes. We have seen that it is possible to separate a flat band from the other bands by a gap when time reversal symmetry is broken. In these situations, the flat band can be viewed as a critical

point (with zero curvature) that separates electron-like from hole-like bands, and we can switch between these two curvatures by changing parameters in the Hamiltonian.

When the gap is closed and the flat band lies between two other bands, one obtains a spin-1 conical spectrum, extending to higher angular momentum the spin-1/2 Dirac-like spectra in topological insulators and in graphene.

Although we made progress in understanding several aspects of flat bands, two points remain open questions and deserve further investigation. First, we do not have a generic proof that time reversal symmetry must be broken to isolate a flat band with finite range hopping. Nonetheless, it is natural to speculate that this is true in general, as it holds in all examples that we have found, in addition to the well-known case of Landau levels. And second, in the example discussed here as well as in a class of tight binding models defined on a line graph [65], the flat bands have zero Chern number. Whether this is an intrinsic property of exact flat bands with a finite number of hoppings remains unclear to us. If it is possible, however, to find other examples of flat bands with non-zero Chern number in the absence of an external magnetic field, this could be an interesting scenario for realizing strongly correlated electronic states with topological order. This question will be addressed in Chapter 5.

Chapter 5

Fractional quantum Hall states without an external magnetic field

Abstract

We investigate topological flatbands with non-zero Chern number, where electron-electron interactions are shown to stabilize a fractional quantum Hall state at 1/3 filling of the band. Various properties of these topological bands are discussed and comparisons are drawn with Landau levels.

5.1 Introduction

Haldane [43] has pointed out that Landau levels are not a necessary ingredient for the integer quantum Hall effect. By considering spinless electrons hopping on a honeycomb lattice with a real valued nearest neighbor hopping amplitudes t_1 (as in graphene), Haldane has shown that a second nearest complex hopping t_2 has the effect of splitting the degeneracy of the Dirac points, thus opening a gap between the

valence and the conduction bands. This complex mass parameter has the non-trivial property that it gives the bands a Chern number of magnitude 1. In this way, this system at half-filling becomes a bulk insulator with a single chiral propagating edge mode and exhibits the integer quantum Hall effect.

Given the equivalence between a filled band with a non-zero Chern number (henceforth referred to as a Chern band) and a filled Landau level, as far the integer quantum Hall effect is concerned, it is legitimate to ask - motivated by the fractional quantum Hall effect in a partially filled Landau level - about the effect of strong electronic interactions in a partially filled Chern band.

In Sec. 5.3 we present exact diagonalization results in a small system which show that electron-electron interactions in a dispersionless Chern band give rise to a fractional quantum Hall state at 1/3 filling. This result revealed by numerical diagonalization is rather non-trivial, when one compares the properties of a Chern band with those of Landau levels.

First, we recall that the single-particle wave functions of the lowest Landau level possess special analytic properties, which are not shared by the wave functions belonging to a given Chern band. This analytic properties were explored by Laughlin [70] to propose trial wave functions of the fractional quantum Hall effect at filling fractions $1/(2m+1)$, $m \in \mathbb{Z}$. Second, in a Chern insulator as in Ref. [43] the total flux accumulated in the unit cell by the complex hopping t_2 is *zero*. By varying the phase of t_2, one can change the band gap, but the number of bands is always fixed ($= 2$). This should be contrasted with the Hofstadter model [51], where small changes in the *non-zero* magnetic flux per unit cell have a drastic effect of the spectrum, de-

pending on whether the flux per unit cell, in units of the fundamental flux quantum $\phi_0 = hc/e$, takes rational or irrational values. Third, in semiconductor structure where the FQHE is observed, the magnetic length ℓ_B is typically much larger than the underlying lattice spacing, implying that lattice effects can be neglected to a good approximation. Contrasting to that, in a Chern band the role of the magnetic length is played by the lattice spacing itself, such that no continuum formulation seems to apply. In Sec. 5.4 we make this statement more precise by showing that the minimum width of the Wannier orbitals in a Chern band is of the order $\sqrt{|C|\mathcal{A}_c}$, where C is the Chern number of the band and $\mathcal{A}_c$ is the area of the lattice unit cell.

In this sec. 5.3 we present numerical results of exact diagonalization in a small system which support the fractional quantum Hall effect at 1/3 filling of the Chern band. This result is quite non-trivial in view of the differences discussed above between a Chern band and a Landau level. Nevertheless, we learn that the combination of interactions and the topology of the band represented by the Chern number makes a FQH state favorable over, say, a charge density wave state.

We close this chapter contrasting, in Sec 5.5, the spectrum of neutral mode excitations within the single mode approximation in a dispersionless Chern band with the early result in the LLL [37].

5.2 Non-interacting band models with non-zero Chern number

Consider the noninteracting two-band Bloch Hamiltonian of the generic form

$$H_0 = \sum_{\boldsymbol{k}\in \mathrm{BZ}} \psi^\dagger_{\boldsymbol{k}} \mathcal{H}_{\boldsymbol{k}} \psi_{\boldsymbol{k}}, \qquad \mathcal{H}_{\boldsymbol{k}} = B_{0,\boldsymbol{k}}\sigma_0 + \boldsymbol{B}_{\boldsymbol{k}}\cdot\boldsymbol{\sigma}. \tag{5.1a}$$

Here, BZ stands for the Brillouin zone, $\psi^\dagger_{\boldsymbol{k}} = \left(c^\dagger_{\boldsymbol{k},\mathrm{A}}, c^\dagger_{\boldsymbol{k},\mathrm{B}}\right)$, where $c^\dagger_{\boldsymbol{k},\mathrm{s}}$ creates a Bloch states on sublattice $\mathrm{s} = \mathrm{A}, \mathrm{B}$, and the 2×2 matrices σ_0 and $\boldsymbol{\sigma}$ are the identity matrix and the three Pauli matrices acting on the sublattice indices. If we define

$$\widehat{\boldsymbol{B}}_{\boldsymbol{k}} = \frac{\boldsymbol{B}_{\boldsymbol{k}}}{|\boldsymbol{B}_{\boldsymbol{k}}|}, \quad \tan\phi_{\boldsymbol{k}} = \frac{\widehat{B}_{2,\boldsymbol{k}}}{\widehat{B}_{1,\boldsymbol{k}}}, \quad \cos\theta_{\boldsymbol{k}} = \widehat{B}_{3,\boldsymbol{k}}, \tag{5.1b}$$

we can write the eigenvalues of Hamiltonian $\mathcal{H}_{\boldsymbol{k}}$ as $\varepsilon_{\boldsymbol{k},\pm} = B_{0,\boldsymbol{k}} \pm |\boldsymbol{B}_{\boldsymbol{k}}|$ and for the corresponding orthonormal eigenvectors

$$u_{\boldsymbol{k},+} = \begin{pmatrix} e^{-\mathrm{i}\phi_{\boldsymbol{k}}/2}\cos\frac{\theta_{\boldsymbol{k}}}{2} \\ e^{+\mathrm{i}\phi_{\boldsymbol{k}}/2}\sin\frac{\theta_{\boldsymbol{k}}}{2} \end{pmatrix}, \quad u_{\boldsymbol{k},-} = \begin{pmatrix} e^{-\mathrm{i}\phi_{\boldsymbol{k}}/2}\sin\frac{\theta_{\boldsymbol{k}}}{2} \\ -e^{+\mathrm{i}\phi_{\boldsymbol{k}}/2}\cos\frac{\theta_{\boldsymbol{k}}}{2} \end{pmatrix}. \tag{5.1c}$$

Two examples of Hamiltonians of the form (5.1a) are the following.

Example 1: The honeycomb lattice.— We introduce the vectors $\boldsymbol{a}^t_1 = (0,-1)$, $\boldsymbol{a}^t_2 = \left(\sqrt{3}/2, 1/2\right)$, $\boldsymbol{a}^t_3 = \left(-\sqrt{3}/2, 1/2\right)$ connecting NN and the vectors $\boldsymbol{b}^t_1 = \boldsymbol{a}^t_2 - \boldsymbol{a}^t_3$, $\boldsymbol{b}^t_2 = \boldsymbol{a}^t_3 - \boldsymbol{a}^t_1$, $\boldsymbol{b}^t_3 = \boldsymbol{a}^t_1 - \boldsymbol{a}^t_2$ connecting NNN from the honeycomb lattice depicted in Figure 5.1 (a). We denote with $\boldsymbol{k}$ a wave vector from the BZ of the reciprocal lattice dual to the triangular lattice spanned by $\boldsymbol{b}_1$ and $\boldsymbol{b}_2$, say. The model is then defined

by the Bloch Hamiltonian [43]

$$B_{0,\boldsymbol{k}} = 2t_2 \cos\Phi \sum_{i=1}^{3} \cos \boldsymbol{k}\cdot\boldsymbol{b_i}, \tag{5.2a}$$

$$\boldsymbol{B_k} = \sum_{i=1}^{3} \begin{pmatrix} t_1 \cos \boldsymbol{k}\cdot\boldsymbol{a_i} \\ t_1 \sin \boldsymbol{k}\cdot\boldsymbol{a_i} \\ -2t_2 \sin\Phi \sin \boldsymbol{k}\cdot\boldsymbol{b_i} \end{pmatrix}, \tag{5.2b}$$

where $t_1 \geq 0$ and $t_2 \geq 0$ are NN and NNN hopping amplitudes, respectively, and the real numbers $\pm\Phi$ are the magnetic fluxes penetrating the two halves of the hexagonal unit cell. For $t_1 \gg t_2$, the gap $\Delta \equiv \min_{\boldsymbol{k}}\varepsilon_{+,\boldsymbol{k}} - \max_{\boldsymbol{k}}\varepsilon_{-,\boldsymbol{k}}$ is proportional to t_2. The width of the lower band is $\delta_- \equiv \max_{\boldsymbol{k}}\varepsilon_{-,\boldsymbol{k}} - \min_{\boldsymbol{k}}\varepsilon_{-,\boldsymbol{k}}$. The flatness ratio δ_-/Δ is extremal for the choice $\cos\Phi = t_1/(4t_2) = 3\sqrt{3/43}$, yielding an almost flat lower band with $\delta_-/\Delta = 1/7$ [see Figure 5.1 (c)].

Example 2: The square lattice.— We introduce the vectors $\boldsymbol{x}^t \equiv \left(1/\sqrt{2}, 1/\sqrt{2}\right)$ and $\boldsymbol{y}^t \equiv \left(-1/\sqrt{2}, 1/\sqrt{2}\right)$ connecting NNN from the square lattice as depicted in Figure 5.1 (b). We denote with $\boldsymbol{k}^t = \left(k_x, k_y\right)$ a wave vector from the BZ of the reciprocal lattice dual to the square lattice spanned by $\boldsymbol{x}$ and $\boldsymbol{y}$. The model is then defined by the Bloch Hamiltonian [135]

$$B_{0,\boldsymbol{k}} = 0, \tag{5.3a}$$

$$\begin{aligned} B_{1,\boldsymbol{k}} + \mathrm{i}B_{2,\boldsymbol{k}} = {} & t_1\, e^{-\mathrm{i}\pi/4}\left[1 + e^{+\mathrm{i}\left(k_y - k_x\right)}\right] \\ & + t_1\, e^{+\mathrm{i}\pi/4}\left[e^{-\mathrm{i}k_x} + e^{+\mathrm{i}k_y}\right], \end{aligned} \tag{5.3b}$$

$$B_{3,\boldsymbol{k}} = 2t_2\left(\cos k_x - \cos k_y\right), \tag{5.3c}$$

where $t_1 \geq 0$ and $t_2 \geq 0$ are NN and NNN hopping amplitudes, respectively. The flatness ratio δ_-/Δ is extremal for the choice $t_1/t_2 = \sqrt{2}$, yielding two almost flat

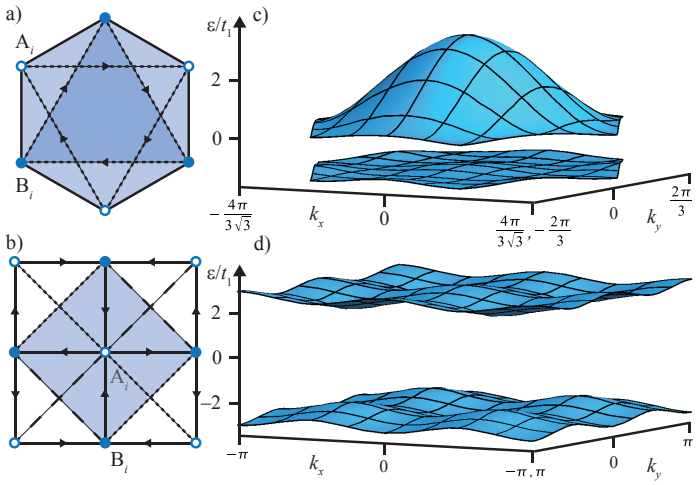

Figure 5.1: (a) Unit cell of Haldane's model on the honeycomb lattice: the NN hopping amplitudes t_1 are real (solid lines) and the NNN hopping amplitudes are $t_2 e^{\mathrm{i}2\pi\Phi/\Phi_0}$ in the direction of the arrow (dotted lines). The flux 3Φ and $-\Phi$ penetrate the dark shaded region and each of the light shaded regions, respectively. For $\Phi = \pi/3$, the model is gauge equivalent to having one flux quantum per unit cell. (b) The chiral-π-flux on the square lattice, where the unit cell corresponds to the shaded area. The NN hopping amplitudes are $t_1 e^{\mathrm{i}\pi/4}$ in the direction of the arrow (solid lines) and the NNN hopping amplitudes are t_2 and $-t_2$ along the dashed and dotted lines, respectively. (c) The band structure of Haldane's model for $\cos\Phi = t_1/(4t_2) = 3\sqrt{3/43}$ with the flatness ratio 1/7. (d) The band structure of the chiral-π-flux for $t_1/t_2 = \sqrt{2}$ with the flatness ratio 1/5. The lower bands can be made exactly flat by adding longer range hoppings.

bands with $\delta_-/\Delta \approx 1/5$ [see Figure 5.1 (d)].

The Chern numbers for the bands labeled by $\pm$ in Eq. (5.1c) are given by

$$C_\pm = \int_{\boldsymbol{k}\in\mathrm{BZ}} \frac{\mathrm{d}^2\boldsymbol{k}}{2\pi\mathrm{i}}\, \epsilon_{\mu\nu} \left(\partial_{k_\mu} u^\dagger_{\boldsymbol{k},\pm}\right) \cdot \left(\partial_{k_\nu} u_{\boldsymbol{k},\pm}\right). \tag{5.4}$$

They have opposite signs if nonzero. All the information about the topology of the Bloch bands of a gaped system is encoded in the single-particle wave functions. For example, the Chern numbers depend solely on the eigenfunctions. Haldane's model (5.2) and the chiral-π-flux (5.3) are topologically equivalent in the sense that

both have two bands with Chern numbers ± 1.

It is yet possible to add a sublattice-staggered chemical potential μ_s that competes with the time-reversal symmetry breaking mass t_2. For the chiral π-flux phase model this is achieved via the substitution $B_{3,\boldsymbol{k}} \to B_{3,\boldsymbol{k}} + 4\mu_{\rm s}$ in Eq. 5.3. Then, defining the dimensionless ration $g \equiv \mu_{\rm s}/t_2$, the two noninteracting bands have a Chern number ± 1 for $g < 1$ and a vanishing Chern number for $g > 1$ with a topological phase transition at the gap closing point $g = 1$.

In order to allow for the possibility of a strongly correlated state, the kinetic effects have to be minimized relative to the inter-particle interactions. In this respect, Landau levels (if one disregards the effects of disorder) form one of the best platforms for the onset of strongly correlated states. On the lattice, the analog of a completely degenerate band with a Chern number is obtained via the Hamiltonian

$$\mathcal{H}_{\boldsymbol{k}}^{\rm flat} \equiv \frac{\mathcal{H}_{\boldsymbol{k}}}{\varepsilon_{\boldsymbol{k},-}}. \tag{5.5}$$

The lowest energy band of this flattened Hamiltonian is degenerate with eigenvalue -1. The flattening procedure does not change the eigenspinors (5.1c) and, thus, does not change the Chern numbers. Typically Hamiltonian (5.1a) is associated with a problem with a finite number of hopping elements, while Hamiltonian (5.5) contains longer range hopping elements, however locally is still preserved by the fact that the longer ranged hoppings decay exponentially due to the non-zero single particle gap.

5.3 Fractional quantum Hall effect at 1/3 filling of the lowest Chern band: A numerical study

An exact diagonalization study [1] is performed to show the existence of a gapped topological ground state for the chiral π-flux phase (5.3) in the presence of interactions. We consider an interaction defined by the repulsive two-body NN potential V according to

$$H_{\text{int}} = V \sum_{\langle ij \rangle} \rho_i \rho_j, \qquad V > 0. \tag{5.6}$$

Directed NN bonds of the square lattice $\Lambda = \text{A} \cup \text{B}$ made of the open and filled circles of Figure 5.1 (b) are here denoted by $\langle ij \rangle$, while ρ_i is the occupation number on the site $i \in \Lambda$.

In order to maximally enhance the effect of interactions, we flatten the lowest energy band of the chiral π-flux phase (5.3) as in (5.5) and perform the numerical diagonalization of the interaction Hamiltonian (5.6) projected into the lowest band.

We work in a lattice of 3×6 unit cells as depicted in Figure 5.1 (b) having $N_{\text{p}} = 6$ particles, corresponding to a filling $\nu = 1/3$ of the total number of states that make up the lowest band.

Two distinctive properties of such a ground state $|\Psi\rangle$ at filling fraction ν (where ν^{-1} is an odd integer) and with periodic boundary conditions (toroidal geometry) are (i) the ν^{-1}-fold topological degeneracy of the ground state manifold and (ii) the quantization of the Hall conductance σ_{xy} in units of $\nu e^2/h$. The Hall conductance

[1] The numerical diagonalization presented in this section was performed by Titus Neupert and appeared in "Fractional quantum Hall states at zero magnetic field," Titus Neupert, Luiz Santos, Claudio Chamon and Christopher Mudry, *Phys. Rev. Lett.* **106**, 236804 (2011).

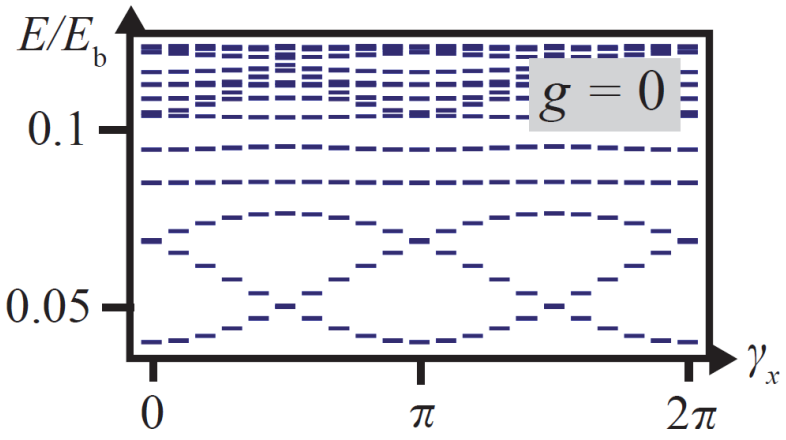

Figure 5.2: The lowest eigenvalues of $H_0^{\text{flat}} + H_{\text{int}}$ for the chiral π-flux phase obtained from exact diagonalization for 6 particles on a 3×6 sublattice A (1/3 filling), normalized by the bandwidth E_{b} subject to twisted boundary conditions as a function of the twisting angle γ_x for $\mu_{\text{s}} = 0$, $t_2 = t_1/\sqrt{2}$ ($g \equiv \mu_{\text{s}}/t_2 = 0$). The level crossings indicate the topological nontrivial nature of the three lowest states.

is related to the Chern-number C of the many-body ground state $|\Psi\rangle$ as $\sigma_{xy} = Ce^2/h$ [87]. Conventionally, the Chern-number is evaluated using twisted boundary conditions

$$\langle \boldsymbol{r} + N_x \boldsymbol{x} | \Psi_{\boldsymbol{\gamma}} \rangle = e^{\mathrm{i}\gamma_x} \langle \boldsymbol{r} | \Psi_{\boldsymbol{\gamma}} \rangle \quad \text{and} \quad \langle \boldsymbol{r} + N_y \boldsymbol{y} | \Psi_{\boldsymbol{\gamma}} \rangle = e^{\mathrm{i}\gamma_y} \langle \boldsymbol{r} | \Psi_{\boldsymbol{\gamma}} \rangle, \tag{5.7}$$

where $\boldsymbol{\gamma}^t = (\gamma_x, \gamma_y)$ is the twisting angle and $N_{\text{c}} \equiv N_x \times N_y$ the number of unit cells. The Chern number is then given by [86]

$$C = \frac{1}{2\pi \mathrm{i}} \int\limits_{\boldsymbol{\gamma} \in [0,2\pi]^2} \mathrm{d}^2 \boldsymbol{\gamma}\, \boldsymbol{\nabla}_{\boldsymbol{\gamma}} \wedge \left\langle \Psi_{\boldsymbol{\gamma}} \left| \boldsymbol{\nabla}_{\boldsymbol{\gamma}} \right| \Psi_{\boldsymbol{\gamma}} \right\rangle . \tag{5.8}$$

The main features of the numerical results displayed in Figure 5.2, which support the $\nu = 1/3$ FQHE are:

- 3 low lying states at the *same* momentum total momentum $\boldsymbol{Q} \equiv \boldsymbol{k}_1 + \cdots +$

$\boldsymbol{k}_{N_\mathrm{p}}$. Because the Hamiltonian of the system is translation invariant, the many-body states can be classified according to different momentum sectors, since the Hamiltonian does not mix states with different momenta. For the 3 low lying states, however, the fact that they are in the same momentum sector causes their degeneracy to be split.

- Upon flux insertion, i.e., upon applying twisted boundary conditions, each one of the 3 topological ground states undergoes two level crossings with the other topological states, as expected for a manifold of 3 ground states with total Chern number $C = 1$ [119].

- Numerical evaluation yields $C = 0.29$, where we attribute the deviations from $C = 1/3$ to the limitations of the small system size.[2]

The fact that the three ground states have the same lattice momentum $\boldsymbol{Q}$ rules out the possibility of a charge density wave, which is a natural competitor of the FQHE. To see that, with 3 degenerate ground states $|\Psi^\alpha_{\boldsymbol{Q}}\rangle$, $\alpha = 1, 2, 3$, at the same momentum $\boldsymbol{Q}$, consider forming a linear combination

$$|\Psi_{\boldsymbol{Q}}\rangle = \sum_{\alpha=1}^{3} c_\alpha \, |\Psi^\alpha_{\boldsymbol{Q}}\rangle. \tag{5.9}$$

A charge density wave is then described by the spatial dependence of the order parameter

$$\langle \widehat{\rho}_{\boldsymbol{r}} \rangle = \langle \Psi_{\boldsymbol{Q}} | \widehat{\rho}_{\boldsymbol{r}} | \Psi_{\boldsymbol{Q}} \rangle = \frac{1}{N_\mathrm{c}} \sum_{\alpha,\alpha'=1}^{3} c^*_{\alpha'} \, c_\alpha \sum_{\boldsymbol{q} \in \mathrm{BZ}} \langle \Psi^{\alpha'}_{\boldsymbol{Q}} | \widehat{\rho}_{\boldsymbol{q}} | \Psi^\alpha_{\boldsymbol{Q}} \rangle \, e^{\,-\mathrm{i}\boldsymbol{q}\cdot\boldsymbol{r}}, \tag{5.10}$$

[2]For a non-degenerate ground state, the the many-body Chern number (5.8) takes only integer values. The value $C = 0.29$ is obtained by "following" one of the three lowest states as γ_x is varied from 0 to 2π. In this way, the Chern number of the ground state manifold is $C_\mathrm{total} = 3 \times \frac{1}{3} = 1$.

where $\widehat{\rho}_{\boldsymbol{r}}$ is the density operator at position $\boldsymbol{r}$ and $\widehat{\rho}_{\boldsymbol{q}}$, its Fourier transform at momentum $\boldsymbol{q}$. Momentum conservation implies that the matrix element $\langle \Psi^{\alpha'}_{\boldsymbol{Q}} | \widehat{\rho}_{\boldsymbol{q}} | \Psi^{\alpha}_{\boldsymbol{Q}} \rangle$ is non-zero only if $\boldsymbol{q} = 0$, which then yields a spatially uniform order parameter $\langle \widehat{\rho}_{\boldsymbol{r}} \rangle$, from which we conclude that $|\Psi_{\boldsymbol{Q}}\rangle$ can not describe a charge density wave state. This, together with the three features listed gives supporting evidence for a 1/3 fractional quantum Hall state on a Chern band with Chern number 1.

5.4 Width of the Wannier states in a Chern band

We now prove a relationship between the Chern number and the spread of the Wannier wavefunctions. We work exclusively with the single-particle eigenstates (5.1c) of the band Hamiltonian (5.1a).

We start with the completeness relation

$$\sum_{\boldsymbol{r}\in A} \sum_{\alpha=A,B} |\, \boldsymbol{r}, \alpha \rangle \, \langle \alpha, \boldsymbol{r} \,| = \mathbb{1} \tag{5.11a}$$

on the bipartite lattice $\Lambda = A \cup B$. The normalized Bloch states $|\varphi_{\boldsymbol{k},\lambda}\rangle$ are defined in terms of the single-particle eigenstates (5.1c) by their overlaps

$$\langle \alpha, \boldsymbol{r} \,| \varphi_{\boldsymbol{k},\lambda} \rangle = \frac{e^{+i\,\boldsymbol{k}\cdot\boldsymbol{r}}}{\sqrt{N_{\mathrm{c}}}}\, u_{\boldsymbol{k},\lambda,\alpha}. \tag{5.11b}$$

The normalization and phase factors are chosen so that the orthonormality condition

$$\langle \varphi_{\boldsymbol{k},\lambda} | \varphi_{\boldsymbol{k},\lambda'} \rangle = \delta_{\lambda,\lambda'} \tag{5.11c}$$

with $\lambda, \lambda' = \pm$ holds for any given wavenumber $\boldsymbol{k} \in \mathrm{BZ}$. The overlap (5.11b) is invariant under the translation $\boldsymbol{k} \to \boldsymbol{k} + \boldsymbol{K}$ for any $\boldsymbol{K}$ that belongs to the reciprocal

lattice of sublattice A owing to the periodicity

$$u_{\boldsymbol{k},\lambda,\alpha} = u_{\boldsymbol{k}+\boldsymbol{K},\lambda,\alpha}. \tag{5.11d}$$

Wannier states are defined in terms of the Bloch states by the unitary transformation

$$|\,\psi_{\boldsymbol{z},\lambda}\rangle = \frac{1}{\sqrt{N_{\rm c}}} \sum_{\boldsymbol{k}\in{\rm BZ}} e^{-i\,\boldsymbol{k}\cdot\boldsymbol{z}}\,|\varphi_{\boldsymbol{k},\lambda}\rangle. \tag{5.12a}$$

The orthonormality (5.11c) of the Bloch states thus carries over to the orthonormality

$$\langle\,\psi_{\boldsymbol{z},\lambda}|\,\psi_{\boldsymbol{z},\lambda'}\rangle = \delta_{\lambda,\lambda'} \tag{5.12b}$$

of the Wannier states. For any λ and α, the representation of the Wannier state on the bipartite lattice $\Lambda = A \cup B$ is the overlap

$$\psi_{\boldsymbol{r},\boldsymbol{z},\lambda,\alpha} \;=\; \langle \boldsymbol{r},\alpha|\,\psi_{\boldsymbol{z},\lambda}\rangle = \frac{1}{N_{\rm c}} \sum_{\boldsymbol{k}\in{\rm BZ}} e^{+i\,\boldsymbol{k}\cdot(\boldsymbol{r}-\boldsymbol{z})}\,u_{\boldsymbol{k},\lambda,\alpha}. \tag{5.12c}$$

We want to estimate the profile in space of the Wannier states (5.12a).

For that purpose, we consider the spread functional

$$R^{(2)}_{\lambda} = \langle\,\psi_{\boldsymbol{z}=0,\lambda}\,|\,\boldsymbol{r}^2|\psi_{\boldsymbol{z}=0,\lambda}\,\rangle - |\,\langle\,\psi_{\boldsymbol{z}=0,\lambda}\,|\,\boldsymbol{r}|\psi_{\boldsymbol{z}=0,\lambda}\,\rangle\,|^2. \tag{5.13}$$

Here, we are assuming, for simplicity, that there is only one band λ that is occupied. If more bands are occupied, we have to carry out a summation over all the occupied bands. Observe that by translational invariance $R^{(2)}_{\lambda}$ is left unchanged under the global translation $\boldsymbol{r},\boldsymbol{z} \to \boldsymbol{r}+\boldsymbol{R},\boldsymbol{z}+\boldsymbol{R}$ for any lattice vector $\boldsymbol{R}$. Hence, the choice $\boldsymbol{z}=0$ in Eq. (5.13) can be done without loss of generality.

We rewrite Eq. (5.13), following Ref. [117], as

$$R^{(2)}_{\lambda} = R^{(2)}_{\mathrm{I}|\lambda} + \tilde{R}^{(2)}_{\lambda}, \tag{5.14a}$$

$$R^{(2)}_{\mathrm{I}|\lambda} = \langle\, \psi_{\boldsymbol{z}=0,\lambda}\,|\,\boldsymbol{r}^2|\psi_{\boldsymbol{z}=0,\lambda}\,\rangle - \sum_{\boldsymbol{z}'} |\,\langle\, \psi_{\boldsymbol{z}=0,\lambda}\,|\,\boldsymbol{r}|\psi_{\boldsymbol{z}',\lambda}\,\rangle\,|^2, \tag{5.14b}$$

$$\tilde{R}^{(2)}_{\lambda} = \sum_{\boldsymbol{z}'\neq\boldsymbol{0}} |\,\langle\, \psi_{\boldsymbol{z}=0,\lambda}\,|\,\boldsymbol{r}|\psi_{\boldsymbol{z}',\lambda}\,\rangle\,|^2. \tag{5.14c}$$

Both $R^{(2)}_{\mathrm{I}|\lambda}$ and $\tilde{R}^{(2)}_{\lambda}$ are non-negative quantities that can be expressed in terms of $\boldsymbol{k}$-space summations as follows. First,

$$\begin{aligned}
R^{(2)}_{\mathrm{I}|\lambda} &= \sum_{j=x,y} \frac{1}{N_{\mathrm{c}}} \sum_{\boldsymbol{k}\in\mathrm{BZ}} \Big[\Big(\partial_{k_j} u^{\dagger}_{\boldsymbol{k},\lambda}\Big) \Big(\partial_{k_j} u_{\boldsymbol{k},\lambda}\Big) - \Big(\partial_{k_j} u^{\dagger}_{\boldsymbol{k},\lambda}\; u_{\boldsymbol{k},\lambda}\Big) \Big(u^{\dagger}_{\boldsymbol{k},\lambda}\; \partial_{k_j} u_{\boldsymbol{k},\lambda}\Big) \Big] \\
&= \sum_{j=x,y} \frac{1}{N_{\mathrm{c}}} \sum_{\boldsymbol{k}\in\mathrm{BZ}} \Big[\langle\, \partial_{k_j} u_{\boldsymbol{k},\lambda}\,|\,\partial_{k_j} u_{\boldsymbol{k},\lambda}\rangle - \langle\, \partial_{k_j} u_{\boldsymbol{k},\lambda}\,|\,u_{\boldsymbol{k},\lambda}\rangle\langle\, u_{\boldsymbol{k},\lambda}\,|\,\partial_{k_j} u_{\boldsymbol{k},\lambda}\,\rangle \Big] \\
&= \sum_{j=x,y} \frac{1}{N_{\mathrm{c}}} \sum_{\boldsymbol{k}\in\mathrm{BZ}} \langle\, \partial_{k_j} u_{\boldsymbol{k},\lambda}\,|\,\big(\mathbb{1} - |\,u_{\boldsymbol{k},\lambda}\,\rangle\,\langle\, u_{\boldsymbol{k},\lambda}|\big)\,|\,\partial_{k_j} u_{\boldsymbol{k},\lambda}\,\rangle \qquad (5.15a) \\
&\equiv \sum_{j=x,y} \frac{1}{N_{\mathrm{c}}} \sum_{\boldsymbol{k}\in\mathrm{BZ}} \langle\, \partial_{k_j} u_{\boldsymbol{k},\lambda}\,|\,Q_{\boldsymbol{k},\lambda}|\,\partial_{k_j} u_{\boldsymbol{k},\lambda}\,\rangle \\
&= \frac{1}{N_{\mathrm{c}}} \sum_{\boldsymbol{k}\in\mathrm{BZ}} \mathrm{tr}\,\big[g_{\boldsymbol{k},\lambda}\big]\,,
\end{aligned}$$

where

$$Q_{\boldsymbol{k},\lambda} \equiv \mathbb{1} - |\,u_{\boldsymbol{k},\lambda}\,\rangle\,\langle\, u_{\boldsymbol{k},\lambda}|, \tag{5.15b}$$

is the single-particle projector operator on all the Bloch states orthogonal to $|\,u_{\boldsymbol{k},\lambda}\,\rangle$, the 2×2 matrix $[g_{\boldsymbol{k},\lambda}]$ has the components

$$g_{\boldsymbol{k},\lambda|i,j} = \mathrm{Re}\,\Big[\,\langle\, \partial_{k_i} u_{\boldsymbol{k},\lambda}\,|\,Q_{\boldsymbol{k},\lambda}|\,\partial_{k_j} u_{\boldsymbol{k},\lambda}\,\rangle\Big]\,, \tag{5.15c}$$

labeled by the Euclidean indices $i,j\in\{x,y\}$ of two-dimensional space, and tr denotes the trace over $i,j\in\{x,y\}$. Second,

$$\tilde{R}^{(2)}_{\lambda} = \sum_{j=x,y} \frac{1}{N} \sum_{\boldsymbol{k}} \big(A_{\boldsymbol{k},\lambda|j} - \bar{A}_{\lambda|j}\big)^2\,, \tag{5.16a}$$

where

$$A_{\boldsymbol{k},\lambda|j} = i\,\langle\, u_{\boldsymbol{k},\lambda}|\,\partial_{k_j} u_{\boldsymbol{k},\lambda}\,\rangle, \tag{5.16b}$$

and

$$\bar{A}_{\lambda|j} = \frac{1}{N}\sum_{\boldsymbol{k}} A_{\boldsymbol{k},\lambda|j} \tag{5.16c}$$

denote the Berry connection and the average of the Berry connection, respectively. Under the gauge transformation

$$|u_{\boldsymbol{k},\lambda}\,\rangle \to e^{i\varphi_{\boldsymbol{k}}}\,|u_{\boldsymbol{k},\lambda}\,\rangle, \tag{5.17}$$

$R^{(2)}_{\mathrm{I}|\lambda}$ remains invariant while $\tilde{R}^{(2)}_{\lambda}$ does not.

We will now establish a lower bound on the gauge invariant quantity $R^{(2)}_{\mathrm{I}|\lambda}$. To this end, we notice that, since $Q_{\boldsymbol{k},\lambda}$ is a projection operator with eigenvalues $0, 1$, then, for any single-particle state $|\Psi_{\boldsymbol{k},\lambda}\rangle$, it follows that

$$\langle\,\Psi_{\boldsymbol{k},\lambda}|Q_{\boldsymbol{k},\lambda}|\Psi_{\boldsymbol{k},\lambda}\,\rangle \geq 0\,. \tag{5.18}$$

In particular, if we choose

$$|\Psi_{\pm,\boldsymbol{k},\lambda}\,\rangle = |\partial_{k_x} u_{\boldsymbol{k},\lambda}\,\rangle \pm i|\partial_{k_y} u_{\boldsymbol{k},\lambda}\,\rangle, \tag{5.19}$$

the inequality (5.18) delivers

$$\mathrm{tr}\,\big[g_{\boldsymbol{k},\lambda}\big] \geq \mp i\,\Big(\langle\,\partial_{k_x} u_{\boldsymbol{k},\lambda}\,|\,\partial_{k_y} u_{\boldsymbol{k},\lambda}\,\rangle - \langle\,\partial_{k_y} u_{\boldsymbol{k},\lambda}\,|\,\partial_{k_x} u_{\boldsymbol{k},\lambda}\,\rangle\Big)\,. \tag{5.20}$$

Summing (5.20) over $\boldsymbol{k}$ and taking the thermodynamic limit $N_{\mathrm{c}} \to \infty$, delivers

$$\begin{aligned} R^{(2)}_{\mathrm{I}|\lambda} &= \frac{\mathcal{A}_c}{(2\pi)^2}\int_{\mathrm{BZ}} d^2\boldsymbol{k}\,\mathrm{tr}\,\big[g_{\boldsymbol{k},\lambda}\big] \\ &\geq \pm\,\frac{\mathcal{A}_c}{2\pi}\int_{\mathrm{BZ}}\frac{d^2\boldsymbol{k}}{2\pi i}\,\Big[\langle\,\partial_{k_x} u_{\boldsymbol{k},\lambda}\,|\,\partial_{k_y} u_{\boldsymbol{k},\lambda}\,\rangle - \langle\,\partial_{k_y} u_{\boldsymbol{k},\lambda}\,|\,\partial_{k_x} u_{\boldsymbol{k},\lambda}\,\rangle\Big] \\ &= \pm\,\frac{\mathcal{A}_c}{2\pi}\,C_\lambda, \end{aligned} \tag{5.21}$$

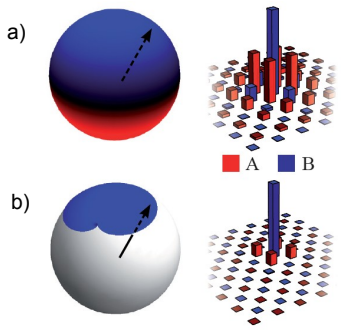

Figure 5.3: Bloch sphere and Wannier orbitals of the chiral π-flux phase (5.3). (a) Left: for a non-zero Chern number, unit vector $\hat{\boldsymbol{B}}(\boldsymbol{k})$ covers the Bloch sphere as $\boldsymbol{k}$ varies over the BZ. Right: The Wannier orbitals are delocalized over many lattice sites, as a consequence of the non-zero Chern number. (b) Left: for a zero Chern number, the unit vector $\hat{\boldsymbol{B}}(\boldsymbol{k})$ only partially covers the Bloch sphere as $\boldsymbol{k}$ varies over the BZ. Right: The Wannier orbitals are more localized than in (a). In the special case $t_2 = 0$ and $\mu_{\rm s} > 0\,(< 0)$, the unit vector $\hat{\boldsymbol{B}}(\boldsymbol{k}) = (0, 0, \pm 1)$ points either to the north or south poles of the bloch sphere and the Wannier are completely localized on a given sublattice.

where $\mathcal{A}_c$ is the area of the unit cell of sublattice A and C_λ are the band-resolved Chern numbers. Since $R^{(2)}_{\mathrm{I}|\lambda} \geq 0$, it then follows

$$R^{(2)}_{\mathrm{I}|\lambda} \geq \frac{\mathcal{A}_c}{2\pi}\,|C_\lambda|, \tag{5.22}$$

as a lower bound, proportional to the band Chern number, on the gauge invariant part of spread of the Wannier states (5.12a). The minimum spread encoded by (5.22) is interpreted as the fact that Chern number does not allow the particles to the localized in a given sublattice, which should be contrasted with the effect of a staggered chemical potential (a non-topological mass) that tends favor sublattice localization (see Figure 5.3). The quantity $\sqrt{\mathcal{A}_c|C_\lambda|}$ has dimensions of length and plays the same role as the magnetic length ℓ_B of the cyclotron orbit of a charge particle in a uniform magnetic field.

5.5 Projected density operator and single-mode approximation in a Chern band

For charged particles in the continuum, the external magnetic field organizes the single-particle spectrum into degenerate Landau levels, whereby two consecutive Landau levels are separated by the energy gap $\hbar\omega_c$. The cyclotron frequency $\omega_c = \hbar/(m_{\rm e}\ell_B^2)$ is proportional to the magnitude B of the uniform magnetic field.

We consider the limit of very strong magnetic fields relative to the characteristic energy scale V of the electron-electron interactions, i.e., $\hbar\omega_c \gg V$. Moreover, we consider a filling fraction $\nu \equiv \Phi/\Phi_0 < 1$ (Φ the magnetic flux and Φ_0 the flux quantum) such that the exact many-body ground state $|\Psi_0\rangle$ does not break spontaneously any symmetry. The translation invariant interacting Hamiltonian $\widehat{H}$ describing a nonvanishing density of spinless fermions moving in a plane perpendicular to an external magnetic field of uniform magnitude B and interacting pairwise with a (screened) Coulomb interaction is then well approximated, as far as low energy properties go, by its projection $\widehat{H}_{\rm LLL}$ onto the vector space spanned by the lowest Landau level.

Upon imposing periodic boundary conditions in an area of linear size L, $\widehat{H}_{\rm LLL}$ is given by

$$\widehat{H}_{\rm LLL} = \sum_{\boldsymbol{q}} v_{\boldsymbol{q}}\, \delta\widehat{\rho}_{-\boldsymbol{q}}\, \delta\widehat{\rho}_{+\boldsymbol{q}}, \tag{5.23a}$$

where

$$v_{\boldsymbol{q}} = v_{\boldsymbol{q}}^* = v_{-\boldsymbol{q}} \tag{5.23b}$$

is the Fourier transform of the screened Coulomb interaction, while

$$\delta\widehat{\rho}_{\boldsymbol{q}} \equiv \widehat{\rho}_{\boldsymbol{q}} - \left\langle\, \Psi_0 \,\middle|\, \widehat{\rho}_{\boldsymbol{q}} \,\middle|\, \Psi_0 \,\right\rangle \tag{5.23c}$$

is the Fourier component of the fermion density operator after projection into the LLL measured relative to its expectation value in the exact many-body ground state $|\Psi_0\rangle$.

Inspired by the early work of Feynman and Bijl in their study of excitations in ^{4}He [23], Girvin, MacDonald and Platzman in Ref. [37] consider the variational state

$$|\phi_{\boldsymbol{k}}\rangle \equiv \delta\widehat{\rho}_{\boldsymbol{k}}\,|\Psi_0\rangle, \tag{5.24}$$

whose energy expectation value $\Delta_{\boldsymbol{k}}$, measured relative to the exact ground state energy E_0, sets a variational upper bound on the spectrum of charge neutral excitations above the ground state $|\Psi_0\rangle$.

Assuming the inversion symmetry

$$\Delta_{+\boldsymbol{k}} = \Delta_{-\boldsymbol{k}}, \tag{5.25a}$$

a direct calculation using Eqs. (5.23) and (5.24) leads to

$$\Delta_{\boldsymbol{k}} = \frac{f_{\boldsymbol{k}}}{s_{\boldsymbol{k}}}, \tag{5.25b}$$

where

$$f_{\boldsymbol{k}} = \frac{1}{2}\,\left\langle \Psi_0 \,\middle|\, \left[\delta\widehat{\rho}_{-\boldsymbol{k}}, \left[\widehat{H}_{\rm LLL}, \delta\widehat{\rho}_{+\boldsymbol{k}}\right]\right] \middle|\, \Psi_0 \right\rangle \tag{5.25c}$$

and

$$s_{\boldsymbol{k}} = \left\langle \Psi_0 \left| \delta\widehat{\rho}_{-\boldsymbol{k}}\,\delta\widehat{\rho}_{+\boldsymbol{k}} \right| \Psi_0 \right\rangle. \tag{5.25d}$$

One recognizes on the right-hand side of Eq. (5.25d) the static structure factor. The insight of Ref. [37] was to realize that the density operators projected onto the LLL close the exact algebra

$$\left[\widehat{\rho}_{\boldsymbol{q}}, \widehat{\rho}_{\boldsymbol{k}}\right] = 2\mathrm{i}\,\sin\left(\frac{1}{2}\,(\boldsymbol{q}\times\boldsymbol{k})\cdot\boldsymbol{e}_3\,\ell_B^2\right)\widehat{\rho}_{\boldsymbol{q}+\boldsymbol{k}} \tag{5.26}$$

(ℓ_B is the magnetic length). In turn, the algebra (5.26) implies that

$$f_{\boldsymbol{k}} \sim |\boldsymbol{k}|^4 \tag{5.27}$$

in the small $|\boldsymbol{k}|$ limit. Hence, in the FQHE, a necessary (but not sufficient) condition for the existence of a finite gap in the thermodynamic limit is to have

$$s_{\boldsymbol{k}} \sim |\boldsymbol{k}|^4 \tag{5.28}$$

also hold in the small $|\boldsymbol{k}|$ limit. In fact, Eq. (5.28) was shown in Ref. [37] to be satisfied when $|\Psi_0\rangle$ is chosen to be any Laughlin state with filling fraction $\nu = 1/m$, where m is an odd integer.

In the spirit of Ref. [37], our starting point is a single-particle Hamiltonian defined on a 2-dimensional lattice. We also assume that there exists at least one band that is independent of the lattice momentum, i.e., a flat band, and, furthermore, that is separated from the other bands by a single-particle gap Δ. We then imagine switching on adiabatically a pairwise interaction that preserves the Bravais lattice point-group symmetry, say a (screened) Coulomb interaction. We shall denote with V the corresponding characteristic interaction energy scale. In the regime for which $\Delta \gg V$, Hamiltonian (5.23) can be reinterpreted as the interacting Hamiltonian projected onto this flat band, provided we identify $v_{\boldsymbol{q}}$ as the Fourier transform with the lattice momentum $\boldsymbol{q}$ of the pairwise fermion interaction, $\delta\widehat{\rho}_{\boldsymbol{q}}$ as the Fourier transform with lattice momentum $\boldsymbol{q}$ of the projected operator describing density fluctuation measured relative to the fermion density with lattice momentum $\boldsymbol{q}$ of the exact many-body ground state $|\Psi_0\rangle$, whereby we assume that $|\Psi_0\rangle$ does not break spontaneously any point-group symmetry of the lattice.

The projected density operator on a flat band reads

$$\widehat{\rho}_{\boldsymbol{k}} = \sum_{\boldsymbol{p}} u^{\dagger}_{\boldsymbol{p}} \cdot u_{\boldsymbol{p}+\boldsymbol{k}}\, \widehat{\chi}^{\dagger}_{\boldsymbol{p}}\, \widehat{\chi}_{\boldsymbol{p}+\boldsymbol{k}} \equiv \sum_{\boldsymbol{p}} M_{\boldsymbol{p},\boldsymbol{k}}\, \widehat{\chi}^{\dagger}_{\boldsymbol{p}}\, \widehat{\chi}_{\boldsymbol{p}+\boldsymbol{k}}, \tag{5.29}$$

where $u_{\boldsymbol{k}}$ denotes the eingespinors of the flatband, while $\widehat{\chi}_{\boldsymbol{k}}$ and $\widehat{\chi}^{\dagger}_{\boldsymbol{k}}$ are the annihilation and creation operators, respectively, of single-particle fermionic eigenstates on the isolated flat band with lattice momentum $\boldsymbol{k}$. Hence, they satisfy the canonical fermionic anticommutation relations

$$\left\{\widehat{\chi}_{\boldsymbol{k}}, \widehat{\chi}_{\boldsymbol{k}'}\right\} = \left\{\widehat{\chi}^{\dagger}_{\boldsymbol{k}}, \widehat{\chi}^{\dagger}_{\boldsymbol{k}'}\right\} = 0, \quad \left\{\widehat{\chi}_{\boldsymbol{k}}, \widehat{\chi}^{\dagger}_{\boldsymbol{k}'}\right\} = \delta_{\boldsymbol{k},\boldsymbol{k}'} \tag{5.30}$$

for any pair $\boldsymbol{k}$ and $\boldsymbol{k}'$ of lattice momentum. In carrying out the program laid out in Eq. (5.25) for a general lattice Hamiltonian with a flat band, one notices two immediate obstacles.

The first one arises from the fact that the commutator of two (projected) density operators does not satisfy the algebra (5.26) valid for the LLL. However, it was noticed in Ref. [89] that, in the limit of small lattice momenta $\boldsymbol{k}$ and $\boldsymbol{k}'$, the commutation relation between two projected density operators reads

$$[\,\widehat{\rho}(\boldsymbol{k}), \widehat{\rho}(\boldsymbol{k}')\,] = \int\limits_{\boldsymbol{p}} \Big[\mathrm{i}\ (\boldsymbol{k} \wedge \boldsymbol{k}') \cdot \boldsymbol{\mathcal{B}}(\boldsymbol{p}) + \cdots\Big]\, \widehat{\chi}^{\dagger}(\boldsymbol{p})\, \widehat{\chi}(\boldsymbol{p}+\boldsymbol{k}+\boldsymbol{k}') \tag{5.31a}$$

in the thermodynamic limit $L \to \infty$, whereby the short-hand notation

$$\int\limits_{\boldsymbol{p}} \equiv \int \frac{\mathrm{d}^2\boldsymbol{p}}{(2\pi/L)^2} \tag{5.31b}$$

is used,

$$\boldsymbol{\mathcal{B}}(\boldsymbol{p}) = -\mathrm{i}\ (\boldsymbol{\nabla} \wedge \boldsymbol{A})\,(\boldsymbol{p}) \tag{5.31c}$$

is the (real-valued) Berry field strength of the flat band, and

$$\boldsymbol{A}(\boldsymbol{p}) = \left(u^\dagger \cdot \boldsymbol{\nabla}\, u\right)(\boldsymbol{p}) \tag{5.31d}$$

is the (imaginary-valued) Berry connection of the flat band, while $\cdots$ in Eq. (5.31a) accounts for higher order terms in powers of $\boldsymbol{k}$ and $\boldsymbol{k}'$. Consequently, Ref. [89] proposed a relationship between 2D Chern bands and Landau levels on the account that, because in a 2D Chern band insulator the integral of the Berry curvature on the Brillouin zone equals the (nonzero) Chern number, replacing $\boldsymbol{\mathcal{B}}(\boldsymbol{p})$ in Eq. (5.31) by its *average*, implies the GMP algebra (5.26) in the long-wavelength limit. However, we would like to stress that for 2D Chern band insulators, the Berry curvature is generically nonuniform; a fact that should be reflected in the exact many-body wavefunction.

The second obstacle to applying the SMA to an interacting lattice model is the fact that no good candidate wavefunction is presently known with which one can compute the static structure factor $s_{\boldsymbol{k}}$ and compare its small $\boldsymbol{k}$ dependence with that of $f_{\boldsymbol{k}}$, as was done by GMP in Ref. [37]. Nevertheless, information about the behavior of $f_{\boldsymbol{k}}$ for small $\boldsymbol{k}$ and the requirement of a finite gap in the thermodynamic limit, i.e., $\Delta_{\boldsymbol{k}} \to \Delta_0 \neq 0$ for $\boldsymbol{k} \to 0$, puts a constraint on the static structure factor for small $\boldsymbol{k}$ and, correspondingly, on the correlations of the exact many-body wavefunction.

In Appendix B.1 we discuss in detail the evaluation of the function $f_{\boldsymbol{k}}$ defined in Eq. (5.25c) to lowest order in $\boldsymbol{k}$. Our main result is that, due to the nonclosure of the density algebra for any 2-dimensional lattice model, the leading contribution to

$f(\boldsymbol{k})$ reads

$$f(\boldsymbol{k}) = \int_{\boldsymbol{q}} \int_{\boldsymbol{p}} \int_{\boldsymbol{p}'} v(\boldsymbol{q}) \Big[(\boldsymbol{k} \wedge \boldsymbol{q}) \cdot \delta\boldsymbol{\mathcal{B}}(\boldsymbol{p}) \Big] \Big[(\boldsymbol{k} \wedge \boldsymbol{q}) \cdot \delta\boldsymbol{\mathcal{B}}(\boldsymbol{p}') \Big] \Big\langle \hat{n}(\boldsymbol{p})\, \hat{n}(\boldsymbol{p}') \Big\rangle$$
$$+ \int_{\boldsymbol{q}} \int_{\boldsymbol{p}} v(\boldsymbol{q})\, \frac{\mathrm{i}}{2}\, (\boldsymbol{k} \wedge \boldsymbol{q}) \cdot \big(\partial_\mu \boldsymbol{\mathcal{B}}\big)\,(\boldsymbol{p}) k^\mu \Big[\Big\langle \delta\widehat{\rho}(-\boldsymbol{q})\, \widehat{\chi}^\dagger(\boldsymbol{p})\, \widehat{\chi}(\boldsymbol{p}+\boldsymbol{q}) \Big\rangle \tag{5.32a}$$
$$- \Big\langle \widehat{\chi}^\dagger(\boldsymbol{p}+\boldsymbol{q})\, \widehat{\chi}(\boldsymbol{p})\, \delta\widehat{\rho}(\boldsymbol{q}) \Big\rangle \Big]$$

where the summation convention is implied over the repeated index $\mu = 1, 2$. In Eq. (5.32a),

$$\hat{n}(\boldsymbol{p}) = \widehat{\chi}^\dagger(\boldsymbol{p})\, \widehat{\chi}(\boldsymbol{p}) \tag{5.32b}$$

is the number operator on the projected Chern band, while

$$\delta\boldsymbol{\mathcal{B}}(\boldsymbol{p}) = \boldsymbol{\mathcal{B}}(\boldsymbol{p}) - \overline{\boldsymbol{\mathcal{B}}} \tag{5.32c}$$

denotes the deviations of the Berry curvature $\boldsymbol{\mathcal{B}}(\boldsymbol{p})$ away from the uniform background value $\overline{\boldsymbol{\mathcal{B}}}$. This uniform background value is defined in such a way that the Chern number

$$\mathrm{C} = \int_{T^2} \frac{\mathrm{d}^2\boldsymbol{p}}{(2\pi)^2} \mathcal{B}(\boldsymbol{p}) \equiv \overline{\mathcal{B}} \int_{T^2} \frac{\mathrm{d}^2\boldsymbol{p}}{(2\pi)^2} \tag{5.33}$$

The result (5.32a) should be contrasted with the calculation in Ref. [37], for which the order $\boldsymbol{k}^2$ term in $f(\boldsymbol{k})$ vanishes identically as a consequence of the algebra (5.26). The formula (5.32a) thus establishes a direct relationship, within the SMA, between the deviations of the Berry field strength away from a uniform configuration and the order $\boldsymbol{k}^2$ contribution to $f(\boldsymbol{k})$

$$f(\boldsymbol{k}) \sim |\boldsymbol{k}|^2 \,. \tag{5.34}$$

The result (5.32a) also indicates that a prerequisite for the existence of a nonvanishing but finite many-body gap to excitations above the many-body ground state is that

the static structure factor $s(\boldsymbol{k})$ has also to vanish as $\boldsymbol{k}^2$ to allow for the possibility of a nonzero ratio $\Delta(\boldsymbol{k}) \equiv f(\boldsymbol{k})/s(\boldsymbol{k})$ and therefore a nonvanishing SMA gap in Eq. (5.25b).

5.6 Conclusions

We have studied the effect of interactions in flatbands with non-zero Chern number, focusing on the simplest example of a two-band model with Chern number 1. Exact diagonalization results on a small system provide supporting evidence of a fractional quantum Hall state at 1/3 filling of the Chern band. At the single particle level, the Chern number is responsible for a delocalization of the Wannier orbitas and the lattice spacing plays the role the "magnetic length". Finally, the analysis within the single-mode approximation of the spectrum on charge neutral excitations above the incompressible ground state in a partially filled Chern band shows that the fluctuations of the Berry field change the leading behavior of the static structure factor - compared to the uniform magnetic field scenario -, which in turn should be reflected in the correlations of the many-body ground state. It remains an interesting open question to try to find out good wave functions describing the FQHE in partially filled Chern bands.

Part III

Topological Field Theories of 2D Fractional Topological Insulators

Chapter 6

Time-reversal symmetric hierarchy of incompressible fluids

Abstract

We provide an effective description of fractional topological insulators that include the fractional quantum spin Hall effect by considering the time-reversal symmetric pendant to the topological quantum field theories that encode the Abelian fractional quantum Hall liquids. We explain the hierarchical construction of such a theory and establish for it a bulk-edge correspondence by deriving the equivalent edge theory for chiral bosonic fields.

6.1 Introduction

Laughlin initiated the theoretical exploration of the fractional quantum Hall effect (FQHE) by proposing wave functions for the ground states of interacting electrons in the lowest Landau level at filling fractions $\nu = 1/(2m+1),\ m \in \mathbb{Z}$. [70] The

experimental observation of a plethora of fractional Hall plateaus at other filling fractions lead to the construction of a hierarchy of wave functions out of Laughlin's wave function, [46, 42, 47, 71, 36, 74, 73] and the development of the composite fermion picture. [59, 60] These approaches were later reconciled, and unified by the effective description of the FQHE in terms of multi-component Chern-Simons theories in $(2+1)$-dimensional space and time. [92, 136, 11, 12, 29, 137, 138, 28] These topological effective theories for the hierarchy of the FQHE deliver a correspondence between the physics in the two-dimensional bulk and the physics along the edges. [69, 45, 129, 132, 131, 27]

It is possible to double the Chern-Simons effective theory representing the universal properties of the FQHE at some filling fraction $\nu = 1/(2m+1),\ m \in \mathbb{Z}$ so as to obtain a time-reversal symmetric theory. This approach has been used to interpret a fully gaped superconductor as an example of a topological phase, [135, 130, 21] and – more generally – to explore the universal properties of interacting theories with an emergent local $\mathbb{Z}_2$ gauge symmetry (see Refs. [95, 133, 81, 107, 78]) that signals the phenomenon of spin and charge separation. [26, 48, 101, 100, 145]

A more urgent impetus for the construction of effective time-reversal symmetric topological field theories in $(2+1)$-dimensional space and time arose with the theoretical prediction of time-reversal symmetric topological band insulators, shortly followed by their experimental discovery. [62, 63, 7, 6, 68] These band insulators realize the counterparts to the integer quantum Hall effect and their discovery suggests that a time-reversal symmetric counterpart to the FQHE might emerge from interacting itinerant electrons in a crystalline environment.

From the outset, this endeavor follows a different line of logic than the FQHE, as it is not based on pre-existing experimental evidence. Past experience with the FQHE has thus guided recent attempts to either construct time-reversal symmetric edge theories or to construct time-reversal symmetric bulk wave functions supporting local excitations carrying fractional quantum numbers. [7, 72, 19, 18, 91, 83, 38]

While numerical support for a time-reversal symmetric topological phase of matter was given by Neupert et al. in their study of a lattice model for interacting itinerant electrons, [83] a description in terms of an effective theory is desirable to reveal the universal properties of such a phase. In Ref. [83], the universal properties such as the topological degeneracies of the ground state manifold were explored with the help of a family of edge theories. In this chapter, we are going to construct the corresponding bulk topological theory by generalizing the hierarchy of Abelian FQHEs to the hierarchy of Abelian fractional quantum spin Hall effects (FQSHEs) in Sec. 6.2. We will show in Sec. 6.3 the correspondence between the bulk theory and the edge theory whose stability to the breaking of translation invariance and residual spin-1/2 U(1) symmetry was studied in Ref. [83].

6.2 Time-reversal symmetric Chern-Simons quantum field theory

Let us start by summarizing some of the results that we will derive in this section. We shall construct a class of incompressible liquids, each of which is the ground state of a time-reversal symmetric (2+1)-dimensional Chern-Simons quantum field theory

that depends on $2N$ flavors of gauge fields $a_{i,\mu}(t,\boldsymbol{x})$, where $i = 1,\ldots,2N$ labels the flavors and $\mu = 0,1,2$ labels the space-time coordinates $x^\mu \equiv (t,\boldsymbol{x})$, with the action

$$\mathcal{S} = \int \mathrm{d}t\, \mathrm{d}^2\boldsymbol{x}\; \epsilon^{\mu\nu\rho} \left(-\frac{1}{4\pi} K_{ij}\; a_{i,\mu}\, \partial_\nu\, a_{j,\rho} + \frac{e}{2\pi}\, Q_i\; A_\mu\, \partial_\nu\, a_{i,\rho} + \frac{s}{2\pi}\, S_i\; B_\mu\, \partial_\nu\, a_{i,\rho} \right). \tag{6.1a}$$

Here, K_{ij} are elements of the symmetric and invertible $2N \times 2N$ integer matrix K. The integer-valued component Q_i of the $2N$-dimensional vector Q represents the i-th electric charge in units of the electronic charge e, which couples to the electromagnetic gauge potential $A_\mu(t,\boldsymbol{x})$. Similarly, S_i is an integer-valued component of the $2N$-dimensional vector S that represents the i-th spin charge in units of s associated to the up or down spin projection along a spin-1/2 quantization axis, which couples to the Abelian (spin) gauge potential $B_\mu(t,\boldsymbol{x})$. The operation of time reversal maps $a_{\mathsf{i},\mu}(t,\boldsymbol{x})$ into $-g^{\mu\nu}\, a_{\mathsf{i}+N,\nu}(-t,\boldsymbol{x})$ for $\mathsf{i} = 1,\cdots,N$ and vice versa. Here, $g_{\mu\nu} = \mathrm{diag}(+,-,-) \equiv g^{\mu\nu}$ is the Lorentz metric. In Eq. (6.1a) $\boldsymbol{x} \in \Omega$, where $\Omega \subset \mathbb{R}^2$ is a region of two-dimensional Euclidean space, which for the discussion of the bulk theory we consider to have no boundary, $\partial\,\Omega = \varnothing$. We will show that time-reversal symmetry imposes that the matrix K and the vectors Q and S are of the block form

$$K = \begin{pmatrix} \kappa & \Delta \\ \Delta^{\mathsf{T}} & -\kappa \end{pmatrix}, \quad Q = \begin{pmatrix} \varrho \\ \varrho \end{pmatrix}, \quad S = \begin{pmatrix} \varrho \\ -\varrho \end{pmatrix}, \tag{6.1b}$$

with ϱ an integer N-vector, while $\kappa = \kappa^{\mathsf{T}}$ and $\Delta = -\Delta^{\mathsf{T}}$ are symmetric and antisymmetric integer-valued $N \times N$ matrices, respectively.

The doubled structure of the theory is even more evident if we express it as a BF

theory, [1] [10, 9] i.e., by defining

$$a^{(\pm)}_{\mathsf{i},\mu} = \frac{1}{2}\left(a_{\mathsf{i},\mu} \pm a_{\mathsf{i}+N,\mu}\right), \qquad \mathsf{i} = 1,\ldots,N\,, \tag{6.2a}$$

for $\mu = 0, 1, 2$. This basis allows to re-express the effective action (6.1a) as

$$\mathcal{S} = \int \mathrm{d}t\, \mathrm{d}^2\boldsymbol{x}\; \epsilon^{\mu\nu\rho}\left(-\frac{1}{\pi}\varkappa_{\mathsf{ij}}\, a^{(+)}_{\mathsf{i},\mu}\,\partial_\nu\, a^{(-)}_{\mathsf{j},\rho} + \frac{e}{\pi}\,\rho_{\mathsf{i}}\, A_\mu \partial_\nu\, a^{(+)}_{\mathsf{i},\rho} + \frac{s}{\pi}\,\rho_{\mathsf{i}}\, B_\mu \partial_\nu\, a^{(-)}_{\mathsf{i},\rho}\right). \tag{6.2b}$$

In this representation, the indices in sans serif fonts i,j run from 1 to N. The coupling between the pair of gauge fields $a^{(+)}$ and $a^{(-)}$ is off-diagonal in the BF labels $\pm$. This is a consequence of time-reversal symmetry, which is implemented by

$$a^{(\pm)}_\mu(t,\boldsymbol{x}) \xrightarrow{\mathcal{T}} \mp g^{\mu\nu}\, a^{(\pm)}_\nu(-t,\boldsymbol{x})\,, \tag{6.2c}$$

that leaves the action (6.2b) invariant. In this representation, the electromagnetic gauge potential A couples to the $+$-species only, while the spin gauge potential B couples to the $-$-species only. The $N \times N$ integer-valued matrix $\varkappa$ in the BF representation is related to the block matrices κ and Δ contained in K from Eq. (6.1b) through

$$\varkappa = \kappa - \Delta. \tag{6.2d}$$

The degeneracy of the ground state is obtained for either description, i.e., the one in terms of the flavors a_i with $i = 1,\cdots,2N$ or the one in terms of the flavors $a^{(\pm)}_{\mathsf{i}}$ with $\mathsf{i} = 1,\cdots,N$, from

$$\mathcal{N}_{\mathrm{GS}} \;=\; \left|\det\begin{pmatrix} 0 & \varkappa \\ \varkappa^{\mathsf{T}} & 0 \end{pmatrix}\right| = (\det\varkappa)^2\,. \tag{6.3}$$

[1] This terminology has no deep meaning. It arose historically in the context of topological field theories and refers to the symbols b and f used to represent a p-form b and the curvature f of a $(d-p)$-form in $(d+1)$-dimensional space and time. [10]

If the underlying microscopic theory describes fermions with a residual spin-1/2 U(1) (easy plane XY) symmetry, it is then meaningful to define the quantized spin Hall resistance

$$\sigma_{\mathrm{sH}} = \frac{e}{2\pi} \times \nu_{\mathrm{s}} \,. \tag{6.4a}$$

The filling fraction ν_{s} is here defined so that it is unity for the integer quantum spin Hall effect and therefore given by

$$\nu_{\mathrm{s}} = \frac{1}{2} Q^{\mathsf{T}} \, K^{-1} \, S = \varrho^{\mathsf{T}} \, \varkappa^{-1} \, \varrho. \tag{6.4b}$$

We now turn to the hierarchical construction of the states described by this quantum field theory. As a warm-up, we begin by reviewing how a one-component Chern-Simons quantum field theory in $(2 + 1)$-dimensional space and time is related to the quantum Hall effect. We then construct recursively the multi-component Chern-Simons quantum field theory in such a way that it respects time-reversal symmetry.

6.2.1 Brief review of the one-component Chern-Simons theory

We start from the Lagrangian density

$$\mathcal{L}_{\mathrm{CS}} = -\frac{p}{4\pi} \, \epsilon^{\mu\nu\lambda} \, a_\mu \, \partial_\nu \, a_\lambda + \frac{e}{2\pi} \, \epsilon^{\mu\nu\lambda} \, A_\mu \, \partial_\nu \, a_\lambda \tag{6.5a}$$

in $(2 + 1)$-dimensional space and time with the action

$$\mathcal{S}_{\mathrm{CS}} = \int\limits_{\mathbb{R}} \mathrm{d}t \int\limits_{\Omega} \mathrm{d}^2 \boldsymbol{x} \, \mathcal{L}_{\mathrm{CS}} \tag{6.5b}$$

and partition function

$$Z_{\mathrm{CS}}[A] = \int \mathcal{D}[a] \, e^{\frac{\mathrm{i}}{\hbar} \mathcal{S}_{\mathrm{CS}}}. \tag{6.5c}$$

The dimensionless integer p is positive. The electromagnetic coupling (electric charge) e is dimensionfull. It measures the strength of the interaction between an external electromagnetic gauge field A with the components $A^\mu \equiv (A^0, \boldsymbol{A})$ and a dynamical gauge field a with the components $a^\mu \equiv (a^0, \boldsymbol{a})$. The symbol $\mathcal{D}[a]$ represents the measure of all gauge orbits stemming from the Abelian group U(1).

The operation $\mathcal{T}$ for reversal of time is defined by

$$a_\mu(t, \boldsymbol{x}) \xrightarrow{\mathcal{T}} +g^{\mu\nu}\, a_\nu(-t, \boldsymbol{x}), \tag{6.6a}$$

$$A_\mu(t, \boldsymbol{x}) \xrightarrow{\mathcal{T}} +g^{\mu\nu}\, A_\nu(-t, \boldsymbol{x}), \tag{6.6b}$$

for $\mu = 0, 1, 2$. We also posit that $\mathcal{T}$ is an anti-unitary linear transformation. If so, one verifies that $\mathcal{L}_{\rm CS}$ is odd under reversal of time.

Define the electromagnetic current to be the 3-vector

$$J^\mu_{\rm CS} \equiv \frac{1}{\hbar}\frac{\delta \mathcal{S}_{\rm CS}}{\delta A_\mu} = \frac{e}{2\pi\hbar}\,\epsilon^{\mu\nu\lambda}\,\partial_\nu\, a_\lambda \tag{6.7a}$$

for $\mu = 0, 1, 2$. Because the Levi-Civita tensor with the component $\epsilon^{012} \equiv 1$ is fully antisymmetric, this current is conserved,

$$\partial_\mu J^\mu_{\rm CS} = 0. \tag{6.7b}$$

Now, the equations of motions

$$0 = \frac{\delta \mathcal{S}_{\rm CS}}{\delta a_\mu} = -\frac{p}{2\pi}\epsilon^{\mu\nu\lambda}\,\partial_\nu\, a_\lambda + \frac{e}{2\pi}\epsilon^{\mu\nu\lambda}\,\partial_\nu\, A_\lambda \tag{6.8}$$

can be used in conjunction with Eq. (6.7) to yield the conserved electromagnetic current

$$J^\mu_{\rm CS} = \frac{1}{p}\,\frac{e^2}{h}\,\epsilon^{\mu\nu\lambda}\,\partial_\nu\, A_\lambda \tag{6.9}$$

which allows us to identify the filling fraction $\nu = p^{-1}$ in this simple example, so that the quantum Hall conductance is given by $\sigma_{\mathrm{H}} = \nu \frac{e^2}{h}$. From now on, we adopt units in which $\hbar = 1$.

6.2.2 One-component BF theory

We start from the Lagrangian density in $(2+1)$-dimensional space and time

$$\mathcal{L}_{\mathrm{BF}}^{\mathrm{TRS}} = -\frac{p}{\pi}\,\epsilon^{\mu\nu\lambda}\,a_\mu^{(+)}\,\partial_\nu\,a_\lambda^{(-)} + \frac{e}{\pi}\,\epsilon^{\mu\nu\lambda}\,A_\mu\,\partial_\nu\,a_\lambda^{(+)} + \frac{s}{\pi}\,\epsilon^{\mu\nu\lambda}\,B_\mu\,\partial_\nu\,a_\lambda^{(-)} \tag{6.10a}$$

with the action

$$\mathcal{S}_{\mathrm{BF}}^{\mathrm{TRS}} = \int\limits_{\mathbb{R}} \mathrm{d}t \int\limits_{\Omega} \mathrm{d}^2\boldsymbol{x}\,\mathcal{L}_{\mathrm{BF}}^{\mathrm{TRS}} \tag{6.10b}$$

and partition function

$$Z_{\mathrm{BF}}^{\mathrm{TRS}}[A,B] = \int \mathcal{D}[a^{(+)},a^{(-)}]\,e^{\mathrm{i}\mathcal{S}_{\mathrm{BF}}^{\mathrm{TRS}}}. \tag{6.10c}$$

Equation (6.10) is a BF theory made of two copies of the Chern-Simons theory (6.5) with the specificity that the integer p enters with opposite signs in the two copies. We have also introduced two external gauge fields A and B with the couplings e and s, respectively. For the gauge field A, e will be interpreted as a total U(1) charge. For the gauge field B, s will be interpreted as a relative U(1) charge. If the underlying microscopic model is built from itinerant electrons, the gauge field A is the U(1) electromagnetic gauge field that couples to the conserved electric charge whereas the gauge field B is the U(1) gauge field that couples to the conserved projection along some quantization axis of the electronic spin, i.e., $s = 1/2$.

This theory is invariant under the operation of time reversal defined by the anti-linear extension of

$$a_\mu^{(\pm)}(t,\boldsymbol{x}) \xrightarrow{\mathcal{T}} \mp g^{\mu\nu}\, a_\nu^{(\pm)}(-t,\boldsymbol{x}) \equiv \mp a^{(\pm)\mu}(\tilde{t},\tilde{\boldsymbol{x}}), \tag{6.11a}$$

$$A_\mu(t,\boldsymbol{x}) \xrightarrow{\mathcal{T}} +g^{\mu\nu}\, A_\nu(-t,\boldsymbol{x}) \equiv +A^\mu(\tilde{t},\tilde{\boldsymbol{x}}), \tag{6.11b}$$

$$B_\mu(t,\boldsymbol{x}) \xrightarrow{\mathcal{T}} -g^{\mu\nu}\, B_\nu(-t,\boldsymbol{x}) \equiv -B^\mu(\tilde{t},\tilde{\boldsymbol{x}}), \tag{6.11c}$$

for $\mu = 0,1,2$. The component A^0 of the external electromagnetic gauge field A is unchanged whereas its vector component $\boldsymbol{A}$ is reversed under reversal of time, just as the vector components of $a^{(-)}$. This behavior is reversed for the components of the external gauge field B that couples to the conserved U(1) spin current and the gauge field $a^{(+)}$.

Since this theory is equivalent to two independent copies of the Chern-Simons theory (6.5), there are two independent conserved currents of the form (6.7),

$$J_\pm^\mu = \frac{e}{\pi}\epsilon^{\mu\nu\lambda}\partial_\nu a_\lambda^{(\pm)}, \tag{6.12}$$

for $\mu = 0,1,2$. Their transformation laws under reversal of time are

$$J_\pm^\mu(x) \xrightarrow{\mathcal{T}} \pm g_{\mu\nu} J_\pm^\nu(\tilde{x}), \tag{6.13}$$

for $\mu = 0,1,2$. If the microscopic model is made of itinerant electrons, we can thus interpret J_+^μ as the charge current and, if the model has a residual U(1) rotation symmetry of the electronic spin, J_-^μ represents the conserved spin current. The equations of motions

$$0 = \frac{\delta \mathcal{S}_{\mathrm{BF}}^{\mathrm{TRS}}}{\delta a_\mu^{(\pm)}} \tag{6.14a}$$

for the dynamical compact gauge fields $a^{(-)}$ and $a^{(+)}$, respectively, deliver the relations

$$\epsilon^{\mu\nu\lambda}\,\partial_\nu\,a^{(+)}_\lambda = \frac{s}{p}\,\epsilon^{\mu\nu\lambda}\,\partial_\nu\,B_\lambda \tag{6.14b}$$

and

$$\epsilon^{\mu\nu\lambda}\,\partial_\nu\,a^{(-)}_\lambda = \frac{e}{p}\,\epsilon^{\mu\nu\lambda}\,\partial_\nu\,A_\lambda, \tag{6.14c}$$

for $\mu = 0, 1, 2$, respectively. We conclude that, on the one hand, the charge current obeys the Hall response

$$J^\mu_+ = 2s \times \frac{e}{2\pi p}\epsilon^{\mu\nu\lambda}\,\partial_\nu\,B_\lambda, \tag{6.15a}$$

with $\mu = 0, 1, 2$ while, on the other hand, the spin current obeys the Hall response

$$J^\mu_- = 2e \times \frac{e}{2\pi p}\,\epsilon^{\mu\nu\lambda}\,\partial_\nu\,A_\lambda, \tag{6.15b}$$

with $\mu = 0, 1, 2$.

6.2.3 Time-reversal symmetric hierarchy

The generic structure of the hierarchical construction is the following. Let $n > 0$ be any positive integer. Define at the level n of the hierarchy the quantum field theory with the partition function

$$Z^{\mathrm{TRS}}_n[A, B] = \int \mathcal{D}\left[a^{(+)}_1, \cdots, a^{(+)}_n, a^{(-)}_1, \cdots, a^{(-)}_n\right] \times e^{\mathrm{i}\mathcal{S}^{\mathrm{TRS}}_n}, \tag{6.16a}$$

where the action is

$$\mathcal{S}^{\mathrm{TRS}}_n = \int\limits_{\mathbb{R}} \mathrm{d}t \int\limits_{\Omega} \mathrm{d}^2\boldsymbol{x}\,\mathcal{L}^{\mathrm{TRS}}_n \tag{6.16b}$$

and the Lagrangian density is

$$\begin{aligned}\mathcal{L}_n^{\mathrm{TRS}} = &-\sum_{\mathsf{i},\mathsf{j}=1}^{n} \frac{1}{\pi}\, \varkappa_{\mathsf{ij}}^{(n)}\, \epsilon^{\mu\nu\lambda}\, a_{\mathsf{i},\mu}^{(+)}\, \partial_\nu\, a_{\mathsf{j},\lambda}^{(-)} + \sum_{\mathsf{i}=1}^{n} \frac{e}{\pi}\, \varrho_{\mathsf{i}}^{(n)}\, \epsilon^{\mu\nu\lambda}\, A_\mu\, \partial_\nu\, a_{\mathsf{i},\lambda}^{(+)} \\ &+ \sum_{\mathsf{i}=1}^{n} \frac{s}{\pi}\, \varrho_{\mathsf{i}}^{(n)}\, \epsilon^{\mu\nu\lambda}\, B_\mu\, \partial_\nu\, a_{\mathsf{i},\lambda}^{(-)}.\end{aligned} \tag{6.16c}$$

Here, the dynamical gauge fields $a^{(\pm)}$ are the n-tuplet with the components

$$\left(a_{\mathsf{i}}^{(\pm)}\right) \equiv \left(a_1^{(\pm)}, \cdots, a_n^{(\pm)}\right)^{\mathsf{T}}. \tag{6.17a}$$

Moreover, the $n \times n$ matrix $\varkappa^{(n)}$ is invertible and has, by assumption, integer-valued matrix elements. The charge vector $\varrho^{(n)}$ has the integer-valued components

$$\varrho^{(n)} = (1, 0, \cdots, 0)^{\mathsf{T}} \in \mathbb{Z}^n. \tag{6.17b}$$

Finally, the compatibility condition

$$(-)^{\varkappa_{\mathsf{ii}}^{(n)}} = (-)^{\varrho_{\mathsf{i}}^{(n)}} \tag{6.17c}$$

for $\mathsf{i} = 1, \cdots, n$ is also assumed.

The operation of time reversal is the rule

$$x^\mu \xrightarrow{\mathcal{T}} \tilde{x}^\mu \equiv -g_{\mu\nu}\, x^\nu \tag{6.18a}$$

together with the anti-linear extension of the rules

$$a_{\mathsf{i}}^{(\pm)\mu}(x) \xrightarrow{\mathcal{T}} \mp g_{\mu\nu}\, a_{\mathsf{i}}^{(\pm)\nu}(\tilde{x}), \tag{6.18b}$$

for $\mu = 0, 1, 2$ and $\mathsf{i} = 1, \cdots, n$ that leaves the Lagrangian density (6.16c) invariant.

The level $n+1$ of the hierarchical construction posits the existence of the pair of quasiparticle 3-currents $j_{\pm,n+1}$ that are conserved, i.e.,

$$\partial_\mu\, j_{\pm,n+1}^\mu = 0. \tag{6.19}$$

It also posits the existence of some *even* integer p_{n+1} and $2n$ integers $l_{\mathsf{i}}^{(+)},\ l_{\mathsf{i}}^{(-)}$ with $\mathsf{i} = 1, \cdots, n$ such that the constraints

$$j^{\mu}_{\pm,n+1} = \frac{\epsilon^{\mu\nu\lambda}}{\pi p_{n+1}} \sum_{\mathsf{i}=1}^{n} l_{\mathsf{i}}^{(\pm)}\, \partial_\nu\, a^{(\pm)}_{\mathsf{i},\lambda} \tag{6.20}$$

for $\mu = 0, 1, 2$ hold. The constraint (6.20) means that any pair of flux quanta, arising when $a_{\mathsf{i}}^{(+)}$ and $a_{\mathsf{i}}^{(-)}$ each support a vortex, creates a quasi-particle with charge $2\, l_{\mathsf{i}}^{(+)}/p_{n+1}$ and spin $2\, l_{\mathsf{i}}^{(-)}/p_{n+1}$ for $\mathsf{i} = 1, \cdots, n$.

This construction can be achieved from the partition function

$$Z^{\mathrm{TRS}}_{n+1}[A, B] = \int \mathcal{D}\left[a_1^{(+)}, \cdots, a_{n+1}^{(+)}, a_1^{(-)}, \cdots, a_{n+1}^{(-)}\right] \times e^{\mathrm{i}\mathcal{S}^{\mathrm{TRS}}_{n+1}}, \tag{6.21a}$$

with the action

$$\mathcal{S}^{\mathrm{TRS}}_{n+1} = \int\limits_{\mathbb{R}} \mathrm{d}t \int\limits_{\Omega} \mathrm{d}^2\boldsymbol{x}\, \mathcal{L}_{n+1} \tag{6.21b}$$

and Lagrangian density

$$\begin{aligned} \mathcal{L}^{\mathrm{TRS}}_{n+1} = \mathcal{L}^{\mathrm{TRS}}_{n} &- \frac{p_{n+1}}{\pi}\, \epsilon^{\mu\nu\lambda}\, a^{(+)}_{n+1,\mu}\, \partial_\nu\, a^{(-)}_{n+1,\lambda} \\ &+ \frac{1}{\pi}\, \epsilon^{\mu\nu\lambda} \sum_{\mathsf{i}=1}^{n} l_{\mathsf{i}}^{(+)}\, a^{(+)}_{\mathsf{i},\mu}\, \partial_\nu\, a^{(-)}_{n+1,\lambda} + \frac{1}{\pi}\, \epsilon^{\mu\nu\lambda} \sum_{\mathsf{i}=1}^{n} l_{\mathsf{i}}^{(-)}\, a^{(-)}_{\mathsf{i},\mu}\, \partial_\nu\, a^{(+)}_{n+1,\lambda}. \end{aligned} \tag{6.21c}$$

Indeed, we can then *define* the conserved quasiparticle currents of type n to be

$$j^{\mu}_{\pm,n+1} \equiv \frac{1}{\pi}\, \epsilon^{\mu\nu\lambda}\, \partial_\nu\, a^{(\pm)}_{n+1,\lambda} \tag{6.22}$$

for $\mu = 0, 1, 2$ and use the equations of motion

$$0 = \frac{\delta \mathcal{S}^{\mathrm{TRS}}_{n+1}}{\delta a^{(\mp)}_{n+1,\mu}} \Longleftrightarrow \frac{p_{n+1}}{\pi} \epsilon^{\mu\nu\lambda} \partial_\nu a^{(\pm)}_{n+1,\lambda} = \frac{\epsilon^{\mu\nu\lambda}}{\pi} \sum_{\mathsf{i}=1}^{n} l_{\mathsf{i}}^{(\pm)}\, \partial_\nu\, a^{(\pm)}_{\mathsf{i},\lambda} \tag{6.23}$$

obeyed by the dynamical gauge fields $a^{(\pm)}_{n+1,\mu}$ to establish that they indeed obey the constraints imposed in Eq. (6.20).

Observe that if we introduce the two $(n+1)$-tuplets $a^{(\pm)}$ given by

$$\left(a_{\mathsf{i}}^{(\pm)}\right)^{\mathsf{T}} \equiv \left(a_1^{(\pm)}, \cdots, a_{n+1}^{(\pm)}\right)^{\mathsf{T}} \tag{6.24a}$$

of dynamical gauge fields, then the Lagrangian $\mathcal{L}_{n+1}^{\mathrm{TRS}}$ defined in Eq. (6.21c) takes the same form as $\mathcal{L}_n^{\mathrm{TRS}}$ defined in Eq. (6.16c) after the substitution $n \to n+1$. The $(n+1)\times(n+1)$ matrix $\varkappa^{(n+1)}$ is then given by

$$\varkappa^{(n+1)} = \begin{pmatrix} \varkappa^{(n)} & -l^{(+)} \\ -l^{(-)\mathsf{T}} & p_{n+1} \end{pmatrix}. \tag{6.24b}$$

The $(n+1)$-component charge vector $\varrho^{(n+1)}$ is given by

$$\varrho^{(n+1)} = (1, 0, \cdots, 0)^{\mathsf{T}} \in \mathbb{Z}^{n+1}, \tag{6.24c}$$

thus imposing a vanishing coupling of the external gauge fields A and B to $a_{n+1}^{(\pm)}$. The compatibility condition

$$(-)^{\varkappa_{\mathsf{ii}}^{(n)}} = (-)^{\varrho_{\mathsf{i}}^{(n)}} \tag{6.24d}$$

for $\mathsf{i} = 1, \cdots, n+1$ holds if and only if the integer p_{n+1} is even.

The representation (6.24) is called the hierarchical representation.

The operation of time reversal obtained from Eq. (6.18) by allowing i to run from 1 up to $n+1$ leaves the Lagrangian of level $n+1$ invariant. Therefore, we have constructed a hierarchical time-reversal symmetric BF theory.

6.2.4 Equivalent representations

We define an equivalence class on all the actions of the form (6.2b) when there exists a linear transformation W with integer valued coefficients and unit determinant

such that

$$\varkappa = W^{\mathsf{T}}\, \varkappa'\, W \tag{6.25a}$$

and

$$\varrho = W^{\mathsf{T}}\, \varrho', \tag{6.25b}$$

between any two given pairs $(\varkappa, \varrho)$ and $(\varkappa', \varrho')$ within an equivalence class.

Example 1: The lower-triangular transformation

$$W^{\mathsf{T}} = \begin{pmatrix} 1 & 0 & \cdots & 0 \\ 1 & -1 & \cdots & 0 \\ \vdots & \vdots & \cdots & \vdots \\ 1 & 0 & \cdots & -1 \end{pmatrix} \tag{6.26a}$$

relates the hierarchical basis characterized by the charge vectors

$$\varrho = (1, 0, \cdots, 0)^{\mathsf{T}} \tag{6.26b}$$

to the so-called symmetric basis characterized by the charge vector

$$\varrho = (1, 1, \cdots, 1)^{\mathsf{T}}. \tag{6.26c}$$

Example 2: The block-diagonal transformation

$$W^{\mathsf{T}} = \begin{pmatrix} \mathbb{1}_{m-1} & & & & \\ & 0 & & -1 & \\ & & \mathbb{1}_{n-1-m} & & \\ & +1 & & 0 & \\ & & & & \mathbb{1}_{N-n} \end{pmatrix} \tag{6.27}$$

with $1 \leq m < n \leq N$ that interchanges $\varkappa_{mm}$ with $\varkappa_{nn}$, $\varkappa_{mn}$ with $-\varkappa_{nm}$, while it substitutes $-\varrho_n$ for ϱ_m and $+\varrho_m$ for ϱ_n.

6.3 Edge theory

In this Section, we study the quantum field theory for $2N$ Abelian Chern-Simons fields as defined in (6.1a) or, equivalently, (6.2b) in a system with a boundary by following a strategy pioneered in Refs. [22] and [134]. However, before relaxing the condition $\partial\,\Omega = \varnothing$, we decompose the action (6.1a) of the bulk theory into

$$\mathcal{S} = \mathcal{S}_K + \mathcal{S}_Q + \mathcal{S}_S, \tag{6.28a}$$

$$\mathcal{S}_K = -\frac{1}{4\pi} \int\limits_{\mathbb{R}} \mathrm{d}t \int\limits_{\Omega} \mathrm{d}^2\boldsymbol{x}\, K_{ij}\, \epsilon^{\mu\nu\rho}\, a_{i,\mu}\, \partial_\nu\, a_{j,\rho}, \tag{6.28b}$$

$$\mathcal{S}_Q = +\int\limits_{\mathbb{R}} \mathrm{d}t \int\limits_{\Omega} \mathrm{d}^2\boldsymbol{x}\, \frac{e}{2\pi}\, Q_i\, \epsilon^{\mu\nu\rho}\, a_{i,\mu}\, \partial_\nu\, A_\rho, \tag{6.28c}$$

$$\mathcal{S}_S = +\int\limits_{\mathbb{R}} \mathrm{d}t \int\limits_{\Omega} \mathrm{d}^2\boldsymbol{x}\, \frac{s}{2\pi}\, S_i\, \epsilon^{\mu\nu\rho}\, a_{i,\mu}\, \partial_\nu\, B_\rho. \tag{6.28d}$$

Notice that we have performed a partial integration in Eq. (6.28c) and Eq. (6.28d) as compared to Eq. (6.1a), so that the gauge fields A and B enter Eq. (6.28) in an explicitly gauge invariant form. In contrast, we are going to make a gauge choice for the fields a_i with $i = 1, \cdots, 2N$ to derive the gauge-invariant effective theory of the edge, once we have relaxed the condition $\partial\,\Omega = \varnothing$.

Let us choose Ω to be the upper-half plane of $\mathbb{R}^2$, i.e.,

$$\Omega = \big\{\, (x, y) \in \mathbb{R}^2 \big|\, y \geq 0 \big\} \tag{6.29}$$

for notational simplicity but without loss of generality. Observe that under the $2N$ independent Abelian gauge transformations of the dynamical Chern-Simons fields

$$a_{i,\mu} \to a_{i,\mu} + \partial_\mu \chi_i \tag{6.30a}$$

for $\mu = 0, 1, 2$ where χ_i with $i = 1, \cdots, 2N$ are real-valued and smooth, the action $\mathcal{S}$ defined in Eq. (6.28) obeys the transformation law

$$\mathcal{S} \to \mathcal{S} + \delta\mathcal{S} \tag{6.30b}$$

with

$$\delta\mathcal{S} = \int\limits_{-\infty}^{+\infty} \mathrm{d}\, t \int\limits_{-\infty}^{+\infty} \mathrm{d}\, x \, \left(\chi_i \, \mathcal{J}_i^2\right)(t, x, 0) \tag{6.30c}$$

and

$$\mathcal{J}_i^2(t, x, y) = \Big[- \frac{1}{4\pi} K_{ij} \, \epsilon^{2\nu\rho} \, \left(\partial_\nu \, a_{j,\rho}\right) + \frac{e}{2\pi} \, Q_i \, \epsilon^{2\nu\rho} \, \left(\partial_\nu \, A_\rho\right) + \frac{s}{2\pi} \, S_i \, \epsilon^{2\nu\rho} \, \left(\partial_\nu \, B_\rho\right) \Big]. \tag{6.30d}$$

The equations of motion

$$K_{ij} \, \epsilon^{\mu\nu\rho} \, \partial_\nu \, a_{j,\rho} = e \, Q_i \, \epsilon^{\mu\nu\rho} \, \partial_\nu \, A_\rho + s \, S_i \, \epsilon^{\mu\nu\rho} \, \partial_\nu \, B_\rho \tag{6.31}$$

for the dynamical gauge field a dictate here that

$$\mathcal{J}_i^\mu(t, x, y) = + \frac{1}{4\pi} K_{ij} \, \epsilon^{\mu\nu\rho} \, \partial_\nu \, a_{j,\rho} \tag{6.32}$$

for $i = 1, \cdots, 2N$ and $\mu = 0, 1, 2$. Hence, the $2N$ components of the quasi-particle 3-current $\mathcal{J}_i$ obey the continuity equation $\partial_\mu \mathcal{J}_i^\mu = 0$ if $\left(\partial_\mu \, \partial_\nu - \partial_\nu \, \partial_\mu\right) a_{i,\rho} = 0$ holds for any $i = 1, \cdots, 2N$ and $\rho = 0, 1, 2$.

We now assume that the $2N$-tuplet χ is constant along the boundary $\partial\Omega$ for all times,

$$\left(\partial_x \chi_i\right)(t, x, y = 0) = \left(\partial_t \, \chi_i\right)(t, x, y = 0) = 0 \tag{6.33}$$

for $i = 1, \cdots, 2N$. In this case, each component χ_i can be pulled outside the integral in Eq. (6.30c) yielding

$$\delta\mathcal{S} = \chi_i \int\limits_{-\infty}^{+\infty} \mathrm{d}\, t \int\limits_{-\infty}^{+\infty} \mathrm{d}\, x \, \mathcal{J}_i^2(t, x, 0). \tag{6.34}$$

Gauge invariance, i.e., $\delta\mathcal{S} = 0$, is then achieved if, in addition to the restriction (6.33), we demand that there is no net accumulation of quasi-particle charge along the boundary arising from the quasi-particle current normal to the boundary, i.e.,

$$0 = \int_{-\infty}^{+\infty} \mathrm{d}\, t \int_{-\infty}^{+\infty} \mathrm{d}\, x\ \mathcal{J}_i^2(t, x, 0). \tag{6.35}$$

Observe that the stronger condition

$$\chi_i(t, x, y = 0) = 0 \tag{6.36}$$

for $i = 1, \cdots, 2N$ achieves gauge invariance, i.e., $\delta\mathcal{S} = 0$, without imposing condition (6.35).

Now that we understand under what conditions the quantum field theory with the action (6.28) is gauge invariant with the choice (6.29) for Ω, we are ready to construct the bulk-edge correspondence. To this end, we are going to extract from the dynamical gauge field a degrees of freedom that are localized on the edge $\partial\Omega$ and invariant under the gauge transformations induced by Eqs. (6.30a), (6.33), and (6.35) on the edge $\partial\Omega$.

6.3.1 Bulk-edge correspondence

We start by fixing the gauge of the $2N$ Abelian Chern-Simons fields through the conditions

$$a_0 = K^{-1}\, V\, a_1. \tag{6.37a}$$

We demand here that V is a symmetric, positive definite $2N \times 2N$ matrix that satisfies

$$V = \Sigma_1\, V\, \Sigma_1, \tag{6.37b}$$

where the $2N \times 2N$ matrices

$$\Sigma_\rho = \sigma_\rho \otimes \mathbb{1}_N, \qquad \rho = 1, 2, 3 \tag{6.37c}$$

are defined by taking the tensor product between any of the Pauli matrices σ_1, σ_2, and σ_3 and the unit $N \times N$ matrix $\mathbb{1}_N$. Condition (6.37b) guarantees that the gauge condition (6.37a) is consistent with reversal of time defined by

$$a_\mu(t, x, y) \xrightarrow{\mathcal{T}} -g^{\mu\nu}\Sigma_1\, a_\nu(-t, x, y). \tag{6.37d}$$

Indeed, the gauge condition (6.37a) then transforms under reversal of time into

$$-\Sigma_1\, a^0(-t, x, y) = K^{-1}\, V\, \Sigma_1\, a_1(-t, x, y), \tag{6.38}$$

which, upon using $K^{-1} = -\Sigma_1\, K^{-1}\, \Sigma_1$, coincides with Eq. (6.37a) if and only if we impose condition (6.37b).

Next, we use the gauge conditions (6.37a) to eliminate the time components a_0 of the dynamical gauge fields from the theory. For that, observe that their equations of motion

$$0 = \frac{\delta \mathcal{S}_K}{\delta a_0} \Longleftrightarrow \partial_1 a_2 - \partial_2 a_1 = 0, \tag{6.39a}$$

which require the vanishing of their field strengths, are automatically satisfied if

$$a_1 = \partial_1 \Phi, \qquad a_2 = \partial_2 \Phi, \tag{6.39b}$$

for

$$(\partial_1 \partial_2 - \partial_2 \partial_1)\, \Phi = 0 \tag{6.39c}$$

then follows if the $2N$ components Φ_i of the vector field Φ are smooth for $i = 1, \cdots, 2N$.

We rewrite the kinetic part (6.28b) of the action (6.28a) using the gauge conditions (6.37a) and the equations of motion (6.39a) and subsequently substitute the gauge fields Φ defined in Eq. (6.39b):

$$\begin{aligned}\mathcal{S}_K &= -\frac{\epsilon^{0\nu\lambda}}{4\pi}\int_{-\infty}^{+\infty}\mathrm{d}t\int_{-\infty}^{+\infty}\mathrm{d}x\int_{0}^{+\infty}\mathrm{d}y\,\left(-a_\nu^\mathsf{T}\,K\,\partial_0\,a_\lambda + a_\nu^\mathsf{T}\,V\,\partial_\lambda\,a_1\right)\\ &= -\frac{\epsilon^{0\nu\lambda}}{4\pi}\int_{-\infty}^{+\infty}\mathrm{d}t\int_{-\infty}^{+\infty}\mathrm{d}x\int_{0}^{+\infty}\mathrm{d}y\,\left(\partial_\nu\Phi\right)^\mathsf{T}\left(K\,\partial_0\,\partial_\lambda\Phi - V\,\partial_\lambda\,\partial_1\Phi\right)\\ &= -\frac{\epsilon^{0\nu\lambda}}{4\pi}\int_{-\infty}^{+\infty}\mathrm{d}t\int_{-\infty}^{+\infty}\mathrm{d}x\int_{0}^{+\infty}\mathrm{d}y\,\partial_\nu\left(\Phi^\mathsf{T}\,K\,\partial_0\,\partial_\lambda\Phi - \Phi^\mathsf{T}\,V\,\partial_\lambda\,\partial_1\Phi\right).\end{aligned} \tag{6.40}$$

We shall demand that $\Phi(t,\boldsymbol{x})$ vanishes for $|\boldsymbol{x}|\to\infty$, in which case

$$\begin{aligned}\mathcal{S}_K &= -\frac{1}{4\pi}\int_{-\infty}^{+\infty}\mathrm{d}t\int_{-\infty}^{+\infty}\mathrm{d}x\,\left(\Phi^\mathsf{T}\,K\,\partial_0\partial_1\Phi - \Phi^\mathsf{T}\,V\,\partial_1\,\partial_1\Phi\right)(t,x,0)\\ &= \frac{1}{4\pi}\int_{-\infty}^{+\infty}\mathrm{d}t\int_{-\infty}^{+\infty}\mathrm{d}x\,\left[\left(\partial_1\Phi\right)^\mathsf{T}\,K\,\partial_0\Phi - \left(\partial_1\Phi\right)^\mathsf{T}\,V\,\partial_1\Phi\right](t,x,0).\end{aligned} \tag{6.41}$$

Under the gauge transformation (6.30a) subject to the constraints (6.33) and (6.35) the $2N$-tuplet Φ transforms as

$$\Phi(t,\boldsymbol{x})\to\Phi(t,\boldsymbol{x})+\chi. \tag{6.42}$$

The fact that χ is independent of time t and space x implies that (a) the edge theory (6.41) is unchanged under Eq. (6.42), as anticipated, and (b) $\left(\partial_1\Phi\right)(t,x,0)$ and $\left(\partial_0\Phi\right)(t,x,0)$ are unchanged under Eq. (6.42) and therefore are physical degrees of freedom at the edge. Their dynamics are controlled by the non-universal matrix V, which is fixed by microscopic details of the physical system near the edge.

So far, we have discussed only the kinetic part of the action. Let us now discuss the couplings to the external gauge potentials A and B given by the actions (6.28c)

and (6.28d), respectively. We assume that the external gauge field A is chosen so that (i) all its components are independent of y, i.e.,

$$A_\mu(t,x,y) = A_\mu(t,x), \tag{6.43a}$$

for $\mu = 0,1,2$ and (ii) they generate the Maxwell equations in a one-dimensional space defined by the boundary $y = 0$, i.e.,

$$A_2(t,x) = 0 \tag{6.43b}$$

for all times t and for all positions x along the one-dimensional boundary $y = 0$. Using (i) and (ii), we can recast $\mathcal{S}_Q$ as

$$\begin{aligned}
\mathcal{S}_Q &= +\frac{e}{2\pi}\int\limits_{\mathbb{R}} \mathrm{d}t \int\limits_{\Omega} \mathrm{d}^2\boldsymbol{x}\, Q_i\, \epsilon^{2\nu\rho}\, a_{i,2}\, \partial_\nu\, A_\rho \\
&= +\frac{e}{2\pi}\int\limits_{\mathbb{R}} \mathrm{d}t \int\limits_{\Omega} \mathrm{d}^2\boldsymbol{x}\, Q_i\, \epsilon^{2\mu\nu}\, \partial_2\, \left(\Phi_i \partial_\mu\, A_\nu\right) \\
&= -\frac{e}{2\pi}\int\limits_{-\infty}^{\infty} \mathrm{d}t \int\limits_{-\infty}^{\infty} \mathrm{d}x\, \left(\epsilon^{\mu\nu}\, A_\mu\, Q^{\mathsf{T}}\, \partial_\nu\, \Phi\right)(t,x,0).
\end{aligned} \tag{6.44}$$

On the last line, the Levi-Civita tensor is defined for $(1+1)$ space and time.

Furthermore, the very same manipulations that lead to Eq. (6.44) can be carried out on $\mathcal{S}_S$ to deliver

$$\mathcal{S}_S = -\frac{s}{2\pi}\int\limits_{-\infty}^{+\infty} \mathrm{d}t \int\limits_{-\infty}^{+\infty} \mathrm{d}x\, \left(\epsilon^{\mu\nu}\, B_\mu\, S^{\mathsf{T}}\, \partial_\nu\, \Phi\right)(t,x,0). \tag{6.45}$$

Finally, the operation of time reversal stated in Eq. (6.37d) in the bulk reduces on the boundary to the transformation law

$$a_1(t,x) = \left(\partial_x \Phi\right)(t,x) \xrightarrow{\mathcal{T}} \Sigma_1\, a_1(-t,x) = \left(\partial_x\, \Sigma_1\, \Phi\right)(-t,x). \tag{6.46}$$

The transformation law of the $2N$-tuplet Φ under reversal of time is thus only fixed unambiguously up to an additive constant $2N$-tuplet. The choice

$$\Phi(t,x) \xrightarrow{\mathcal{T}} \Sigma_1\,\Phi(-t,x) + \pi K^{-1}\,\Sigma^{\downarrow}\,Q, \tag{6.47a}$$

with

$$\Sigma^{\uparrow} = \frac{1}{2}\left(\Sigma_0 + \Sigma_3\right), \qquad \Sigma^{\downarrow} = \frac{1}{2}\left(\Sigma_0 - \Sigma_3\right), \tag{6.47b}$$

guarantees that at least one Kramers doublet of fermions exists as local fields in the edge theory, as was shown in Ref. [83].

6.4 Summary

In this chapter, we first derived a hierarchy of FQSHEs, the universal properties of which are encoded by equivalence classes of BF theories of the form

$$\mathcal{L} = -\frac{1}{\pi}\epsilon^{\mu\nu\lambda}\,a_\mu^{(+)\mathsf{T}}\,\varkappa\,\partial_\nu\,a_\lambda^{(-)} + \frac{e}{\pi}\epsilon^{\mu\nu\lambda}\,A_\mu\,\varrho^{\mathsf{T}}\,\partial_\nu\,a_\lambda^{(+)} + \frac{s}{\pi}\epsilon^{\mu\nu\lambda}\,B_\mu\,\varrho^{\mathsf{T}}\,\partial_\nu\,a_\lambda^{(-)}. \tag{6.48}$$

The $N \times N$ invertible and integer-valued matrix $\varkappa$ couples the N flavors of the dynamical gauge field $a^{(+)}$ to the N flavors of the dynamical gauge field $a^{(-)}$. The N-tuplets $a^{(+)}$ and $a^{(-)}$ also couple linearly to the external gauge fields A and B, respectively, through the vector $\varrho \in \mathbb{Z}^N$, where the integer ϱ_{i} shares the same parity as the integer $\varkappa_{\mathsf{ii}}$ for $\mathsf{i} = 1, \cdots, N$. Correspondingly, there exists two independent conserved currents, a charge current associated to the gauge field $a^{(+)}$ and a spin current associated to the gauge field $a^{(-)}$.

Time-reversal symmetry implies the vanishing of the charge Hall conductivity

$$\sigma_{\mathrm{H}} = \frac{e^2}{2\pi} \times \nu = 0. \tag{6.49}$$

The non-vanishing spin filling fraction

$$\nu_{\mathrm{s}} = \varrho^{\mathsf{T}} \varkappa^{-1} \varrho \tag{6.50a}$$

can be interpreted as the spin Hall conductance

$$\sigma_{\mathrm{sH}} = \frac{e}{2\pi} \times \nu_{\mathrm{s}} \tag{6.50b}$$

if the U(1) conservation law associated to the current of $a^{(-)}$ arises microscopically from a residual spin-1/2 U(1) (easy plane XY) symmetry. The topological ground state degeneracy, if two-dimensional space Ω has a toroidal geometry,

$$(\det \varkappa)^2 \tag{6.51}$$

is always the square of an integer as a consequence of time-reversal symmetry. Equivalent pairs $(\varkappa, \varrho)$ and $(\varkappa', \varrho')$, as defined by Eq. (6.25), share the same spin Hall conductivity and topological degeneracy.

The theory (6.48) is topological when two-dimensional space Ω has no boundary, i.e., the Hamiltonian density associated to the Lagrangian density (6.48) vanishes. This is not true anymore if the boundary $\partial\Omega$ is a one-dimensional manifold. We have shown that imposing gauge invariance delivers a gapless theory with all excitations propagating along the boundary $\partial\Omega$. These excitations can all be constructed out of N pairs of counter-propagating chiral bosons whose non-universal velocities along the boundary $\partial\Omega$ derive from a gauge-fixing condition. The stability of this edge theory to the (time-reversal symmetric) breaking of translation invariance along the boundary (including the breaking of the spin conservation law associated to the spin vector S) was studied in Ref. [83].

Chapter 7

Conclusion and perspectives

Modern condensed matter physics makes ever more use of concepts from topology. Since the discovery of the quantum Hall effect (QHE) in semiconductor heterostructures, a wide range of physical phenomena in condensed matter are known to be of topological origin. Recently, band insulators were shown to be divided into two categories: "trivial" insulators and topological insulators (TI). TI's, besides a gap separating valence and conduction bands, have robust gapless surface states, which are protected from localization by disorder provided time-reversal symmetry is not broken. Similarly to the topological invariant (Chern number) characterizing the QHE, an invariant index carrying information about the topology of the band structure determines whether the insulator belongs to the "trivial" or to the topological class. The recent extensive classification of topological phases has so far been almost entirely within the realm of non-interacting systems, with interactions being regarded as a small perturbation. It is inevitable, though, to raise the question as to what happens in the regime where the band structure is topologically non-trivial and concomitantly the interaction strength is large compared with kinetic effects such

that the single particle picture breaks down. Do interactions stabilize a many-body ground state that inherits the band's topological characteristics?

In Chapter 4 we have studied conditions to obtain flat band models as a natural platform for strongly correlated physics and in Chapter 5 we have began to address the interplay between topology and strong interactions by demonstrating that models with partially filled flat bands with non-zero Chern number give rise to the FQHE without an external magnetic field, despite the fact that no obvious connection *a priori* existed between the lattice problem and the FQHE observed in semiconductor heterostructures in the presence of a large uniform magnetic field. Surrounding this topic, there are still many open and relevant questions, which deserve further investigation and go beyond the scope of this thesis, such as: What are the similarities and, more interestingly, the differences between these FQHE states on a Chern band and the ones observed in semiconductor heterostructures? Are there materials with such non-trivial flat bands with a hierarchy of energy scales capable of realizing quantum Hall phases at temperatures much higher than the typically low temperature scales required in order to observe the QHE in semiconductors with an external magnetic field? What is the relation between the Chern number, the filling fraction and the hierarchy of FQHE states that can be achieved?

On another front, a challenge that lies ahead is the search, in theory and in experiment, for strongly interacting phases with time reversal symmetry. In 2D, the FQHE is the quintessential strongly correlated topological phase and it is sometimes possible to conceptually visualize time-reversal invariant topological states in 2D in terms of time-reversed pairs of FQH states. In Chapter 6 we have explored this con-

nection to establish a hierarchical construction of such time-reversal invariant fluids with fractionalized excitations. In 3D, on the other hand, the absence of quantum Hall effect calls for a fresh look at the question of how to think about strongly interacting topological systems. In other words, it remains a vary challenging question to determine - if it exists - what would be the quintessential strongly correlated system in 3D playing the analogous role of the FQHE in 2D. Besides, given a time-reversal invariant interacting Hamiltonian, no guarantee exists that the ground state will also be time-reversal invariant, for the presence of strong interactions can, in principle, break time-reversal symmetry spontaneously, which could lead to many interesting phases.

Topological states of matter have gained a renewed interest in recent years for their potential applications to Topological Quantum Computation, which proposes to overcome decoherence effects by working with qubits made out of delocalized excitations of a many-body quantum state. One of the most discussed realizations of such protected qubits is via pairs of Majorana fermions in spatially separated superconductor vortices. Central to the ability of creating qubits immune to decoherence is the parity of the number of Majorana fermions per vortex. In Chapter 2, we have elucidated the mechanism behind the stability of Majorana qubits in 2D lattice systems with a free particle band structure containing "Dirac particles", similar to that of graphene. The obstacle imposed by the fermion doubling to the construction of decoherent free qubits is overcome by fermion masses which break time-reversal symmetry and compete with the superconductor order parameter, thus allowing the possibility of an odd number of Majorana fermions per vortex. Motivated by the important consequences

of fermion zero modes, either as Majorana fermions in superconductors, or for the phenomenon of fractionalization in charge conserving systems, we have developed in Chapter 3 a method for counting the number of zero modes bound to a point defect.

Appendix A

Appendix to Chapter 3

A.1 Counting the zero modes with the induced charge

In this Appendix, we review an identity that relates the total number of zero modes of any single-particle Hamiltonian $\mathcal{H}$ with charge-conjugation symmetry to its Euclidean Green function $\mathcal{G}(\omega) = (\mathrm{i}\omega - \mathcal{H})^{-1}$. This identity appears implicitly in Ref. [112] and explicitly in Ref. [58]. [139] We will only assume that the single-particle Hamiltonian $\mathcal{H}$ has the property that there exists a transformation $\mathcal{C}$ such that

$$\mathcal{C}^{-1}\,\mathcal{H}\,\mathcal{C} = -\mathcal{H}, \tag{A.1}$$

whereby the transformation $\mathcal{C}$ is norm preserving, i.e., it can either be an unitary or an antiunitary transformation. We call $\mathcal{C}$ the operation of charge conjugation.

To simplify notation, we take the spectrum

$$\{0\,,\,\mathrm{sgn}(n)\,\varepsilon_{|n|}\,|\,n = \pm 1, \pm 2, \cdots\} \tag{A.2}$$

of $\mathcal{H}$ to be discrete up to finite degeneracies of the eigenvalues. This is the case if $\mathcal{H}$ describes the single-particle physics of a lattice Hamiltonian. The spectral decomposition of $\mathcal{H}$ thus reads

$$\mathcal{H} = \sum_{n=\pm1,\pm2,\cdots} \mathrm{sgn}(n)\varepsilon_{|n|}|\psi_n\rangle\langle\psi_n|, \qquad \varepsilon_{|n|} > 0, \tag{A.3}$$

with the single-particle orthonormal basis obeying

$$\begin{aligned} &\langle\psi_n|\psi_{n'}\rangle = \delta_{n,n'}, \qquad \langle\psi_n|\alpha\rangle = 0, \qquad \langle\alpha|\alpha'\rangle = \delta_{\alpha,\alpha'}, \\ &\mathbb{1} = \sum_{\alpha=1}^{N} |\alpha\rangle\langle\alpha| + \sum_{n=\pm1,\pm2,\cdots} |\psi_n\rangle\langle\psi_n| \,. \end{aligned} \tag{A.4}$$

We have assumed the existence of N zero modes labeled by the index α. The relation

$$|\psi_n\rangle = \mathcal{C}|\psi_{-n}\rangle \tag{A.5}$$

holds for any finite energy eigenstate labeled by the index $n = \pm1, \pm2, \cdots$ as a result of the charge-conjugation symmetry (A.1).

On the lattice, we denote the value of the energy eigenfunctions at site i by

$$\psi_{\mathrm{sgn}(n)\varepsilon_{|n|},i} = \langle i|\psi_n\rangle, \qquad n = \pm1, \pm2, \cdots, \tag{A.6}$$

for the finite-energy eigenvalues and

$$\psi_{\alpha,i} = \langle i|\alpha\rangle, \qquad \alpha = 1, \cdots, N, \tag{A.7}$$

for the N zero modes. For any two lattice sites i and j,

$$\begin{aligned} \delta_{i,j} =& \langle i|j\rangle \\ =& \langle i|\hat{1}|j\rangle \\ =& \sum_{n=-1,-2,\cdots} \psi^*_{-|n|,j}\psi_{-|n|,i} + \sum_{n=-1,-2,\cdots} (\mathcal{C}\psi)^*_{-|n|,j} (\mathcal{C}\psi)_{-|n|,i} + \sum_{\alpha=1}^{N} \psi^*_{\alpha,j}\psi_{\alpha,i}, \end{aligned} \tag{A.8}$$

where we have used the completeness relation defined in Eq. (A.4). When $i = j$, we find the local sum rule

$$1 = 2 \sum_{n=-1,-2,\cdots} \psi^*_{-|n|,i} \psi_{-|n|,i} + \sum_{\alpha=1}^{N} \psi^*_{\alpha,i} \psi_{\alpha,i} \tag{A.9}$$

owing to the fact that $\mathcal{C}$ is norm preserving.

We now assume that there exists a single-particle Hamiltonian

$$\begin{aligned} \mathcal{H}_0 &= \sum_{n=\pm 1,\pm 2,\cdots} \mathrm{sgn}(n) \varepsilon^0_{|n|} |\phi_n\rangle\langle\phi_n| \\ &= - \mathcal{C}^{-1} \mathcal{H}_0 \mathcal{C} \end{aligned} \tag{A.10}$$

such that $\mathcal{H}_0$ *does not support zero modes*. Evidently, the local sum rule

$$1 = 2 \sum_{n=-1,-2,\cdots} \phi^*_{-|n|,i} \phi_{-|n|,i} \tag{A.11}$$

also applies.

After subtracting Eq. (A.11) from Eq. (A.9), the local local sum rule

$$-2 \sum_{n=-1,-2,\cdots} \left(\psi^*_{-|n|,i} \psi_{-|n|,i} - \phi^*_{-|n|,i} \phi_{-|n|,i} \right) = \sum_{\alpha=1}^{N} \psi^*_{\alpha,i} \psi_{\alpha,i} \tag{A.12}$$

follows. In turn, after summing over all lattice sites and making use of the fact that the zero modes are normalized to one, the global sum rule

$$\frac{N}{2} = \sum_{n=-1,-2,\cdots} \sum_{i} \left(\phi^*_{-|n|,i} \phi_{-|n|,i} - \psi^*_{-|n|,i} \psi_{-|n|,i} \right) \tag{A.13}$$

follows. The global sum rule is only meaningful in the thermodynamic limit after this subtraction procedure has been taken.

We now present the global sum rule (A.13) with the help of Euclidean single-particle Green functions. We thus define the Euclidean single-particle Green functions

$$\mathcal{G}(\omega) = \frac{1}{\mathrm{i}\omega - \mathcal{H}} \tag{A.14a}$$

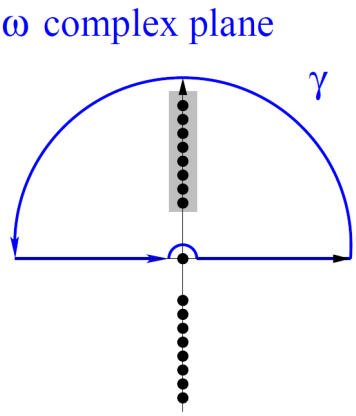

Figure A.1: Definition of the integration contour γ that picks up the discrete negative energy eigenvalues of the single-particle Hamiltonian. The shaded box represents the Fermi sea. The filled circles represent the discrete energy eigenvalues. The contour γ avoids the zero mode.

and

$$\mathcal{G}_0(\omega) = \frac{1}{\mathrm{i}\omega - \mathcal{H}_0} \tag{A.14b}$$

for any real-valued and non-vanishing ω. Next, we choose γ to be the contour in the complex ω plane that runs counterclockwise along the real axis $\omega \in \mathbb{R}$, avoids the origin $\omega = 0$ by an infinitesimal deformation into the upper complex plane $\mathrm{Re}\,\omega > 0$, and closes through a semi-circle in the very same upper complex plane (see Figure A.1). With the help of the residue theorem, it then follows that

$$\sum_{n=-1,-2,\cdots} \psi^*_{-|n|,i}\psi_{-|n|,i} = \int_\gamma \frac{\mathrm{d}\omega}{2\pi} \langle i\,|\mathcal{G}(\omega)|\,i\rangle \tag{A.15a}$$

and

$$\sum_{n=-1,-2,\cdots} \phi^*_{-|n|,i}\phi_{-|n|,i} = \int_\gamma \frac{\mathrm{d}\omega}{2\pi} \langle i\,|\mathcal{G}_0(\omega)|\,i\rangle\,. \tag{A.15b}$$

Equation (A.13) can now be rewritten in the desired form

$$\frac{N}{2} = -\mathrm{Tr} \int_\gamma \frac{\mathrm{d}\omega}{2\pi} \left[\mathcal{G}(\omega) - \mathcal{G}_0(\omega)\right]. \tag{A.16a}$$

Equation (A.16a) can be expressed in terms of the local "lattice charge" ρ_i through

$$\begin{aligned} \frac{N}{2} &= -\sum_i \rho_i \equiv -Q, \\ \rho_i &\equiv \int_\gamma \frac{\mathrm{d}\omega}{2\pi} \left\langle i \left| \left[\mathcal{G}(\omega) - \mathcal{G}_0(\omega)\right] \right| i \right\rangle, \end{aligned} \tag{A.16b}$$

or the local "continuum charge" through "charge" $\rho(\boldsymbol{r})$

$$\begin{aligned} \frac{N}{2} &= -\int \mathrm{d}^d\boldsymbol{r}\, \rho(\boldsymbol{r}) \equiv -Q, \\ \rho(\boldsymbol{r}) &\equiv \int_\gamma \frac{\mathrm{d}\omega}{2\pi} \left\langle \boldsymbol{r} \left| \left[\mathcal{G}(\omega) - \mathcal{G}_0(\omega)\right] \right| \boldsymbol{r} \right\rangle. \end{aligned} \tag{A.16c}$$

A.2 Zero modes of $\mathcal{H}_d^{\mathrm{Dirac}}$

This Appendix provides intermediary steps for Sec. 3.3.3.

A.2.1 Dirac fermions in one-dimensional space

Definition

When $d = 1$, Eq. (3.52) simplifies to

$$\mathcal{H}_1^{\mathrm{Dirac}}\big(\hat{p}, \boldsymbol{\phi}(x)\big) = \sigma_3 \hat{p} + \sigma_1 \phi_1(x) + \sigma_2 \phi_2(x). \tag{A.17}$$

The $(R = 2)$-dimensional representation of the Clifford algebra is here generated from the Pauli matrices σ_1, σ_2, and σ_3. If the doublet of Higgs fields $\boldsymbol{\phi}_0$ is constant through

one-dimensional space (x), the single-particle spectrum of Hamiltonian (A.17) has a gap controlled by the Higgs components adding in quadrature,

$$\varepsilon_0^2(\boldsymbol{p}) = \boldsymbol{p}^2 + \boldsymbol{\phi}_0^2 = \boldsymbol{p}^2 + \phi_{0\,1}^2 + \phi_{0\,2}^2. \tag{A.18}$$

The generator of the chiral symmetry of the Dirac Hamiltonian (A.17) is

$$\mathcal{C}_{\text{ch}} = \sigma_2 \tag{A.19a}$$

if

$$\phi_2 = 0 \tag{A.19b}$$

everywhere in Euclidean space $x \in \mathbb{R}$.

The operation of time-reversal is implemented by

$$\mathcal{T}_1\,\mathsf{K} = \sigma_1\,\mathsf{K} \tag{A.20}$$

where K denotes complex conjugation. It is a symmetry of the Dirac Hamiltonian (A.17) for any Higgs configuration ϕ_1 and ϕ_2.

The operation of particle-hole exchange is implemented by

$$\mathcal{C}_{\text{ph}} = \mathcal{T}_1\,\mathsf{K}\,\mathcal{C}_{\text{ch}} = -\mathrm{i}\sigma_3\,\mathsf{K} \tag{A.21}$$

and it is only a symmetry of the Dirac Hamiltonian (A.17) provided $\phi_2 = 0$.

The discovery that this model supports zero modes was made by Jackiw and Rebbi in Ref. [56]. Its relevance to the physics of polyacetylene was made by Su, Schrieffer, and Heeger in Refs. [113] and [114]. In polyacetylene, the kinetic energy results from linearizing the dispersion around the two Fermi points of a single-band nearest-neighbor tight-binding model at half-filling in the left- and right-mover basis.

The Higgs field $\phi_1 \equiv \varphi_1$ realizes a modulation of the nearest-neighbor hopping amplitude that is mediated by phonons. A Peierls transition opens up a single-particle electronic gap through the breaking of the translation symmetry by one lattice spacing down to a residual translation symmetry by two lattice spacings. A domain wall in φ_1 that interpolates between the two possible dimer ground states binds one zero mode per electronic spin (which we have ignored so far). The Higgs field ϕ_2 breaks the sublattice symmetry of the tight-binding model. The quasiparticle charge density induced by a domain wall with a non-vanishing charge-conjugation symmetry breaking ϕ_2 was computed by Goldstone and Wilczek in Ref. [39] and shown to vary continuously with ϕ_2. We are going to reproduce all these results using the adiabatic approximation (3.23).

Counting zero modes

We start from the expansion (3.20a) of the quasiparticle charge density which, for a Dirac Hamiltonian, is exact and consider the contribution from $n = 1$. The adiabatic approximation to the quasiparticle charge density is

$$\rho_{\text{adia}}(x) = \int \frac{\mathrm{d}\omega \mathrm{d}p}{(2\pi)^2} \frac{2\epsilon_{\mathsf{ab}} \left(\partial_x \phi_{\mathsf{a}}\right)(x)\, \phi_{\mathsf{b}}(x)}{\left[\omega^2 + p^2 + \phi_1^2(x) + \phi_2^2(x)\right]^2} = \frac{\epsilon_{\mathsf{ab}}}{2\pi} \frac{\left(\partial_x \phi_{\mathsf{a}}\right)(x)\, \phi_{\mathsf{b}}(x)}{\left[\phi_1^2(x) + \phi_2^2(x)\right]}. \tag{A.22}$$

For a constant $\phi_2 > 0$ that breaks the conjugation symmetry, integration over one-dimensional Euclidean space (x) gives the adiabatic approximation to the induced charge

$$Q_{\text{adia}}(\phi_2) = \int_{\phi_1(x=-\infty)}^{\phi_1(x=+\infty)} \frac{\mathrm{d}\phi_1}{2\pi} \frac{\phi_2}{(\phi_1^2 + \phi_2^2)} = (2\pi)^{-1} \left(\arctan \frac{\phi_1(x)}{\phi_2} \right) \Bigg|_{x=-\infty}^{x=+\infty}. \tag{A.23}$$

The single domain wall with the asymptotic values

$$\phi_1(\pm\infty) = \mp\varphi_0, \qquad \varphi_0 > 0, \tag{A.24}$$

here chosen in such a way that any zero mode is shifted in energy by $\phi_2 > 0$ *above* the chemical potential, induces the *negative* charge

$$\lim_{\phi_2 \to 0^+} Q_{\text{adia}}(\phi_2) = -\frac{1}{2}. \tag{A.25}$$

Having restored the charge-conjugation symmetry by removing ϕ_2 in Eq. (A.25), the counting formula (3.14) can, in turn, be used to deliver the *positive* number of unoccupied zero modes

$$N = 1 \tag{A.26}$$

bound to this single domain wall.

Chern number

Whereas the counting formula (3.14) relies on the charge-conjugation symmetry, the adiabatic approximation to the quasiparticle charge density does not. We are going to take advantage of this freedom to relate the induced charge to *the first Chern number*.

To this end, we compactify the base space $x \in \mathbb{R}$ to the circle $x \in S^1$ by imposing periodic boundary conditions. We then parametrize the doublet of Higgs fields according to the polar decomposition

$$\boldsymbol{\phi}(x) = \begin{pmatrix} \phi_1(x) \\ \phi_2(x) \end{pmatrix} = m \begin{pmatrix} \sin\theta(x) \\ \cos\theta(x) \end{pmatrix}. \tag{A.27}$$

We have thus compactified the target space $\boldsymbol{\phi}(x) \in \mathbb{R}^2$ to the unit circle $\theta(x) \in S^1$.

In the adiabatic approximation (3.23), the charge is

$$Q_{\text{adia}} = \frac{1}{2(2\pi)^2} \int \mathrm{d}\omega \int_0^{2\pi} \mathrm{d}p \int_0^{2\pi} \mathrm{d}x \, (-\mathrm{i}) \frac{\partial \theta}{\partial x} \times \mathrm{tr} \left(\mathcal{G} \frac{\partial \mathcal{G}^{-1}}{\partial p} \mathcal{G} \frac{\partial \mathcal{G}^{-1}}{\partial \theta} \mathcal{G} - \mathcal{G} \frac{\partial \mathcal{G}^{-1}}{\partial \theta} \mathcal{G} \frac{\partial \mathcal{G}^{-1}}{\partial p} \mathcal{G} \right)_0 . \tag{A.28}$$

The integrand can be written in a more compact and symmetric form by observing that

$$\left(\frac{\partial \mathcal{G}^{-1}}{\partial \omega} \right)_0 = \mathrm{i}, \qquad \mathrm{i}\, \mathcal{G}_0 = \left(\mathcal{G} \frac{\partial \mathcal{G}^{-1}}{\partial \omega} \right)_0 , \tag{A.29}$$

and by introducing the three-momentum

$$K_\nu \equiv (\omega, p, \theta) \ \in \mathbb{R} \times S^1 \times S^1. \tag{A.30}$$

Equation (A.28) is then nothing but *the first Chern number*, [123] for

$$Q_{\text{adia}} = \frac{-1}{24\pi^2} \int_{\mathbb{R}\times S^1 \times S^1} \mathrm{d}^3 K \epsilon_{\mu\nu\lambda} \mathrm{tr} \left(\mathcal{G} \frac{\partial \mathcal{G}^{-1}}{\partial K_\mu} \mathcal{G} \frac{\partial \mathcal{G}^{-1}}{\partial K_\nu} \mathcal{G} \frac{\partial \mathcal{G}^{-1}}{\partial K_\lambda} \right)_0 . \tag{A.31}$$

We infer that the charge induced by the adiabatic winding of the Higgs doublet around the circle takes integer values.

Moreover, the domain wall from Sec. A.2.1 is a half-winding of the unit circle S^1. More precisely, evaluation of the trace in the integrand of *the first Chern number* (A.31) gives the adiabatic approximation to the charge

$$Q_{\text{adia}} = \frac{1}{2\pi} \int \mathrm{d}x \, \frac{\epsilon_{\mathsf{ab}} \phi_{\mathsf{a}} \partial_x \phi_{\mathsf{b}}}{|\boldsymbol{\phi}|^2} = \text{winding number in } \boldsymbol{\phi}. \tag{A.32}$$

The integrand is nothing but the space (x) and time (t) dependent quasiparticle charge density

$$j^0 := \frac{1}{2\pi |\boldsymbol{\phi}|^2} \epsilon_{\mathsf{ab}} \phi_{\mathsf{a}} \partial_x \phi_{\mathsf{b}} \tag{A.33a}$$

that obeys the continuity equation [39]

$$\partial_\nu j^\nu = 0 \tag{A.33b}$$

with

$$j^\nu = \frac{1}{2\pi\boldsymbol{\phi}^2}\epsilon^{\nu\nu'}\epsilon_{\mathsf{a}\mathsf{a}'}\phi_{\mathsf{a}}\partial_{\nu'}\phi_{\mathsf{a}'}. \tag{A.33c}$$

A.2.2 Dirac fermions in two-dimensional space

Definition

When $d = 2$, Eq. (3.52) simplifies to

$$\mathcal{H}_2^{\text{Dirac}}\big(\hat{p}, \boldsymbol{\phi}(x)\big) = \alpha_1\hat{p}_1 + \alpha_2\hat{p}_2 + \beta_1\phi_1 + \beta_2\phi_2 + \beta_3\phi_3. \tag{A.34a}$$

The $(R = 4)$-dimensional representation of the Clifford algebra can be chosen to be generated from the five traceless and Hermitian matrices

$$\Gamma_\nu = (\alpha_1, \alpha_2, \beta_1, \beta_2, \beta_3) \tag{A.34b}$$

with

$$\alpha_1 = \sigma_3 \otimes \tau_1, \qquad \alpha_2 = \sigma_3 \otimes \tau_2, \tag{A.34c}$$

and

$$\beta_1 = \sigma_1 \otimes \tau_0, \qquad \beta_2 = \sigma_2 \otimes \tau_0, \qquad \beta_3 = \sigma_3 \otimes \tau_3. \tag{A.34d}$$

A second set of Pauli matrices τ_1, τ_2, and τ_1 has been introduced, together with the unit 2×2 matrices σ_0 and τ_0. If the triplet of Higgs field $\boldsymbol{\phi}_0$ is constant throughout two-dimensional space ($\boldsymbol{x}$), the single-particle spectrum of Hamiltonian (A.34) has a gap controlled by the Higgs components adding in quadrature,

$$\varepsilon_0^2(\boldsymbol{p}) = \boldsymbol{p}^2 + \boldsymbol{\phi}_0^2 = \boldsymbol{p}^2 + \phi_{0\,1}^2 + \phi_{0\,2}^2 + \phi_{0\,3}^2. \tag{A.35}$$

The generator of the chiral symmetry of the Dirac Hamiltonian (A.34) is

$$\mathcal{C}_{\text{ch}} = \beta_3 = \sigma_3 \otimes \tau_3 \tag{A.36a}$$

if

$$\phi_3 = 0 \tag{A.36b}$$

everywhere in Euclidean space $\boldsymbol{x} \in \mathbb{R}^2$.

The operation of time-reversal is implemented by

$$\mathcal{T}_2 \, \mathsf{K} = \sigma_1 \otimes \tau_1 \, \mathsf{K} \tag{A.37}$$

where K denotes complex conjugation. It is a symmetry of the Dirac Hamiltonian (A.34) for any Higgs configuration ϕ_1, ϕ_2, and ϕ_3.

The operation of particle-hole exchange is implemented by

$$\mathcal{C}_{\text{ph}} = \mathcal{T}_2 \, \mathsf{K} \, \mathcal{C}_{\text{ch}} = -\sigma_2 \otimes \tau_2 \, \mathsf{K} \tag{A.38}$$

and it is only a symmetry of the Dirac Hamiltonian (A.34) provided $\phi_3 = 0$.

The discovery that this model supports zero modes (Majorana fermions) was made by Jackiw and Rossi in Ref. [57] within an interpretation of Hamiltonian (A.34) as a relativistic superconductor. Weinberg shortly thereafter proved an index theorem in Ref. [128] for these zero modes. The effect on the induced charge by a triplet of Higgs fields was investigated by Jaroszewicz in Ref. [61] (see also Refs. [16, 50, 146]). It was proposed by Hou, Chamon, and Mudry in Ref. [52] that graphene could realize Hamiltonian (A.34) with the Higgs doublet ϕ_1 and ϕ_2 responsible for a Kekulé bond-density-wave instability and the charge-conjugation-symmetry-breaking ϕ_3 responsible for a charge-density-wave instability (see also Refs. [14, 15, 98]).

Counting zero modes

We start from the expansion (3.20a) of the quasiparticle charge density induced by a static triplet of Higgs fields $\boldsymbol{\phi}$ which, for a Dirac Hamiltonian, is exact. We compute first the contribution from $n = 1$. It vanishes. The adiabatic approximation to the quasiparticle charge density is in fact given by Eq. (3.24)

$$\rho_{\text{adia}}(\boldsymbol{x}) = \int \frac{\mathrm{d}\omega \mathrm{d}^2\boldsymbol{p}}{(2\pi)^3} \frac{8\epsilon_{\mathsf{abc}} \left(\partial_1 \phi_{\mathsf{a}}\right) \left(\partial_2 \phi_{\mathsf{b}}\right) \phi_{\mathsf{c}}}{\left[\omega^2 + \boldsymbol{p}^2 + \boldsymbol{\phi}^2(\boldsymbol{x})\right]^3} = \frac{\epsilon_{\mathsf{abc}}}{4\pi} \frac{\left(\partial_1 \phi_{\mathsf{a}}\right) \left(\partial_2 \phi_{\mathsf{b}}\right) \phi_{\mathsf{c}}}{|\boldsymbol{\phi}(\boldsymbol{x})|^3}. \tag{A.39}$$

For a constant ϕ_3, the integration over $\boldsymbol{x}$ gives the adiabatic approximation to the charge

$$Q_{\text{adia}}(\phi_3) = \frac{1}{4\pi} \int \mathrm{d}\Theta \int_0^{\Delta_0} \mathrm{d}\rho\, \rho \, \frac{\phi_3}{\left(\rho^2 + \phi_3^2\right)^{3/2}} \tag{A.40a}$$

where the parametrization

$$\begin{pmatrix} \phi_1 \\ \phi_2 \end{pmatrix} = \begin{pmatrix} \rho(r) \cos \Theta(\theta) \\ \rho(r) \sin \Theta(\theta) \end{pmatrix} \tag{A.40b}$$

is assumed for the charge-conjugation-symmetric doublet of Higgs fields with r and θ denoting the polar coordinates of $\boldsymbol{x} \in \mathbb{R}^2$. In the limit in which ϕ_3 tends to zero, the induced charge

$$Q_{\text{adia}}(\phi_3) = \frac{\operatorname{sgn}(\phi_3)}{2} \times \text{winding number in } (\phi_1, \phi_2) \tag{A.41}$$

follows. To compute the number of unoccupied zero modes N with the counting formula (3.14), we choose the sign of the charge-conjugation-symmetry-breaking ϕ_3 such that it shifts the zero mode in energy above the chemical potential, i.e., with the opposite sign to the winding number of the Higgs doublet (ϕ_1, ϕ_2). We then take

the limit $\phi_3 \to 0$. If so, for a unit winding

$$N = 1. \tag{A.42}$$

Observe that the number of zero modes (A.40a) agrees with Weinberg's index theorem in Ref. [128] applied to a single vortex with unit vorticity.

Chern number

We use the notation $\mathcal{G} \equiv (\mathrm{i}\omega - \mathcal{H}_{d=2}^{\mathrm{Dirac}})^{-1}$ and compactify both space and the order-parameter space,

$$\boldsymbol{x} \in S^2, \qquad \boldsymbol{\phi}(\boldsymbol{\theta}) \in S^2 \subset \mathbb{R}^3, \tag{A.43}$$

where $\boldsymbol{\theta} = (\theta_1, \theta_2)$ are the spherical coordinates on the two-sphere $S^2 \subset \mathbb{R}^3$.

With the general manipulations of Appendix A.2.3, it is then possible to write

$$Q_{\mathrm{adia}} = \frac{-\mathrm{i}(2\pi)^2}{60} \int\limits_K \epsilon_{\nu_1 \cdots \nu_5} \mathrm{tr}_4 \left(\mathcal{G}\partial_{\nu_1}\mathcal{G}^{-1} \cdots \mathcal{G}\partial_{\nu_5}\mathcal{G}^{-1} \right)_0 \tag{A.44a}$$

where we have introduced the family of indices ν

$$\nu_1, \cdots, \nu_5 = 1, \cdots, 5, \tag{A.44b}$$

the momentum

$$K_\nu = (\omega, p_1, p_2, \theta_1, \theta_2), \tag{A.44c}$$

and the domain of integration

$$\int\limits_K \equiv \int \frac{\mathrm{d}\omega}{2\pi} \int\limits_{\boldsymbol{p}\in S^2} \frac{\mathrm{d}\Omega_2(\boldsymbol{p})}{(2\pi)^2} \int\limits_{\boldsymbol{\theta}\in S^2} \frac{\mathrm{d}\Omega_2(\boldsymbol{\theta})}{(2\pi)^2}. \tag{A.44d}$$

The "surface" element of the sphere S^2 is here denoted by $\mathrm{d}\Omega_2$. The subscript 0 refers to the semi-classical Green function (3.22). Equation (A.44) is *the second Chern number*. [90] It takes integer values only.

A.2.3 Chern number for Dirac fermions in d-dimensional space

To prove Eq. (3.58), imagine that we integrate out the Dirac fermions in the background, not necessarily static, of the Higgs fields in Eq. (3.52d) subject to the constraint

$$\boldsymbol{\phi}(\boldsymbol{\theta}) \in S^d \subset \mathbb{R}^{d+1}, \tag{A.45a}$$

where $\boldsymbol{\theta}$ are the polar coordinates of the d-sphere $S^d \subset \mathbb{R}^{d+1}$. The conserved current of the fermionic single-particle Dirac Hamiltonian must induce a conserved current j^ν_{adia} with $\nu = 0, 1, \cdots, d$ for the Higgs fields. Its time-like component j^0_{adia} enters in the counting formula (3.14). Relativistic covariance, current conservation, dimensional analysis, and the constraint (A.45a) all conspire to bring this current to the form

$$j^\nu_{\text{adia}} \propto \epsilon^{\nu\nu_1\cdots\nu_d}\epsilon_{\mathsf{a}_1\cdots\mathsf{a}_d\mathsf{a}_{d+1}}\phi_{\mathsf{a}_{d+1}}\partial_{\nu_d}\phi_{\mathsf{a}_d}\cdots\partial_{\nu_1}\phi_{\mathsf{a}_1}. \tag{A.45b}$$

Here, summation convention over the repeated indices

$$\begin{aligned} &\nu, \nu_1, \cdots, \nu_d = 0, 1, \cdots, d, \\ &\mathsf{a}_1, \cdots, \mathsf{a}_d, \mathsf{a}_{d+1} = d+1, \cdots, 2d+1, \end{aligned} \tag{A.45c}$$

is implied. (Compared to our convention in the definition (3.52d) of the Dirac Hamiltonian, we have shifted the values taken by the family of indices $\mathsf{a} = d+1, \cdots, 2d+1$ to stress that it differs from the family of indices $i = 1, \cdots, d$.)

If we compare Eq. (A.45) with the gradient expansion (3.26), we deduce that the leading non-vanishing contribution to the gradient expansion (3.26) must be of order $n = d$ and, for a static Higgs background, given by

$$j^0_{\text{adia}}(\boldsymbol{x}) = (-\mathrm{i})^d \mathcal{I}_{i_d\mathsf{a}_d\cdots i_1\mathsf{a}_1}\left(\partial_{i_d}\phi_{\mathsf{a}_d}\right)\cdots\left(\partial_{i_1}\phi_{\mathsf{a}_1}\right)(\boldsymbol{x}). \tag{A.46a}$$

The summation convention over the two distinct families of indices

$$\begin{aligned} i_1, \cdots, i_d &= 1, \cdots, d, \\ \mathsf{a}_1, \cdots, \mathsf{a}_d &= d+1, \cdots, 2d+1, \end{aligned} \tag{A.46b}$$

is implied and the expansion coefficients are

$$\mathcal{I}_{i_d \mathsf{a}_d \cdots i_1 \mathsf{a}_1} = -\mathrm{i} \int \frac{\mathrm{d}\omega}{2\pi} \int_{\boldsymbol{p}} \mathrm{tr}_R \left[\left(\mathcal{G} \frac{\partial \mathcal{G}^{-1}}{\partial p_{i_d}} \mathcal{G} \frac{\partial \mathcal{G}^{-1}}{\partial \phi_{\mathsf{a}_d}} \right) \cdots \left(\mathcal{G} \frac{\partial \mathcal{G}^{-1}}{\partial p_{i_1}} \mathcal{G} \frac{\partial \mathcal{G}^{-1}}{\partial \phi_{\mathsf{a}_1}} \right) \left(\mathcal{G} \frac{\partial \mathcal{G}^{-1}}{\partial \omega} \right) \right]_0 . \tag{A.46c}$$

Any permutation of the indices on the left-hand side is defined by the same permutation of the differentials in the trace of the right-hand side.

We are first going to prove that

$$Q_{\mathrm{adia}} = \int_{S^d} \mathrm{d}^d \boldsymbol{x}\, j^0_{\mathrm{adia}}(\boldsymbol{x}) = \frac{(-)^{d(d-1)/2} (-\mathrm{i})^d}{d!} \int_{\boldsymbol{\theta} \in S^d} \epsilon_{i_d \mathsf{b}_d \cdots i_1 \mathsf{b}_1} \mathcal{J}_{i_d \mathsf{b}_d \cdots i_1 \mathsf{b}_1}(\boldsymbol{\theta}) \tag{A.47a}$$

where the target space $S^d \subset \mathbb{R}^{d+1}$ of the order-parameter is parametrized by the d-independent spherical coordinates

$$\boldsymbol{\theta} \equiv (\theta_{d+1}, \cdots, \theta_{2d}), \tag{A.47b}$$

the integral

$$\int_{\boldsymbol{\theta} \in S^d} \equiv \int_{S^d} \mathrm{d}\Omega_d \tag{A.47c}$$

with $\mathrm{d}\Omega_d$ the "surface" element of the d-sphere, and

$$\mathcal{J}_{i_d \mathsf{b}_d \cdots i_1 \mathsf{b}_1} = -\mathrm{i} \int \frac{\mathrm{d}\omega}{2\pi} \int_{\boldsymbol{p}} \mathrm{tr}_R \left[\left(\mathcal{G} \frac{\partial \mathcal{G}^{-1}}{\partial p_{i_d}} \mathcal{G} \frac{\partial \mathcal{G}^{-1}}{\partial \theta_{\mathsf{b}_d}} \right) \cdots \left(\mathcal{G} \frac{\partial \mathcal{G}^{-1}}{\partial p_{i_1}} \mathcal{G} \frac{\partial \mathcal{G}^{-1}}{\partial \theta_{\mathsf{b}_1}} \right) \left(\mathcal{G} \frac{\partial \mathcal{G}^{-1}}{\partial \omega} \right) \right]_0 . \tag{A.47d}$$

Again any permutation of the indices on the left-hand side is defined by the same permutation of the differentials in the trace of the right-hand side.

Proof. To evaluate the trace in the integrand (A.46c), the semi-classical Green functions are re-massaged so as to bring all the Dirac matrices in the numerator,

$$\mathcal{G}_{\text{s-c}}(\omega, \boldsymbol{p}, \boldsymbol{x}) = \frac{1}{\mathrm{i}\omega - \Gamma_i p_i - \Gamma_{\mathsf{a}}\phi_{\mathsf{a}}(\boldsymbol{x})} = -\frac{\mathrm{i}\omega + \Gamma_i p_i + \Gamma_{\mathsf{a}}\phi_{\mathsf{a}}(\boldsymbol{x})}{\omega^2 + \boldsymbol{p}^2 + \boldsymbol{\phi}^2(\boldsymbol{x})}. \tag{A.48}$$

Multiplying out all Green functions in the trace from the integrand in Eq. (A.46c) yields in the numerator terms made of the product from $2d$ Γ-matrices, $2d+1$ Γ-matrices, ..., $2d+2j$ Γ-matrices, $2d+2j+1$ Γ-matrices, ..., $2d+2d$ Γ-matrices, and $2d+2d+1$ Γ-matrices. Any trace over an even number $2d+2j$ of Γ-matrices is odd under $\omega \to -\omega$ since it comes multiplied by the power $\omega^{2d+1-2j}$ in the numerator. Such a trace does not contribute to the ω integration since the denominator is an even function of ω. Any trace over an odd number $2d+2j+1$ of Γ-matrices is even under $\omega \to -\omega$ since it comes multiplied by the power $\omega^{2d+1-2j-1}$. Such a trace can only be nonvanishing if $\Gamma_1, \cdots, \Gamma_{2d+1}$ all appear in the trace and all an odd number of times. [147] For such traces, the Clifford algebra delivers another key identity in that

$$\mathrm{tr}_R\left(\Gamma_{2d+1}\Gamma_{\mu_1}\cdots\Gamma_{\mu_{2d}}\right) = R\,(+\mathrm{i})^d \epsilon_{\mu_1\cdots\mu_{2d}} \tag{A.49}$$

if $\mu_j = 1, \cdots, 2d$ for $j = 1, \cdots, 2d$. Here, $R = 2^d$ and Γ_{2d+1} was defined in Eq. (3.55b). The coefficients (A.46c) inherit the antisymmetry of Eq. (A.49) in that they are fully antisymmetric under any exchange of the indices (A.46b).

We need to overcome the fact that the ranges of i and a are unequal in cardinality. To this end, we change variables on the target space and introduce the spherical coordinates (A.47b) of the target space $S^d \subset \mathbb{R}^{d+1}$. The adiabatic approximation (A.46a) to the quasiparticle charge density becomes

$$j^0_{\text{adia}}(\boldsymbol{x}) = (-\mathrm{i})^d \mathcal{J}_{i_d \mathsf{b}_d \cdots i_1 \mathsf{b}_1}\left(\partial_{i_d}\theta_{\mathsf{b}_d}\right)\cdots\left(\partial_{i_1}\theta_{\mathsf{b}_1}\right)(\boldsymbol{x}). \tag{A.50}$$

Now, it is the summation convention over the two distinct families of indices

$$\begin{aligned} &i_1, \cdots, i_d = 1, \cdots, d, \\ &\mathsf{b}_1, \cdots, \mathsf{b}_d = d+1, \cdots, 2d, \end{aligned} \tag{A.51}$$

that replaces (A.46b), whereby the expansion coefficients (A.50) are related to the expansion coefficients (A.46c) through the chain rule for differentiation, i.e.,

$$\mathcal{J}_{i_d \mathsf{b}_d \cdots i_1 \mathsf{b}_1} = \mathcal{I}_{i_d \mathsf{a}_d \cdots i_1 \mathsf{a}_1} \left(\frac{\partial \phi_{\mathsf{a}_d}}{\partial \theta_{\mathsf{b}_d}} \right) \cdots \left(\frac{\partial \phi_{\mathsf{a}_1}}{\partial \theta_{\mathsf{b}_1}} \right). \tag{A.52}$$

Here, any permutation of the indices of $\mathcal{J}$ on the left-hand side is defined by the same permutation on the indices of $\mathcal{I}$ on the right-hand side.

By linearity, the antisymmetry (A.49) thus carries over to

$$\mathcal{J}_{i_d \mathsf{b}_d \cdots i_1 \mathsf{b}_1} = \mathcal{N}_d \, \epsilon_{i_d \mathsf{b}_d \cdots i_1 \mathsf{b}_1} \tag{A.53}$$

where $\mathcal{N}_d$ is a normalization constant. We will not need the explicit dependence of the normalization $\mathcal{N}_d$. We will only make use of the fact that it obeys the identity

$$\mathcal{N}_d(\boldsymbol{\theta}) = \frac{1}{(d!)^2} \epsilon_{i_d \mathsf{b}_d \cdots i_1 \mathsf{b}_1} \mathcal{J}_{i_d \mathsf{b}_d \cdots i_1 \mathsf{b}_1}(\boldsymbol{\theta}). \tag{A.54}$$

This follows from contracting the Levi-Civita antisymmetric tensor $\epsilon_{i_d \mathsf{b}_d \cdots i_1 \mathsf{b}_1}$ with itself and observing that the two sets of indices i and b run over d distinct values each.

The Jacobian of the map from $\boldsymbol{x} \in S^d$ to $\boldsymbol{\theta} \in S^d \subset \mathbb{R}^{d+1}$ is

$$\begin{aligned} \left| \frac{\partial \boldsymbol{\theta}}{\partial \boldsymbol{x}} \right| &= \epsilon_{i_d \cdots i_1} \partial_{i_d} \theta_{2d} \cdots \partial_{i_1} \theta_{d+1} \\ &= \frac{1}{d!} \epsilon_{i_d \cdots i_1} \epsilon_{\mathsf{b}_d \cdots \mathsf{b}_1} \partial_{i_d} \theta_{\mathsf{b}_d} \cdots \partial_{i_1} \theta_{\mathsf{b}_1} \\ &= \frac{1}{d!} \epsilon_{i_d \cdots i_1 \mathsf{b}_d \cdots \mathsf{b}_1} \partial_{i_d} \theta_{\mathsf{b}_d} \cdots \partial_{i_1} \theta_{\mathsf{b}_1} \\ &= \frac{(-)^{d(d-1)/2}}{d!} \epsilon_{i_d \mathsf{b}_d \cdots i_1 \mathsf{b}_1} \partial_{i_d} \theta_{\mathsf{b}_d} \cdots \partial_{i_1} \theta_{\mathsf{b}_1}. \end{aligned} \tag{A.55}$$

The charge then becomes

$$\begin{aligned} Q_{\text{adia}} =& \int\limits_{\boldsymbol{x}\in S^d} j^0_{\text{adia}} \\ =&(-\mathrm{i})^{d+1} \int\limits_{\boldsymbol{x}\in S^d} \mathcal{J}_{i_d \mathsf{b}_d \cdots i_1 \mathsf{b}_1} \partial_{i_d} \theta_{\mathsf{b}_d} \cdots \partial_{i_1} \theta_{\mathsf{b}_1} \\ =&(-\mathrm{i})^{d+1} \int\limits_{\boldsymbol{x}\in S^d} \mathcal{N}_d \, \epsilon_{i_d \mathsf{b}_d \cdots i_1 \mathsf{b}_1} \partial_{i_d} \theta_{\mathsf{b}_d} \cdots \partial_{i_1} \theta_{\mathsf{b}_1} \\ =&(-\mathrm{i})^{d+1} (-)^{d(d-1)/2} d! \int\limits_{\boldsymbol{\theta}\in S^d} \mathcal{N}_d(\boldsymbol{\theta}) \\ =& \frac{(-)^{d(d-1)/2} (-\mathrm{i})^{d+1}}{d!} \int\limits_{\boldsymbol{\theta}\in S^d} \epsilon_{i_d \mathsf{b}_d \cdots i_1 \mathsf{b}_1} \mathcal{J}_{i_d \mathsf{b}_d \cdots i_1 \mathsf{b}_1}(\boldsymbol{\theta}) \end{aligned} \tag{A.56}$$

with the help of Eq. (A.54) to reach the last equality.

□

For convenience, we introduce another family of indices μ through

$$\begin{aligned} &\mu_1, \cdots, \mu_{2d} = 1, \cdots, 2d, \\ &i_1, \cdots, i_d = 1, \cdots, d, \\ &\mathsf{b}_1, \cdots, \mathsf{b}_d = d+1, \cdots, 2d. \end{aligned} \tag{A.57}$$

For any tensor $\mathcal{J}_{\mu_1 \cdots \mu_{2d}}$ that reduces to the fully antisymmetric tensor $\mathcal{J}_{i_d \mathsf{b}_d \cdots i_1 \mathsf{b}_1}$, we have the identity

$$\epsilon_{\mu_1 \cdots \mu_{2d}} \mathcal{J}_{\mu_1 \cdots \mu_{2d}} = \frac{(2d)!}{(d!)^2} \, \epsilon_{i_d \mathsf{b}_d \cdots i_1 \mathsf{b}_1} \mathcal{J}_{i_d \mathsf{b}_d \cdots i_1 \mathsf{b}_1}, \tag{A.58}$$

since the contraction on the left-hand side of this equation yields a combinatorial factor of $(2d)!$ whereas the contraction on the right-hand side yields a combinatorial factor of $d! \times d!$, i.e., one $d!$ for the family i of indices and another $d!$ for the distinct

family b of indices. In particular, we can choose

$$\mathcal{J}_{\mu_1\cdots\mu_{2d}} = \int_{\omega}\int_{\boldsymbol{p}\in S^d} \mathrm{tr}_R\left(\mathcal{G}\partial_{\mu_1}\mathcal{G}^{-1}\cdots\mathcal{G}\partial_{\mu_{2d}}\mathcal{G}^{-1}\mathcal{G}\partial_{\omega}\mathcal{G}^{-1}\right)_0 \tag{A.59}$$

where the subscript 0 refers to the semi-classical Green function (A.48).

At last, we add the non-compact imaginary-time label with the introduction of the family ν of indices,

$$\begin{aligned}
&\nu_1,\cdots,\nu_{2d+1} = 0,1,\cdots,2d,\\
&\mu_1,\cdots,\mu_{2d} = 1,\cdots,2d,\\
&i_1,\cdots,i_d = 1,\cdots,d,\\
&\mathsf{b}_1,\cdots,\mathsf{b}_d = d+1,\cdots,2d.
\end{aligned} \tag{A.60}$$

Define

$$\begin{aligned}
&K_\nu = (\omega, p_1,\cdots,p_d,\theta_{d+1},\cdots,\theta_{2d}),\\
&\mathcal{J}_{\nu_1\cdots\nu_{2d+1}} = \int_{\omega}\int_{\boldsymbol{p}\in S^d} \mathrm{tr}_R\left(\mathcal{G}\partial_{\nu_1}\mathcal{G}^{-1}\cdots\mathcal{G}\partial_{\nu_{2d+1}}\mathcal{G}^{-1}\right)_0,\\
&\int_K \equiv \int_{\omega}\int_{\boldsymbol{p}\in S^d}\int_{\boldsymbol{\theta}\in S^d} \equiv \int\frac{\mathrm{d}\omega}{2\pi}\int_{S^d}\frac{\mathrm{d}\Omega_d(\boldsymbol{p})}{(2\pi)^d}\int_{S^d}\frac{\mathrm{d}\Omega_d(\boldsymbol{\theta})}{(2\pi)^d}.
\end{aligned} \tag{A.61a}$$

The "surface" element of S^d is here denoted by $\mathrm{d}\Omega_d$. It follows that

$$Q_{\mathrm{adia}} = \frac{(-)^{d(d-1)/2}(-\mathrm{i})^{d+1}d!}{(2d+1)!}(2\pi)^d \times \int_K \epsilon_{\nu_1\cdots\nu_{2d+1}}\mathrm{tr}_R\left(\mathcal{G}\partial_{\nu_1}\mathcal{G}^{-1}\cdots\mathcal{G}\partial_{\nu_{2d+1}}\mathcal{G}^{-1}\right)_0 \tag{A.61b}$$

thereby completing the proof of Eq. (3.58). This is *the d-th Chern number* in $(2d+1)$-dimensional Euclidean space and time.

Appendix B

Appendix to Chapter 5

B.1 SMA for a flat band

We present some of the intermediate steps needed to derive Eq. (5.32a). (For ease of presentation, we use Latin instead of Greek indices for the momentum components in what follows. Summation convention over repeated indices is also implied.)

Our aim is to evaluate Eq. (5.25c) up to order $\boldsymbol{q}^2\boldsymbol{k}^2$. The commutator in Eq. (5.25c) can be conveniently broken into four contributions,

$$f_{\boldsymbol{k}} = f_{1,\boldsymbol{k}} + f_{2,\boldsymbol{k}} + f_{3,\boldsymbol{k}} + f_{4,\boldsymbol{k}}, \tag{B.1a}$$

each of which read

$$f_{1,\boldsymbol{k}} := \frac{1}{2}\sum_{\boldsymbol{q}} v_{\boldsymbol{q}} \left\langle \left[\delta\widehat{\rho}_{-\boldsymbol{k}}, \delta\widehat{\rho}_{-\boldsymbol{q}}\right]\left[\delta\widehat{\rho}_{+\boldsymbol{q}}, \delta\widehat{\rho}_{+\boldsymbol{k}}\right]\right\rangle, \tag{B.1b}$$

$$f_{2,\boldsymbol{k}} := \frac{1}{2}\sum_{\boldsymbol{q}} v_{\boldsymbol{q}} \left\langle \left[\delta\widehat{\rho}_{-\boldsymbol{q}}, \delta\widehat{\rho}_{+\boldsymbol{k}}\right]\left[\delta\widehat{\rho}_{-\boldsymbol{k}}, \delta\widehat{\rho}_{+\boldsymbol{q}}\right]\right\rangle, \tag{B.1c}$$

$$f_{3,\boldsymbol{k}} := \frac{1}{2}\sum_{\boldsymbol{q}} v_{\boldsymbol{q}} \left\langle \delta\widehat{\rho}_{-\boldsymbol{q}}\left[\delta\widehat{\rho}_{-\boldsymbol{k}}, \left[\delta\widehat{\rho}_{+\boldsymbol{q}}, \delta\widehat{\rho}_{+\boldsymbol{k}}\right]\right]\right\rangle, \tag{B.1d}$$

and

$$f_{4,\boldsymbol{k}} := \frac{1}{2} \sum_{\boldsymbol{q}} v_{\boldsymbol{q}} \Big\langle \left[\delta\widehat{\rho}_{-\boldsymbol{k}}, \left[\delta\widehat{\rho}_{-\boldsymbol{q}}, \delta\widehat{\rho}_{+\boldsymbol{k}}\right]\right] \delta\widehat{\rho}_{+\boldsymbol{q}} \Big\rangle. \tag{B.1e}$$

The commutator of two projected density operators can be expressed, with the aid of Eq. (5.30), as

$$\left[\widehat{\rho}_{\boldsymbol{q}}, \widehat{\rho}_{\boldsymbol{k}}\right] = \sum_{\boldsymbol{p}} R_{\boldsymbol{p},\boldsymbol{q},\boldsymbol{k}}\, \widehat{\chi}^{\dagger}_{\boldsymbol{p}}\, \widehat{\chi}_{\boldsymbol{p}+\boldsymbol{q}+\boldsymbol{k}}, \tag{B.2a}$$

where

$$R_{\boldsymbol{p},\boldsymbol{q},\boldsymbol{k}} := M_{\boldsymbol{p},\boldsymbol{q}}\, M_{\boldsymbol{p}+\boldsymbol{q},\boldsymbol{k}} - M_{\boldsymbol{p}+\boldsymbol{k},\boldsymbol{q}}\, M_{\boldsymbol{p},\boldsymbol{k}}. \tag{B.2b}$$

The nested commutators of three projected density operators can be expressed, with the aid of Eq. (5.30), as

$$\Big[\, \widehat{\rho}_{\boldsymbol{k}}, \left[\widehat{\rho}_{\boldsymbol{q}}, \widehat{\rho}_{\boldsymbol{k}}\right] \Big] = \sum_{\boldsymbol{p}} \Lambda_{\boldsymbol{p},\boldsymbol{q},\boldsymbol{k}}\, \widehat{\chi}^{\dagger}_{\boldsymbol{p}}\, \widehat{\chi}_{\boldsymbol{p}+\boldsymbol{q}}, \tag{B.3a}$$

where

$$\Lambda_{\boldsymbol{p},\boldsymbol{q},\boldsymbol{k}} := R_{\boldsymbol{p}-\boldsymbol{k},\boldsymbol{q},\boldsymbol{k}}\, M_{\boldsymbol{p},-\boldsymbol{k}} - R_{\boldsymbol{p},\boldsymbol{q},\boldsymbol{k}}\, M_{\boldsymbol{p}+\boldsymbol{q}+\boldsymbol{k},-\boldsymbol{k}}. \tag{B.3b}$$

Observe here that the identity

$$\Big[\, \widehat{\rho}_{\boldsymbol{k}}, \left[\widehat{\rho}_{\boldsymbol{q}}, \widehat{\rho}_{\boldsymbol{k}}\right] \Big]^{\dagger} = \Big[\, \widehat{\rho}_{-\boldsymbol{k}}, \left[\widehat{\rho}_{-\boldsymbol{q}}, \widehat{\rho}_{-\boldsymbol{k}}\right] \Big] \tag{B.4}$$

implies that

$$\Lambda^{*}_{\boldsymbol{p},\boldsymbol{q},\boldsymbol{k}} = \Lambda_{\boldsymbol{p}+\boldsymbol{q},-\boldsymbol{q},-\boldsymbol{k}}. \tag{B.5}$$

Needed is the expansion of $R_{\boldsymbol{p},\boldsymbol{q},\boldsymbol{k}}$ and $\Lambda_{\boldsymbol{p},\boldsymbol{q},\boldsymbol{k}}$ up to order $\boldsymbol{q}^2\boldsymbol{k}^2$. We start with

$$\begin{aligned} M_{\boldsymbol{p},\boldsymbol{q}} &= u^\dagger_{\boldsymbol{p}} \cdot u_{\boldsymbol{p}+\boldsymbol{q}} \\ &= u^\dagger_{\boldsymbol{p}} \cdot \left(u_{\boldsymbol{p}} + q^i\, \partial_i\, u_{\boldsymbol{p}} + \frac{1}{2}\, q^i q^j\, \partial_i\, \partial_j\, u_{\boldsymbol{p}} + \cdots \right) \\ &= 1 + q^i\, u^\dagger_{\boldsymbol{p}} \cdot \partial_i\, u_{\boldsymbol{p}} + \frac{1}{2}\, q^i q^j\, u^\dagger_{\boldsymbol{p}} \cdot \partial_i\, \partial_j\, u_{\boldsymbol{p}} + \cdots \\ &= 1 + q^i\, A_{i,\boldsymbol{p}} + \frac{1}{2}\, q^i q^j\, u^\dagger_{\boldsymbol{p}} \cdot \partial_i\, \partial_j\, u_{\boldsymbol{p}} + \cdots \end{aligned} \tag{B.6a}$$

where we have introduced the (imaginary-valued) Berry connection

$$A_{i,\boldsymbol{p}} \equiv u^\dagger_{\boldsymbol{p}} \cdot \partial_i\, u_{\boldsymbol{p}} \tag{B.6b}$$

and the summation convention over repeated indices $i, j = 1, \cdots, d$ is implied. The symbol ∂_i with $i = 1, \cdots, d$ is to be regarded as a derivative with respect to the argument of the function on which it acts. Similarly,

$$\begin{aligned} M_{\boldsymbol{p}+\boldsymbol{q},\boldsymbol{k}} = 1 &+ k^i\, A_i + q^i k^j \partial_i\, u^\dagger \cdot \partial_j\, u + \frac{1}{2}\left(k^i k^j + 2 q^i k^j\right)\, u^\dagger \cdot \partial_i\, \partial_j\, u \\ &+ \frac{1}{2}\left(q^i q^j k^m + k^i k^j q^m\right)\, u^\dagger \cdot \partial_i\, \partial_j\, \partial_m u + \frac{1}{2}\left(k^i k^j q^m + 2 q^m q^i k^j\right)\, \partial_m u^\dagger \cdot \partial_i\, \partial_j\, \partial_m u \\ &+ \frac{1}{2}\, q^i q^j k^m\, \partial_i\, \partial_j\, u^\dagger \cdot \partial_m u + \frac{1}{4}\, q^i q^j k^l k^m\, u^\dagger \cdot \partial_i\, \partial_j\, \partial_l\, \partial_m u \\ &+ \frac{1}{2}\, k^i k^j q^l q^m\, \partial_l\, u^\dagger \cdot \partial_i\, \partial_j\, \partial_m u + \frac{1}{2}\, q^i q^j k^l k^m\, \partial_i\, \partial_j\, u^\dagger \cdot \partial_l\, \partial_m \partial_m u + \cdots \end{aligned} \tag{B.7}$$

where the summation convention over the repeated indices $i, j, l, m = 1, \cdots, d$ is implied.

We multiply Eq. (B.6a) by Eq. (B.7) and antisymmetrize with respect to the interchange of $\boldsymbol{q}$ and $\boldsymbol{k}$. We obtain

$$R(\boldsymbol{p}, \boldsymbol{q}, \boldsymbol{k}) = q^i k^j \left(T^{(2)}_{ij}\right)(\boldsymbol{p}) + \left(k^i k^j q^m - q^i q^j k^m\right) \left(T^{(3)}_{ij;m}\right)(\boldsymbol{p}) + k^i k^j q^l q^m \left(T^{(4)}_{ij;lm}\right)(\boldsymbol{p}), \tag{B.8a}$$

where the summation convention over the repeated indices $i, j, l, m = 1, \cdots, d$ is implied and we have introduced the short-hand notation

$$\left(T^{(2)}_{ij}\right)(\boldsymbol{p}) \equiv \left(F_{ij}\right)(\boldsymbol{p}) \equiv \left(\partial_i A_j - \partial_i A_j\right)(\boldsymbol{p}), \tag{B.8b}$$

$$\left(T^{(3)}_{ij;m}\right)(\boldsymbol{p}) \equiv \frac{1}{2}\left(\partial_m u^\dagger \cdot \partial_i \partial_j u - \partial_i \partial_j u^\dagger \cdot \partial_m u - 2\partial_j u^\dagger \cdot \partial_i \partial_m u - 2A_j \partial_i A_m\right)(\boldsymbol{p}), \tag{B.8c}$$

and

$$\begin{aligned}\left(T^{(4)}_{ij;lm}\right)(\boldsymbol{p}) \equiv \frac{1}{4}\Big[&\partial_l \partial_m u^\dagger \cdot \partial_i \partial_j u - \partial_i \partial_j u^\dagger \cdot \partial_l \partial_m u + 2A_l \partial_m \left(u^\dagger \cdot \partial_i \partial_j u\right) \\ &- 2A_i \partial_j \left(u^\dagger \cdot \partial_l \partial_m u\right) + 2\partial_l u^\dagger \cdot \partial_i \partial_j \partial_m u - 2\partial_i u^\dagger \cdot \partial_l \partial_j \partial_m u\Big](\boldsymbol{p})\end{aligned} \tag{B.8d}$$

for $i, j, l, m = 1, \cdots, d$. We evaluate

$$\begin{aligned}\Lambda(\boldsymbol{p}, \boldsymbol{q}, \boldsymbol{k}) &= R(\boldsymbol{p} - \boldsymbol{k}, \boldsymbol{q}, \boldsymbol{k})\, M(\boldsymbol{p}, -\boldsymbol{k}) - R(\boldsymbol{p}, \boldsymbol{q}, \boldsymbol{k})\, M(\boldsymbol{p} + \boldsymbol{q} + \boldsymbol{k}, -\boldsymbol{k}) \\ &= \Big[R(\boldsymbol{p}, \boldsymbol{q}, \boldsymbol{k}) - k^a \partial_a R(\boldsymbol{p}, \boldsymbol{q}, \boldsymbol{k}) + \cdots\Big]\Big[1 - k^b A_b(\boldsymbol{p}) + \cdots\Big] \\ &\quad - R(\boldsymbol{p}, \boldsymbol{q}, \boldsymbol{k})\Big[1 - k^a A_a(\boldsymbol{p}) - k^a q^b \partial_b A_a(\boldsymbol{p}) + \cdots\Big] \\ &= -q^i k^j k^a \left(\partial_a T^{(2)}_{ij}\right)(\boldsymbol{p}) + q^i q^j k^m k^a \left(\partial_a T^{(3)}_{ij;m}\right)(\boldsymbol{p}) \\ &\quad + q^b k^a q^i k^j \partial_b A_a(\boldsymbol{p}) \left(T^{(2)}_{ij}\right)(\boldsymbol{p}) + \cdots\end{aligned} \tag{B.9}$$

where the summation convention over the repeated indices $a, b, i, j, m = 1, \cdots, d$ is implied.

At last, we are in a position to evaluate the terms contributing to the function $f_{\boldsymbol{k}}$

in Eq. (B.1). We start with

$$
\begin{aligned}
f_{1,\boldsymbol{k}} &= \frac{1}{2}\sum_{\boldsymbol{q}} v_{\boldsymbol{q}} \left\langle [\delta\widehat{\rho}_{-\boldsymbol{k}}, \delta\widehat{\rho}_{-\boldsymbol{q}}][\delta\widehat{\rho}_{\boldsymbol{q}}, \delta\widehat{\rho}_{\boldsymbol{k}}] \right\rangle \\
&= \frac{1}{2}\sum_{\boldsymbol{q}} v_{\boldsymbol{q}} \left\langle \sum_{\boldsymbol{p}} R(\boldsymbol{p}, -\boldsymbol{k}, -\boldsymbol{q})\, \widehat{\chi}^{\dagger}_{\boldsymbol{p}}\, \widehat{\chi}_{\boldsymbol{p}-\boldsymbol{k}-\boldsymbol{q}} \sum_{\boldsymbol{p}'} R(\boldsymbol{p}', \boldsymbol{q}, \boldsymbol{k})\, \widehat{\chi}^{\dagger}_{\boldsymbol{p}'}\, \widehat{\chi}_{\boldsymbol{p}'+\boldsymbol{k}+\boldsymbol{q}} \right\rangle \\
&= \frac{1}{2}\sum_{\boldsymbol{q}} v_{\boldsymbol{q}} \sum_{\boldsymbol{p},\boldsymbol{p}'} R(\boldsymbol{p}, -\boldsymbol{k}, -\boldsymbol{q})\, R(\boldsymbol{p}', \boldsymbol{q}, \boldsymbol{k}) \left\langle \widehat{\chi}^{\dagger}_{\boldsymbol{p}}\, \widehat{\chi}_{\boldsymbol{p}-\boldsymbol{k}-\boldsymbol{q}}\, \widehat{\chi}^{\dagger}_{\boldsymbol{p}'}\, \widehat{\chi}_{\boldsymbol{p}'+\boldsymbol{k}+\boldsymbol{q}} \right\rangle \\
&= \frac{1}{2}\sum_{\boldsymbol{q}} \sum_{\boldsymbol{p},\boldsymbol{p}'} v_{\boldsymbol{q}} \Big[(-k^a)(-q^b) \left(T^{(2)}_{ab}\right)(\boldsymbol{p}) + \cdots\Big] \Big[q^i k^j \left(T^{(2)}_{ij}\right)(\boldsymbol{p}') + \cdots\Big] \\
&\qquad\qquad \times \left\langle \widehat{\chi}^{\dagger}_{\boldsymbol{p}}\, \widehat{\chi}_{\boldsymbol{p}-\boldsymbol{k}-\boldsymbol{q}}\, \widehat{\chi}^{\dagger}_{\boldsymbol{p}'}\, \widehat{\chi}_{\boldsymbol{p}'+\boldsymbol{k}+\boldsymbol{q}} \right\rangle \\
&= -\frac{1}{2}\sum_{\boldsymbol{q},\boldsymbol{p},\boldsymbol{p}'} v_{\boldsymbol{q}} \Big[k^a q^b \left(F_{ab}\right)(\boldsymbol{p})\Big] \Big[k^i q^j \left(F_{ij}\right)(\boldsymbol{p}')\Big] \left\langle \widehat{\chi}^{\dagger}_{\boldsymbol{p}}\, \widehat{\chi}_{\boldsymbol{p}-\boldsymbol{k}-\boldsymbol{q}}\, \widehat{\chi}^{\dagger}_{\boldsymbol{p}'}\, \widehat{\chi}_{\boldsymbol{p}'+\boldsymbol{k}+\boldsymbol{q}} \right\rangle + \cdots \\
&= -\frac{1}{2}\sum_{\boldsymbol{q},\boldsymbol{p},\boldsymbol{p}'} v_{\boldsymbol{q}} \Big[(\boldsymbol{k}\wedge\boldsymbol{q})\cdot\boldsymbol{B}(\boldsymbol{p})\Big] \Big[(\boldsymbol{k}\wedge\boldsymbol{q})\cdot\boldsymbol{B}(\boldsymbol{p}')\Big] \left\langle \widehat{\chi}^{\dagger}_{\boldsymbol{p}}\, \widehat{\chi}_{\boldsymbol{p}-\boldsymbol{k}-\boldsymbol{q}}\, \widehat{\chi}^{\dagger}_{\boldsymbol{p}'}\, \widehat{\chi}_{\boldsymbol{p}'+\boldsymbol{k}+\boldsymbol{q}} \right\rangle + \cdots ,
\end{aligned}
\tag{B.10}
$$

where we used that $B^i = \epsilon^{ijm}\partial_j A_m = \frac{1}{2}\epsilon^{ijm}F_{jm}$ or, equivalently, $F_{ij} = \epsilon_{ijm}B^m$. We now break the Berry field strength into two contributions, i.e., $\boldsymbol{B}(\boldsymbol{p}) = \overline{\boldsymbol{B}} + \delta\boldsymbol{B}(\boldsymbol{p})$.

If so,

$$
\begin{aligned}
f_{1,\boldsymbol{k}} &= -\frac{1}{2}\sum_{\boldsymbol{q},\boldsymbol{p},\boldsymbol{p}'} v_{\boldsymbol{q}}\Big[\,(\boldsymbol{k}\wedge\boldsymbol{q})\cdot\big(\overline{\boldsymbol{B}}+\delta\boldsymbol{B}(\boldsymbol{p})\big)\Big]\Big[\,(\boldsymbol{k}\wedge\boldsymbol{q})\cdot\big(\overline{\boldsymbol{B}}+\delta\boldsymbol{B}(\boldsymbol{p}')\big)\,\Big] \\
&\qquad\qquad \Big\langle \widehat{\chi}^{\dagger}_{\boldsymbol{p}}\widehat{\chi}_{\boldsymbol{p}-\boldsymbol{k}-\boldsymbol{q}}\widehat{\chi}^{\dagger}_{\boldsymbol{p}'}\widehat{\chi}_{\boldsymbol{p}'+\boldsymbol{k}+\boldsymbol{q}}\Big\rangle + \cdots \\
&= -\frac{1}{2}\sum_{\boldsymbol{q}} v_{\boldsymbol{q}}\Big[\,(\boldsymbol{k}\wedge\boldsymbol{q})\cdot\overline{\boldsymbol{B}}\Big]\Big[\,(\boldsymbol{k}\wedge\boldsymbol{q})\cdot\overline{\boldsymbol{B}}\Big]\Big\langle \widehat{\rho}_{-\boldsymbol{k}-\boldsymbol{q}}\,\widehat{\rho}_{\boldsymbol{k}+\boldsymbol{q}}\Big\rangle \\
&\quad -\frac{1}{2}\sum_{\boldsymbol{q},\boldsymbol{p}'} v_{\boldsymbol{q}}\Big[\,(\boldsymbol{k}\wedge\boldsymbol{q})\cdot\overline{\boldsymbol{B}}\Big]\Big[\,(\boldsymbol{k}\wedge\boldsymbol{q})\cdot\delta\boldsymbol{B}(\boldsymbol{p}')\Big]\Big\langle \widehat{\rho}_{-\boldsymbol{k}-\boldsymbol{q}}\,\widehat{\chi}^{\dagger}_{\boldsymbol{p}'}\,\widehat{\chi}_{\boldsymbol{p}'+\boldsymbol{k}+\boldsymbol{q}}\Big\rangle \\
&\quad -\frac{1}{2}\sum_{\boldsymbol{q},\boldsymbol{p},\boldsymbol{p}'} v_{\boldsymbol{q}}\Big[\,(\boldsymbol{k}\wedge\boldsymbol{q})\cdot\delta\boldsymbol{B}(\boldsymbol{p})\Big]\Big[\,(\boldsymbol{k}\wedge\boldsymbol{q})\cdot\overline{\boldsymbol{B}}\Big]\Big\langle \widehat{\chi}^{\dagger}_{\boldsymbol{p}}\,\widehat{\chi}_{\boldsymbol{p}-\boldsymbol{k}-\boldsymbol{q}}\,\widehat{\rho}_{\boldsymbol{k}+\boldsymbol{q}}\Big\rangle \\
&\quad -\frac{1}{2}\sum_{\boldsymbol{q},\boldsymbol{p},\boldsymbol{p}'} v_{\boldsymbol{q}}\Big[\,(\boldsymbol{k}\wedge\boldsymbol{q})\cdot\delta\boldsymbol{B}(\boldsymbol{p})\Big]\Big[\,(\boldsymbol{k}\wedge\boldsymbol{q})\cdot\delta\boldsymbol{B}(\boldsymbol{p}')\Big]\Big\langle \widehat{\chi}^{\dagger}_{\boldsymbol{p}}\,\widehat{\chi}_{\boldsymbol{p}-\boldsymbol{k}-\boldsymbol{q}}\,\widehat{\chi}^{\dagger}_{\boldsymbol{p}'}\,\widehat{\chi}_{\boldsymbol{p}'+\boldsymbol{k}+\boldsymbol{q}}\Big\rangle \\
&\quad +\cdots .
\end{aligned}
\tag{B.11}
$$

In a uniform liquid-like ground state we have $\langle\,\widehat{\rho}_{\boldsymbol{k}}\,\rangle \propto \delta_{\boldsymbol{k},\boldsymbol{0}}$ and, due to the relation $k^a q^b\, F_{ab} = (\boldsymbol{k}\wedge\boldsymbol{q})\cdot\boldsymbol{B}$, we can replace $\widehat{\rho}_{\pm\boldsymbol{k}\pm\boldsymbol{q}}$ by $\delta\widehat{\rho}_{\pm\boldsymbol{k}\pm\boldsymbol{q}}$. As a consequence, we can drop the first three terms on the last equality of (B.11) up to order $\boldsymbol{q}^2\boldsymbol{k}^2$. We are then left with:

$$
f_{1,\boldsymbol{k}} = -\frac{1}{2}\sum_{\boldsymbol{q}}\sum_{\boldsymbol{p},\boldsymbol{p}'} v_{\boldsymbol{q}}\Big[\,(\boldsymbol{k}\wedge\boldsymbol{q})\cdot\delta\boldsymbol{B}(\boldsymbol{p})\Big]\Big[\,(\boldsymbol{k}\wedge\boldsymbol{q})\cdot\delta\boldsymbol{B}(\boldsymbol{p}')\Big]\Big\langle \hat{n}_{\boldsymbol{p}}\hat{n}_{\boldsymbol{p}'}\Big\rangle + \cdots , \tag{B.12}
$$

where $\hat{n}_{\boldsymbol{p}} \equiv \widehat{\chi}^{\dagger}_{\boldsymbol{p}}\,\widehat{\chi}_{\boldsymbol{p}}$ is the number operator projected on the lowest band. Similarly,

$$
\begin{aligned}
f_{2,\boldsymbol{k}} &= \frac{1}{2}\sum_{\boldsymbol{q}} v_{\boldsymbol{q}}\Big\langle [\delta\widehat{\rho}_{-\boldsymbol{q}},\delta\widehat{\rho}_{\boldsymbol{k}}][\delta\widehat{\rho}_{-\boldsymbol{k}},\delta\widehat{\rho}_{\boldsymbol{q}}]\Big\rangle \\
&= \frac{1}{2}\sum_{\boldsymbol{q}} v_{\boldsymbol{q}}\Big\langle [\delta\widehat{\rho}_{\boldsymbol{k}},\delta\widehat{\rho}_{-\boldsymbol{q}}][\delta\widehat{\rho}_{\boldsymbol{q}},\delta\widehat{\rho}_{-\boldsymbol{k}}]\Big\rangle \\
&= f_{1,-\boldsymbol{k}} \\
&= -\frac{1}{2}\sum_{\boldsymbol{q}}\sum_{\boldsymbol{p},\boldsymbol{p}'} v_{\boldsymbol{q}}\Big[\,(\boldsymbol{k}\wedge\boldsymbol{q})\cdot\delta\boldsymbol{B}(\boldsymbol{p})\Big]\Big[\,(\boldsymbol{k}\wedge\boldsymbol{q})\cdot\delta\boldsymbol{B}(\boldsymbol{p}')\Big]\Big\langle \hat{n}_{\boldsymbol{p}}\hat{n}_{\boldsymbol{p}'}\Big\rangle + \cdots ,
\end{aligned}
\tag{B.13}
$$

while

$$\begin{aligned} f_{3,\boldsymbol{k}} &= \frac{1}{2}\sum_{\boldsymbol{q}} v_{\boldsymbol{q}} \Big\langle \delta\widehat{\rho}_{-\boldsymbol{q}} \left[\delta\widehat{\rho}_{-\boldsymbol{k}}, \left[\delta\widehat{\rho}_{\boldsymbol{q}}, \delta\widehat{\rho}_{\boldsymbol{k}}\right]\right] \Big\rangle \\ &= \frac{1}{2}\sum_{\boldsymbol{q}} v_{\boldsymbol{q}} \Big\langle \delta\widehat{\rho}_{-\boldsymbol{q}} \sum_{\boldsymbol{p}} \Lambda(\boldsymbol{p},\boldsymbol{q},\boldsymbol{k})\, \widehat{\chi}^{\dagger}_{\boldsymbol{p}}\, \widehat{\chi}_{\boldsymbol{p}+\boldsymbol{q}} \Big\rangle \\ &= \frac{1}{2}\sum_{\boldsymbol{q}}\sum_{\boldsymbol{p}} v_{\boldsymbol{q}}\, \Lambda(\boldsymbol{p},\boldsymbol{q},\boldsymbol{k}) \Big\langle \delta\widehat{\rho}_{-\boldsymbol{q}}\, \widehat{\chi}^{\dagger}_{\boldsymbol{p}}\, \widehat{\chi}_{\boldsymbol{p}+\boldsymbol{q}} \Big\rangle. \end{aligned} \tag{B.14}$$

The matrix element $\left\langle \delta\widehat{\rho}_{-\boldsymbol{q}}\, \widehat{\chi}^{\dagger}_{\boldsymbol{p}}\, \widehat{\chi}_{\boldsymbol{p}+\boldsymbol{q}} \right\rangle$ vanishes in the limit $\boldsymbol{q} \to 0$ and, therefore, the only term that contributes to $f_{3,\boldsymbol{k}}$ up to order $\boldsymbol{q}^2\boldsymbol{k}^2$ is

$$\begin{aligned} f_{3,\boldsymbol{k}} &= \frac{1}{2}\sum_{\boldsymbol{q}}\sum_{\boldsymbol{p}} v_{\boldsymbol{q}} \Big[-q^i k^j k^a \left(\partial_a F_{ij}\right)(\boldsymbol{p}) \Big] \Big\langle \delta\widehat{\rho}_{-\boldsymbol{q}}\, \widehat{\chi}^{\dagger}_{\boldsymbol{p}}\, \widehat{\chi}_{\boldsymbol{p}+\boldsymbol{q}} \Big\rangle \\ &= \frac{1}{2}\sum_{\boldsymbol{q}}\sum_{\boldsymbol{p}} v_{\boldsymbol{q}} \Big[(\boldsymbol{k}\wedge\boldsymbol{q})\cdot\left(\frac{\partial \boldsymbol{B}}{\partial p^a}\right)(\boldsymbol{p}) \Big] k^a \Big\langle \delta\widehat{\rho}_{-\boldsymbol{q}}\, \widehat{\chi}^{\dagger}_{\boldsymbol{p}}\, \widehat{\chi}_{\boldsymbol{p}+\boldsymbol{q}} \Big\rangle. \end{aligned} \tag{B.15}$$

The condition (B.5) implies that $f_{4,\boldsymbol{k}} = f^{*}_{3,\boldsymbol{k}}$, which then delivers

$$f_{4,\boldsymbol{k}} = \frac{1}{2}\sum_{\boldsymbol{q}}\sum_{\boldsymbol{p}} v_{\boldsymbol{q}} \Big[-(\boldsymbol{k}\wedge\boldsymbol{q})\cdot\left(\frac{\partial \boldsymbol{B}}{\partial p^a}\right)(\boldsymbol{p}) \Big] k^a \Big\langle \widehat{\chi}^{\dagger}_{\boldsymbol{p}+\boldsymbol{q}}\, \widehat{\chi}_{\boldsymbol{p}} \delta\widehat{\rho}_{\boldsymbol{q}} \Big\rangle, \tag{B.16}$$

where we have used that $(\boldsymbol{B}(\boldsymbol{p}))^{*} = -\boldsymbol{B}(\boldsymbol{p})$.

Putting together all the contributions, we obtain

$$\begin{aligned} f_{\boldsymbol{k}} = &-\sum_{\boldsymbol{q}}\sum_{\boldsymbol{p},\boldsymbol{p}'} v_{\boldsymbol{q}} \Big[(\boldsymbol{k}\wedge\boldsymbol{q})\cdot\delta\boldsymbol{B}(\boldsymbol{p}) \Big] \Big[(\boldsymbol{k}\wedge\boldsymbol{q})\cdot\delta\boldsymbol{B}(\boldsymbol{p}') \Big] \Big\langle \hat{n}_{\boldsymbol{p}}\hat{n}_{\boldsymbol{p}'} \Big\rangle \\ &+ \frac{k^a}{2}\sum_{\boldsymbol{q}}\sum_{\boldsymbol{p}} v_{\boldsymbol{q}} \Big[(\boldsymbol{k}\wedge\boldsymbol{q})\cdot\left(\frac{\partial \boldsymbol{B}}{\partial p^a}\right)(\boldsymbol{p}) \left\langle \delta\widehat{\rho}_{-\boldsymbol{q}}\, \widehat{\chi}^{\dagger}_{\boldsymbol{p}}\, \widehat{\chi}_{\boldsymbol{p}+\boldsymbol{q}} \right\rangle \\ &\qquad - (\boldsymbol{k}\wedge\boldsymbol{q})\cdot\left(\frac{\partial \boldsymbol{B}}{\partial p^a}\right)(\boldsymbol{p}) \Big\langle \widehat{\chi}^{\dagger}_{\boldsymbol{p}+\boldsymbol{q}}\, \widehat{\chi}_{\boldsymbol{p}}\, \delta\widehat{\rho}_{\boldsymbol{q}} \Big\rangle \Big] \end{aligned} \tag{B.17}$$

where the summation convention over the repeated indices $a = 1, \cdots, d$ is implied. Finally, the analytical continuation $\boldsymbol{\mathcal{B}} \equiv -\mathrm{i}\boldsymbol{B}$ delivers Eq. (5.32a).

Bibliography

[1] A. Altland and M. R. Zirnbauer. Nonstandard symmetry classes in mesoscopic normal-superconducting hybrid structures. *Phys. Rev. B*, **55**, 1142 (1997).

[2] D. Arovas, J. R. Schrieffer, and F. Wilczek. Fractional statistics and the quantum Hall effect. *Phys. Rev. Lett.*, **53**, 722 (1984).

[3] D. Bercioux, D. Urban, H. Grabert, and W. Häusler. Massless Dirac-Weyl fermions in a t3 optical lattice. *Phys. Rev. A*, **80**, 063603 (2009).

[4] D. L. Bergman, C. Wu, and L. Balents. Band touching from real-space topology in frustrated hopping models. *Phys. Rev. B*, **78**, 125104 (2008).

[5] N. Berline, E. Getzler, and M. Vergne. *Heat Kernels and Dirac Operators*. Springer, Berlin, 2004.

[6] B. A. Bernevig, T. L. Hughes, and S.-C. Zhang. Quantum spin Hall effect and topological phase transition in HgTe quantum wells. *Science*, **314**, 1757 (2006).

[7] B. A. Bernevig and S.-C. Zhang. Spin quantum hall effect. *Phys. Rev. Lett.*, **96**, 106802 (2006).

[8] M. V. Berry. Quantal phase factors accompanying adiabatic changes. *Proc. R. Soc. Lond. A*, **392**, 45 (1984).

[9] A. Blasi, A. Braggio, M. Carrega, D. Ferraro, N. Maggiore, and N. Magnoli. Non-abelian BF theory for 2+1 dimensional topological states of matter. *New J. Phys.*, **14**, 013060 (2012).

[10] M. Blau and G. Thompson. Topological gauge theories of antisymmetric tensor fields. *Ann. Phys.*, **205**, 130 (1991).

[11] B. Blok and X. G. Wen. Effective theories of the fractional quantum Hall effect at generic filling fractions. *Phys. Rev. B*, **42**, 8133 (1990).

[12] B. Blok and X. G. Wen. Structure of the microscopic theory of the hierarchical fractional quantum Hall effect. *Phys. Rev. B*, **43**, 8337 (1991).

[13] C. Callan and J. Harvey. Anomalies and fermion zero modes on strings and domain walls. *Nucl. Phys. B*, **250**, 427 (1985).

[14] C. Chamon, C.-Y. Hou, R. Jackiw, C. Mudry, S.-Y. Pi, and A. P. Schnyder. Irrational versus rational charge and statistics in two-dimensional quantum systems. *Phys. Rev. Lett.*, **100**, 110405 (2008).

[15] C. Chamon, C.-Y. Hou, R. Jackiw, C. Mudry, S.-Y. Pi, and G. Semenoff. Electron fractionalization for two-dimensional Dirac fermions. *Phys. Rev. B*, **77**, 235431 (2008).

[16] Y.-H. Chen and F. Wilczek. Induced quantum numbers in some $2+1$ dimensional models. *Int. J. Mod. Phys. B*, **3**, 117 (1989).

[17] Y. L. Chen, J. G. Analytic, J.-H. Chu, Z. K. Liu, S.-K. Mo, X. L. Qi, H. J. Zhang, D. H. Lu, X. Dai, Z. Fang, S. C. Zhang, I. R. Fisher, Z. Hussain, and Z.-X. Shen. Experimental realization of a three-dimensional topological insulator, Bi2Te3. *Science*, **325**, 178 (2009).

[18] G. Y. Cho and J. E. Moore. Quantum phase transition and fractional excitations in a topological insulator thin film with Zeeman and excitonic masses. *Phys. Rev. B*, **84**, 165101 (2011).

[19] G. Y. Cho and J. E. Moore. Topological BF field theory description of topological insulators. *Ann. Phys.*, **326**, 1515 (2011).

[20] E. Dagotto, E. Fradkin, and A. Moreo. A comment on the Nielsen-Ninomiya theorem. *Phys. Lett. B*, **172**, 383 (1986).

[21] M. C. Diamantini, P. Sodano, and C. Trugenberger. Superconductors with topological order. *Eur. Phys. J.*, **B53**, 19 (2006).

[22] S. Elitzur, G. Moore, A. Schwimmer, and N. Seiberg. Remarks on the canonical quantization of the Chern-Simons-Witten theory. *Nucl. Phys. B*, **326**, 108 (1989).

[23] R. P. Feynman. *Statistical Mechanics*. Benjamin Reading, Mass., 1972.

[24] E. Fradkin, E. Dagotto, and D. Boyanovsky. Physical realization of the parity anomaly in condensed matter physics. *Phys. Rev. Lett.*, **57**, 2967 (1986).

[25] M. Freedman, M. B. Hastings, C. Nayak, X.-L. Qi, K. Walker, and Z. Wang. Projective ribbon permutation statistics: a remnant of non-abelian braiding in higher dimensions. *Phys. Rev. B*, **83**, 115132 (2011).

[26] M. Freedman, C. Nayak, K. Shtengel, K. Walker, and Z. Wang. A class of (P,T)-invariant topological phases of interacting electrons. *Ann. of Phys. (N.Y.)*, **310**, 428 (2004).

[27] J. Fröhlich and T. Kerler. Universality in quantum Hall systems. *Nucl. Phys. B*, **354**, 369 (1991).

[28] J. Fröhlich and E. Thiran. Integral quadratic forms, kac-moody algebras and fractional quantum Hall effect. *J. Stat. Phys.*, **76**, 209 (1994).

[29] J. Fröhlich and A. Zee. Large scale physics of the quantum Hall fluid. *Nucl. Phys. B*, **364**, 517 (1991).

[30] L. Fu and C. L. Kane. Topological insulators with inversion symmetry. *Phys. Rev. B*, **76**, 045302 (2007).

[31] L. Fu and C. L. Kane. Sc proximity effect and Majorana fermions at the surface of a topological insulator. *Phys. Rev. Lett.*, **100**, 096407 (2008).

[32] L. Fu, C. L. Kane, and E. J. Mele. Topological insulators in three dimensions. *Phys. Rev. Lett.*, **98**, 106803 (2007).

[33] T. Fukui and T. Fujiwara. Topological stability of Majorana zero modes in superconductortopological insulator systems. *J. Phys. Soc. Jpn.*, **79**, 033701 (2010).

[34] P. Ghaemi and F. Wilczek. Near-zero modes in superconducting graphene. *Phys. Scr. T*, **146**, 014019 (2012).

[35] P. B. Gilkey. *Invariance Theory, the Heat Equation, and the Atiyah-Singer Theorem.* Publish or Perish Inc, USA, 1984.

[36] S. M. Girvin. Particle-hole symmetry in the anomalous quantum Hall effect. *Phys. Rev. B*, **29**, 6012 (1984).

[37] S. M. Girvin, A. H. MacDonald, and P. M. Platzman. Collective-excitation gap in the fractional quantum Hall effect. *Phys. Rev. Lett.*, **54**, 581 (1985).

[38] M. O. Goerbig. From fractional chern insulators to a fractional quantum spin Hall effect. *Eur. Phys. J. B*, **85**, 15 (2012).

[39] J. Goldstone and F. Wilczek. Fractional quantum numbers on solitons. *Phys. Rev. Lett.*, **47**, 986 (1981).

[40] H.-M. Guo and M. Franz. Topological insulator on the kagome lattice. *Phys. Rev. B*, **80**, 113102 (2009).

[41] V. Gurarie and L. Radzihovsky. Zero modes of two-dimensional chiral p-wave superconductors. *Phys. Rev. B*, **75**, 212509 (2007).

[42] F. D. M. Haldane. Fractional quantization of the Hall effect: A hierarchy of incompressible quantum fluid states. *Phys. Rev. Lett.*, **51**, 605 (1983).

[43] F. D. M. Haldane. Model for a quantum Hall effect without Landau levels: Condensed-matter realization of the "parity anomaly". *Phys. Rev. Lett.*, **61**, 2015 (1988).

[44] F. D. M. Haldane. Berry curvature on the Fermi surface: Anomalous Hall effect as a topological Fermi-liquid property. *Phys. Rev. Lett.*, **93**, 206602 (2004).

[45] B. I. Halperin. Quantized Hall conductance, current-carrying edge states, and the existence of extended states in a two-dimensional disordered potential. *Phys. Rev. B*, **25**, 2185 (1982).

[46] B. I. Halperin. Theory of the quantized Hall conductance. *Helv. Phys. Acta*, **56**, 75 (1983).

[47] B. I. Halperin. Statistics of quasiparticles and the hierarchy of fractional quantized Hall states. *Phys. Rev. Lett.*, **52**, 1583 (1984).

[48] T. H. Hansson, V. Oganesyan, and S. L. Sondhi. Superconductors are topologically ordered. *Ann. of Phys.*, **313**, 497 (2004).

[49] I. F. Herbut and C.-K. Lu. Spectrum of the Dirac Hamiltonian with the mass hedgehog in arbitrary dimension. *Phys. Rev. B*, **83**, 125412 (2011).

[50] Z. Hlousek, D. Senechal, and S. H. H. Tye. Induced Hopf term in the nonlinear σ model. *Phys. Rev. D*, **41**, 3773 (1990).

[51] D. R. Hofstadter. Energy levels and wave functions of Bloch electrons in rational and irrational magnetic fields. *Phys. Rev. B*, **14**, 2239 (1976).

[52] C.-Y. Hou, C. Chamon, and C. Mudry. Electron fractionalization in two-dimensional graphenelike structures. *Phys. Rev. Lett.*, **98**, 186809 (2007).

[53] D. Hsieh, D. Qian, L. Wray, Y. Xia, Y. S. Hor, R. J. Cava, , and M. Z. Hasan. A topological Dirac insulator in a quantum spin Hall phase. *Nature (London)*, **452**, 970 (2008).

[54] D. A. Ivanov. Non-abelian statistics of half-quantum vortices in p-wave superconductors. *Phys. Rev. Lett.*, **86**, 268 (2001).

[55] R. Jackiw and S.-Y. Pi. Chiral gauge theory for graphene. *Phys. Rev. Lett.*, **98**, 266402 (2007).

[56] R. Jackiw and C. Rebbi. Solitons with fermion number 1/2. *Phys. Rev. D*, **13**, 3398 (1976).

[57] R. Jackiw and P. Rossi. Zero modes of the vortex-fermion system. *Nucl. Phys. B*, **190**, 681 (1981).

[58] R. Jackiw and J. R. Schrieffer. Solitons with fermion number 1/2 in condensed matter and relativistic field theories. *Nucl. Phys. B*, **190**, 253 (1981).

[59] J. K. Jain. Composite-fermion approach for the fractional quantum Hall effect. *Phys. Rev. Lett.*, **63**, 199 (1989).

[60] J. K. Jain. Incompressible quantum Hall states. *Phys. Rev. B*, **40**, 8079 (1989).

[61] T. Jaroszewicz. Induced fermion current in the σ model in $(2+1)$ dimensions. *Phys. Lett. B*, **146**, 337 (1984).

[62] C. L. Kane and E. J. Mele. Quantum spin Hall effect in graphene. *Phys. Rev. Lett.*, **95**, 226801 (2005).

[63] C. L. Kane and E. J. Mele. Z2 topological order and the quantum spin Hall effect. *Phys. Rev. Lett.*, **95**, 146802 (2005).

[64] D. Kaplan. A method for simulating chiral fermions on the lattice. *Phys. Lett. B*, **288**, 342 (1992).

[65] H. Katsura, I. Maruyama, A. Tanaka, and H. Tasaki. Ferromagnetism in the Hubbard model with topological/non-topological flat bands. *Europhys Lett.*, **91**, 57007 (2010).

[66] A. Kitaev. Fault-tolerant quantum computation by anyons. *Ann. Phys.*, **303**, 2 (2003).

[67] A. Kitaev. Periodic table for topological insulators and superconductors. *AIP Conf. Proc.*, **1134**, 22 (2009).

[68] M. König, S. Wiedmann, C. Brüne, A. Roth, H. Buhmann, L. W. Molenkamp, X.-L. Qi, and S.-C. Zhang. Quantum spin Hall insulator state in HgTe quantum wells. *Science*, **318**, 766 (2007).

[69] R. B. Laughlin. Quantized Hall conductivity in two dimensions. *Phys. Rev. B*, **23**, 5632 (1981).

[70] R. B. Laughlin. Anomalous quantum Hall effect: An incompressible quantum fluid with fractionally charged excitations. *Phys. Rev. Lett.*, **50**, 1395 (1983).

[71] R. B. Laughlin. Primitive and composite ground states in the fractional quantum Hall effect. *Surf. Sci.*, **142**, 163 (1984).

[72] M. Levin and A. Stern. Fractional topological insulators. *Phys. Rev. Lett.*, **103**, 196803 (2009).

[73] A. H. MacDonald, G. C. Aers, and M. W. C. Dharma-wardana. Hierarchy of plasmas for fractional quantum Hall states. *Phys. Rev. B*, **31**, 5529 (1985).

[74] A. H. MacDonald and D. B. Murray. Particle-hole symmetry in the anomalous quantum Hall effect. *Phys. Rev. B*, **32**, 2707 (1985).

[75] E. Majorana. Teoria simetrica dell'elettrone e del positrone. *Nuovo Cimento*, **5**, 171 (1937).

[76] R. B. Melrose. *The Atiyah-Patodi-Singer Index Theorem*. Peters, A K, Limited, Wellesley, 1993.

[77] M.Kohmoto. Topological invariant and the quantization of the Hall conductance. *Ann. Phys.*, **160**, 343 (1985).

[78] R. Moessner, S. L. Sondhi, and E. Fradkin. Short-ranged resonating valence bond physics, quantum dimer models, and Ising gauge theories. *Phys. Rev. B*, **65**, 024504 (2001).

[79] G. Moore and N. Read. Nonabelions in the fractional quantum Hall effect. *Nucl. Phys. B*, **360**, 362 (1991).

[80] J. E. Moore and L. Balents. Topological invariants of time-reversal-invariant band structures. *Phys. Rev. B*, **75**, 121306 (2007).

[81] C. Mudry and E. Fradkin. Mechanism of spin and charge separation in one-dimensional quantum antiferromagnets. *Phys. Rev. B*, **50**, 11409 (1994).

[82] A. H. C. Neto, F. Guinea, N. M. Peres, K. S. Novoselov, and A. K. Geim. The electronic properties of graphene. *Rev. Mod. Phys.*, **81**, 109 (2009).

[83] T. Neupert, L. Santos, S. Ryu, C. Chamon, and C. Mudry. Fractional topological liquids with time-reversal symmetry and their lattice realization. *Phys. Rev. B*, **84**, 165107 (2011).

[84] H. B. Nielsen and M. Ninomiya. Absence of neutrinos on a lattice: (i). proof by homotopy theory. *Nucl. Phys. B*, **185**, 20 (1981).

[85] A. Niemi and G. Semenoff. Fermion number fractionization in quantum field theory. *Phys. Rep.*, **135**, 99 (1986).

[86] Q. Niu and D. J. Thouless. Quantized adiabatic charge transport in the presence of substrate disorder and many-body interaction. *J. Phys. A*, **17**, 2453 (1984).

[87] Q. Niu, D. J. Thouless, and Y.-S. Wu. Quantized Hall conductance as a topological invariant. *Phys. Rev. B*, **31**, 3372 (1985).

[88] K. Ohgushi, S. Murakami, and N. Nagaosa. Spin anisotropy and quantum Hall effect in the kagom lattice: Chiral spin state based on a ferromagnet. *Phys. Rev. B*, **62**, R6065 (2000).

[89] S. Parameswaran, R. Roy, and S. Sondhi. Fractional Chern insulators and the W-infinity algebra. arXiv:1106.4025 (2011).

[90] X. Qi, T. Hughes, and S. Zhang. Topological field theory of time-reversal invariant insulators. *Phys. Rev. B*, **78**, 195424 (2008).

[91] X.-L. Qi. Generic wavefunction description of fractional quantum anomalous Hall states and fractional topological insulators. *Phys. Rev. Lett.*, **107**, 126803 (2011).

[92] N. Read. Excitation structure of the hierarchy scheme in the fractional quantum Hall effect. *Phys. Rev. Lett.*, **65**, 1502 (1990).

[93] N. Read. Conformal invariance of chiral edge theories. *Phys. Rev. B*, **79**, 245304 (2009).

[94] N. Read and D. Green. Paired states of fermions in two dimensions with breaking of parity and time-reversal symmetries and the fractional quantum Hall effect. *Phys. Rev. B*, **61**, 10267 (2000).

[95] N. Read and S. Sachdev. Large-n expansion for frustrated quantum antiferromagnets. *Phys. Rev. Lett.*, **66**, 1773 (1991).

[96] R. Roy. Z_2 classification of quantum spin Hall systems: An approach using time-reversal invariance. *Phys. Rev. B*, **79**, 195321 (2009).

[97] R. Roy. Topological Majorana and Dirac zero modes in superconducting vortex cores. *Phys. Rev. Lett.*, **105**, 186401 (2010).

[98] S. Ryu, C. Mudry, C.-Y. Hou, and C. Chamon. Masses in graphenelike two-dimensional electronic systems: Topological defects in order parameters and their fractional exchange statistics. *Phys. Rev. B*, **80**, 205319 (2009).

[99] S. Ryu, A. P. Schnyder, A. Furusaki, and A. W. W. Ludwig. Topological insulators and superconductors: tenfold way and dimensional hierarchy. *New J. Phys.*, **12**, 065010 (2010).

[100] M. L. S.-P. Kou and X.-G. Wen. Mutual chern-simons theory for $\mathbb{Z}2$ topological order. *Phys. Rev. B*, **78**, 155134 (2008).

[101] X.-L. Q. S.-P. Kou and Z.-Y. Weng. Mutual Chern-Simons effective theory of doped antiferromagnets. *Phys. Rev. B*, **71**, 235102 (2005).

[102] L. Santos, T. Neupert, C. Chamon, and C. Mudry. Superconductivity on the surface of topological insulators and in two-dimensional noncentrosymmetric materials. *Phys. Rev. B*, **81**, 184502 (2010).

[103] M. Sato. Topological odd-parity superconductors. *Phys. Rev. B*, **81**, 220504(R) (2010).

[104] M. Sato and S. Fujimoto. Topological phases of noncentrosymmetric superconductors: Edge states, Majorana fermions, and non-abelian statistics. *Phys. Rev. B*, **79**, 094504 (2009).

[105] J. Sau, R. Lutchyn, S. Tewari, and S. D. Sarma. Generic new platform for topological quantum computation using semiconductor heterostructures. *Phys. Rev. Lett.*, **104**, 040502 (2010).

[106] A. P. Schnyder, S. Ryu, A. Furusaki, and A. W. W. Ludwig. Classification of topological insulators and superconductors in three spatial dimensions. *Phys. Rev. B*, **78**, 195125 (2008).

[107] T. Senthil and M. P. Fisher. Quasiparticle localization in superconductors with spin-orbit scattering. *Phys. Rev. B*, **61**, 9690 (2000).

[108] T. Senthil, M. P. Fisher, L. Balents, and C. Nayak. Quasiparticle transport and localization in high- Tc superconductors. *Phys. Rev. Lett.*, **81**, 4704 (1998).

[109] B. Simon. Holonomy, the quantum adiabatic theorem, and Berry's phase. *Phys. Rev. Lett.*, **51**, 2167 (1983).

[110] H. L. Stormer, A. Chang, D. C. T. J. C. M. Hwang, A. C. Gossard, and W. Wiegmann. Fractional quantization of the Hall effect. *Phys.Rev. Lett.*, **50**, 1953 (1983).

[111] J. P. Straley. Band structure of a tight-binding Hamiltonian. *Phys. Rev. B*, **6**, 4086 (1972).

[112] W. P. Su and J. R. Schrieffer. Fractionally charged excitations in charge-density-wave systems with commensurability 3. *Phys. Rev. Lett.*, **46**, 738 (1981).

[113] W. P. Su, J. R. Schrieffer, and A. J. Heeger. Solitons in polyacetylene. *Phys. Rev. Lett.*, **42**, 1698 (1979).

[114] W. P. Su, J. R. Schrieffer, and A. J. Heeger. Soliton excitations in polyacetylene. *Phys. Rev. B*, **22**, 2099 (1980).

[115] J. C. Y. Teo and C. L. Kane. Topological defects and gapless modes in insulators and superconductors. *Phys. Rev. B*, **82**, 115120 (2010).

[116] S. Tewari, S. D. Sarma, and D. H. Lee. An index theorem for the Majorana zero modes in chiral p-wave superconductors. *Phys. Rev. Lett.*, **99**, 037001 (2007).

[117] T. Thonhauser and D. Vanderbilt. Insulator/chern-insulator transition in the Haldane model. *Phys. Rev. B*, **74**, 235111 (2006).

[118] M. F. Thorpe and D. L. Weaire. Electronic properties of an amorphous solid. ii. Further aspects of the theory. *Phys. Rev. B*, **4**, 3518 (1971).

[119] D. J. Thouless. Level crossing and the fractional quantum Hall effect. *Phys. Rev. B*, **40**, 12034 (1989).

[120] D. J. Thouless, M. Kohmoto, M. P. Nightingale, and M. den Nijs. Quantized Hall conductance in a two-dimensional periodic potential. *Phys. Rev. Lett.*, **49**, 405 (1982).

[121] D. C. Tsui, H. L. Stormer, and A. C. Gossard. Two-dimensional magnetotransport in the extreme quantum limit. *Phys.Rev. Lett.*, **48**, 1559 (1982).

[122] K. v. Klitzing, G. Dorda, and M. Pepper. New method for high-accuracy determination of the fine-structure constant based on quantized Hall resistance. *Phys.Rev. Lett.*, **45**, 494 (1980).

[123] G. E. Volovik. Analog of quantum Hall effect in superfuid ^{3}He film. *Sov. Phys. JETP*, **67**, 1804 (1988).

[124] G. E. Volovik. Localized fermions on quantized vortices in superfluid ^{3}He-B. *J. Phys. Condens. Matter*, **3**, 357 (1991).

[125] G. E. Volovik. *The Universe in a Helium Droplet.* Clarendon Press, Oxford, 2003.

[126] D. Weaire. Existence of a gap in the electronic density of states of a tetrahedrally bonded solid of arbitrary structure. *Phys. Rev. Lett.*, **26**, 1541 (1971).

[127] D. L. Weaire and M. F. Thorpe. Electronic properties of an amorphous solid. i. A simple tight-binding theory. *Phys. Rev. B*, **4**, 2508 (1971).

[128] E. J. Weinberg. Index calculations for the fermion-vortex system. *Phys. Rev. D*, **24**, 2669 (1981).

[129] X.-G. Wen. Electrodynamical properties of gapless edge excitations in the fractional quantum Hall states. *Phys. Rev. Lett.*, **64**, 2206 (1990).

[130] X. G. Wen. Topological orders in rigid states. *Int. J. Mod. Phys. B*, **4**, 239 (1990).

[131] X.-G. Wen. Edge transport properties of the fractional quantum Hall states and weak-impurity scattering of a one-dimensional charge-density wave. *Phys. Rev. B*, **44**, 5708 (1991).

[132] X.-G. Wen. Gapless boundary excitations in the quantum Hall states and in the chiral spin states. *Phys. Rev. B*, **43**, 11025 (1991).

[133] X. G. Wen. Mean-field theory of spin-liquid states with finite energy gap and topological orders. *Phys. Rev. B*, **44**, 2664 (1991).

[134] X.-G. Wen. Topological orders and edge excitations in fractional quantum Hall states. *Advances In Physics*, **44**, 405 (1995).

[135] X. G. Wen, F. Wilczek, and A. Zee. *Phys. Rev. B*, **39**, 11413 (1989).

[136] X. G. Wen and A. Zee. Quantum statistics and superconductivity in two spatial dimensions. *Nucl. Phys. B*, **15**, 135 (1990).

[137] X. G. Wen and A. Zee. Classification of Abelian quantum Hall states and matrix formulation of topological fluids. *Phys. Rev. B*, **46**, 2290 (1992).

[138] X. G. Wen and A. Zee. Neutral superfluid modes and "magnetic" monopoles in multilayered quantum Hall systems. *Phys. Rev. Lett.*, **69**, 1811 (1992).

[139] F. Wilczek. Some basic aspects of fractional charge. In N. Bonesteel and L. Gorkov, editors, *Selected Papers of J. Robert Schrieffer*. (World Scientific, 2002.

[140] F. Wilczek. Majorana returns. *Nature Physics*, **5**, 614 (2009).

[141] K. Wilson. *New Phenomena in Subnuclear Physics*. Plenum, New York, 1977.

[142] C. Wu, D. Bergman, L. Balents, and S. D. Sarma. Flat bands and Wigner crystallization in the honeycomb optical lattice. *Phys. Rev. Lett.*, **99**, 070401 (2007).

[143] Y. Xia, D. Qian, D. Hsieh, L. Wray, A. Pal, H. Lin, A. Bansil, D. Grauer, Y. S. Hor, R. J. Cava, and M. Z. Hasan. Observation of a large-gap topological-insulator class with a single Dirac cone on the surface. *Nature Phys.*, **5**, 398 (2009).

[144] Y. Xiao, V. Pelletier, P. M. Chaikin, and D. A. Huse. Landau levels in the case of two degenerate coupled bands:kagomé lattice tight-binding spectrum. *Phys. Rev. B*, **67**, 104505 (2003).

[145] C. Xu and S. Sachdev. Global phase diagrams of frustrated quantum antiferromagnets in two dimensions: Doubled Chern-Simons theory. *Phys. Rev. B*, **79**, 064405 (2009).

[146] V. M. Yakovenko. Chern-simons terms and n field in Haldane's model for the quantum hall effect without Landau levels. *Phys. Rev. Lett.*, **65**, 251 (1990).

[147] J. Z.-Justin. *Quantum Field Theory and Critical Phenomena*. Oxford University Press, New York, 2002.